ADDIS ABABA UNIVERSITY

ADDIS ABABA INSTITUTE OF TECHNOLOGY

SCHOOL OF CIVIL AND ENVIRONMENTAL ENGINEERING

Evaluation of Behavior Factor Provision of ES EN for RC Ductile Regular and Plan Irregular Building Structures using Nonlinear Analysis

A Thesis Submitted in Partial Fulfillment
of the Requirements for the Degree of Master of Science in Structural Engineering

By:

Getahun Asres

Nov, 2018

Addis Ababa, Ethiopia

The undersigned have examined the thesis entitled '**Evaluation of Behavior Factor Provision of ES EN for RC Ductile Regular and Plan Irregular Building Structures using Nonlinear Analysis**' presented by **Getahun Asres**, a candidate for the degree of **Master of Science** and hereby certify that it is worthy of acceptance.

Dr. Ing. Girma Zerayohannes	_____	_____
Advisor	Signature	Date
_____	_____	_____
External Examiner	Signature	Date
_____	_____	_____
Internal Examiner	Signature	Date
_____	_____	_____
Chairman	Signature	Date

UNDERTAKING

I hereby declare that all information in this document has been obtained and presented in accordance with academic rules and ethical conduct. I also declare that, as required by these rules and conduct, I have fully cited and referenced all materials and results that are not original to this work.

Name: Getahun Asres

Signature: _____

ACKNOWLEDGEMENTS

Above all, I would like to thank the Almighty GOD, who gives me the courage and strength to do this work. Next, I would like to express my appreciation and thanks to my advisor, **Dr. Ing. Girma Zerayohannes**, who provided me with opportunity to work with him. He has been of immense help, advising and guiding me during my studies. Discussion with him during the times of difficulties and his appreciation has put me back to my original ambition and path of accomplishment.

I would further like to thank all the staffs of the department of Civil and Environmental Engineering for their commitment to teach me during various academic courses that I took at the University of Addis Ababa Institute of Technology.

I would also like to thank the loved ones who surround me. Their existence all the way through my education not only helped me maintain sanity, but also gave rise to lifelong friendships I now treasure.

I would like to express my profound heartfelt thanks to my all-time best friend, **Mr. Belete Desale** for his special support. Had it not been your genuine co-operation, it would have not been possible to conduct this research.

Last but not list I would like to express my thanks to my friend **Mr. Aklilu Shiferaw** who allow me use a server machine for the analysis of the models used in this research.

ABSTRACT

Most recent seismic codes include response modification factors (R in US practice) or behavior factors (q in European practice) in the definition of equivalent lateral force method of analysis used for the design of earthquake resistant buildings. Seismic design makes use of energy absorption and dissipation to reduce the design forces in order to achieve economy. The behavior factor (q) or response modification factors (R) plays a central role in seismic design process, since it is used to reduce the linear elastic design spectrum to account for the energy dissipation capacity of the structure. In this study the evaluation of behavior factor for regular and irregular ductile reinforced concrete structures using nonlinear analysis is investigated. The evaluation is done by designing regular and irregular structures for different ductility classes with the provision of our seismic code and by checking their performance through non-linear analysis using CSI ETABS. In this paper parametric studies have been conducted and the effects of different parameters (seismic location, ground type, number of stories, ductility class and 3D modelling effects) on behavior factor are presented in detail. Moreover, the evaluation of behavior factor using different models under favorable and unfavorable conditions along with performance comparison of structures designed for different ductility classes were done and the results are discussed and presented in this study. Furthermore, the evaluation of behavior factor for 3D plan irregular reinforced concrete structure under unfavorable conditions is done using non-linear dynamic analysis and the findings are presented as well.

KEY WORDS: Behavior factors, Ductility class

TABLE OF CONTENTS

LIST OF TABLES

LIST OF FIGURES

CHAPTER 1 INTRODUCTION

1.1 Overview

Earthquake engineering is requiring building structures to be designed to sustain post-elastic deformations during strong earthquake events. As part of the input seismic energy is dissipated hysterically and the kinetic energy of the structure is reduced, the design forces, compared to the linear elastic forces, can be taken significantly smaller according to seismic codes, and lead to a more economical design. This reduction is expressed in most codes through the well-known response reduction factor R or behavior factor q, strongly depend on the energy dissipation capacity of the structural system, and/or the ductility of the structural members and their connections.

In our seismic code, linear elastic analysis is usually required and the non-linear behavior of the structure is considered by the introduction of the global response reduction factor or behavior factor q. The value of the factor q is depending on various parameters like the type of the framing structure, ductility class and regularity of the structure.

1.2 Response Reduction Factor / Behavior Factor

It is the factor by which the actual base shear force that would be generated if the structure were to remain elastic during its response to the Design Basis Earthquake (DBE) shaking, shall be reduced to obtain the design lateral force. This factor permits a designer to use a linear elastic force-based design while accounting for non-linear behavior and deformation limits.
Thus, Seismic codes consider a decrease in design loads, taking benefit of the fact that the structures possess substantial reserve strength (over-strength) and capacity to dissipate energy (ductility). The over strength and the ductility are incorporated in structural design through a force reduction or a response modification factor. This factor represents ratio of maximum seismic force on a structure through specified ground motion, if it was to remain elastic to the design seismic force. Thus, seismic forces are reduced by the factor *R* to obtain design forces.

1.3 Component of 'R' Factor

Generally, (*Kashyap N. Patel and Jignesh A. Amin* 2017) defines the response reduction factor as a component of various parameters such as strength, ductility and redundancy of the structural system.

$R = Rs * R\mu * R_R$……1.1

Strength Factor (Rs): Strength factor (Rs) accounts for the yielding of a structure at load higher than the design load due to various partial safety factors, strain hardening, oversized members, confinement of concrete. Non-structural elements also contribute to the over strength. The over strength factor generally, vary with seismic zones, height of structure and design gravity loads. The strength factor (Rs) is ratio of maximum base shear (Vu) to the design base shear (Vd).

Ductility Factor (Rμ): The seismic response parameters of displacement capacity, ductility and ductility ratio are closely inter-related. Displacement ductility ratio is generally defined as the ratio of maximum displacement to the displacement at yield.

Redundancy Factor (RR): It mainly relies on the vertical seismic framing numbers. Yielding at one location in the structure does not indicate yielding of the whole structure. Hence, the load distribution, due to redundancy of the structure, provides additional safety margin. RC structural systems with lateral load resisting frames are normally considered as redundant structure, as each of the seismic frames is designed to transfer the seismic forces to the soil.

1.4 Behavior Factors for Horizontal Seismic Actions According to ES EN 1998:1-2015

The following points are stated in our seismic code (ES EN 1998:1-2015) about the behavior factor (q).

1. The upper limit value of the behavior factor q, to account for energy dissipation capacity, shall be derived for each design direction as follows.

$$q = qo * kw \geq 1.5 \quad \text{……...1.2}$$

where;

qo: is the basic value of the behavior factor, dependent on the type of the structural system and on its regularity in elevation;

kw: is the factor reflecting the prevailing failure mode in structural systems with walls.

2. For buildings that are regular in elevation, the basic values of *qo* for the various structural types are given as follows.

Table 1.1: Basic value of the behavior factor, qo, for systems regular in elevation

Structural Type	DCM	DCH
Frame system, dual system, coupled wall system	$3.0\alpha_u/\alpha_1$	$4.5\alpha_u/\alpha_1$
Uncoupled wall system	3.0	$4.0\alpha u/\alpha_1$
Torsionally flexible system	2.0	3.0
Inverted pendulum system	1.5	2.0

For buildings which are not regular in elevation, the value of q_o should be reduced by 20%

α_l and α_u are defined as follows:

α_1 is the value by which the horizontal seismic design action is multiplied in order to first reach the flexural resistance in any member in the structure, while all other design actions remain constant;

α_u is the value by which the horizontal seismic design action is multiplied, in order to form plastic hinges in a number of sections sufficient for the development of overall structural instability, while all other design actions remain constant. The factor α_u may be obtained from a nonlinear static (pushover) global analysis.

When the multiplication factor α_u/α_1 has not been evaluated through an explicit calculation, for buildings which are regular in plan the following approximate values of α_u/α_1 may be used.

a) Frames or frame-equivalent dual systems.

- One-story buildings: αu/α1=1.1;
- multistory, one-bay frames: αu/α1=1.2;
- multistory, multi-bay frames or frame-equivalent dual structures: αu/α1=1.3.

b) Wall- or wall-equivalent dual systems.

- Wall systems with only two uncoupled walls per horizontal direction: $\alpha_u/\alpha_l = 1.0$;
- other uncoupled wall systems: $\alpha_u/\alpha_1 = 1.1$;
- Wall-equivalent dual, or coupled wall systems: $\alpha_u/\alpha_1 = 1.2$.

3. For buildings which are not regular in plan the approximate value of α_u/α_1 that may be used when calculations are not performed for its evaluation are equal to the average of (a) 1,0 and of (b).
4. Values of α_u/α_1 higher than those given in (a) and (b) may be used, provided that they are confirmed through a nonlinear static (pushover) global analysis.
5. The maximum value of α_u/α_1 that may be used in the design is equal to 1.5, even when the analysis mentioned in (4) results in higher values.
6. The value of q_o given for inverted pendulum systems may be increased, if it can be shown that a correspondingly higher energy dissipation is ensured in the critical region of the structure.
7. If a special and formal Quality System Plan is applied to the design, procurement and construction in addition to normal quality control schemes, the values of q_o given in table 1.1 may be increased by 20%. Such a specific plan must consider the stages from design through to construction and include aspects including the accuracy of the analysis methods implemented and the verification of the correct positioning of the steel in critical zones.

1.5 Statement of The Problem

Ductile RC building structures are commonly used in urban areas worldwide as the dominant mode of building construction. The usual procedure followed by seismic building codes to specify the minimum design strength to resist earthquake ground motions is to prescribe a spectrum based on the linear elastic response of the structure to a design ground motion, combined with response modification factors to reduce the spectral values to account for the capacity of the structural system to dissipate energy when stiffened beyond its elastic limit.

From a general point of view, our seismic code does not consider the influence of the natural period of vibration and ground acceleration in the reduction of the linear elastic spectral values allowed by the ductile inelastic behavior of the structure.

Response reduction factor provisions for both regular and irregular reinforced concrete frames given in ES EN: 1998-2015 are too general. As a result, the adequacy of our seismic code to inhibit collapse of building structures under extreme scenarios as well as its accuracy to result in economical design under favorable situations has to be questioned. In addition, a number of assessments of code-designed plan irregular structures have also shown that specifications subscribed by current major seismic codes need re-examination in order to properly deal with nonlinear behavior.

1.6 Objectives

1.6.1 General Objective

- The primary objective of this study will be to evaluate the adequacy and accuracy of behavior factors given in our seismic code ES EN 1998:1-2015 for RC regular and plan irregular moment resisting buildings using nonlinear analysis.

1.6.2 Specific Objectives

In addition to the primary objective specified, this paper will also try;

- Testing if there is an underestimation or overestimation in response reduction factors for seismic zones of ground acceleration 0.1g, 0.15g and 0.2g.
- Comparing the performance of a structure designed for different ductility classes
- To study and identify the parameters that affects behavior factor

1.7 Scope of The Work

The present study will be limited to three dimensional RC frames with and without irregularities. The stiffness and strength of Infill walls will not be considered. The soil structure interface effects will not be considered in the study. The flexibility of floor diaphragms will be ignored and considered as stiff diaphragm. The column bases are assumed to be fixed in the study. Evaluation of response reduction factors for different ductility classes will be done using CSI ETABS.

1.8 Organization of this Research

Chapter 1: presents a general introduction to the concept of behavior factor, the motivation and objectives of this research.

Chapter 2: gives a detailed review on the calculation of behavior factor and a review of the nonlinear analysis techniques used for the calculation of behavior factor. Previous research works relating to behavior factor are also presented here.

Chapter 3: presents a description of the configuration of the study buildings. Member sizes and material properties used in the design are described. It also defines the seismic loading parameters, capacity design principles and detailing rules used for the design for the design of the models according to ES EN 1998:1-2015.

Chapter 4: presents about modeling and generation of nonlinear hinge properties, types of hysteresis models, procedures of the nonlinear analysis techniques used for this research, verification of the software using experimental results. In addition, parametric study on behavior factor, the summery of the results of each models used in this study and seismic performance comparison of structures designed for different ductility classes are discussed in detail.

Chapter 5: presents a summary of the work and major findings. Recommendations for future work are also described here.

CHAPTER 2 LITERATURE REVIEW

2.1 Introduction

There are many natural hazards in the world but earthquakes are one of the most destructive natural hazards that can result in severe social and economic impact. The devastating potential of an earthquake can have major consequences on infrastructures and lifelines, while annual economic losses, taking major toll on nation's economy.

Earthquake engineering has developed as a branch of engineering concerned with the estimation of earthquake impacts, since last few decades. It has become an interdisciplinary subject involving seismologists, structural engineer, geotechnical engineers, architects, urban planners, information technologists and social scientists. In the past few years, the earthquake engineering community has been reassessing its procedures, in the wake of devastating earthquakes which have caused extensive damage, loss of life and property. These procedures involve assessment of seismic force demands on the structure and then developing design procedures for the structure to withstand the applied actions.

Conventional seismic design in codes of practice is entirely force-based, with a final check on structural displacements. Force-based design is suited to design for actions that are permanently applied. Members are designed to resist the effects of these actions. Seismic design follows the same procedure, except for the fact that inelastic deformations may be utilized to absorb certain levels of energy leading to reduction in the forces for which structures are designed. This leads to the creation of the Response Modification Factor (R factor); the all-important parameter that accounts for over-strength, energy absorption and dissipation as well as structural capacity to redistribute forces from inelastic highly stressed regions to other less stressed locations in the structure. The concept of Response Modification Factor or also commonly known as Force Reduction Factor, has emerged as a single most important number, reflecting the capability of the structure to dissipate energy through inelastic behavior.

In our seismic code, linear elastic analysis is usually required and the non-linear behavior of the structure is considered by the introduction of the global response reduction factor or behavior factor q. The value of the factor q is depending on various parameters like the type

of the framing structure, the type of the material, the geometric configuration, the local ductility of the members, the stiffness distribution, the capacity design criteria, the over strength etc.

2.2 Introduction to Basic Concept of Seismic Design

Design requirements for lateral loads, such as winds or earthquakes, are inherently different from those for gravity (dead and live) loads. Due to frequency of loading scenario, design for wind loads is a primary requirement. But in areas of high seismicity, structures have to be designed to withstand earth quick loads as well.

In earthquake engineering, the aim is to have a control on the type, location and extent of the damage along with detailing process. As it is illustrated in Figure 2.1, where the elastic and inelastic responses are depicted, and the concept of equal energy (discussed further in subsequent sections) is employed to reduce the design force from V_e to V_d (denoting elastic and design force levels).

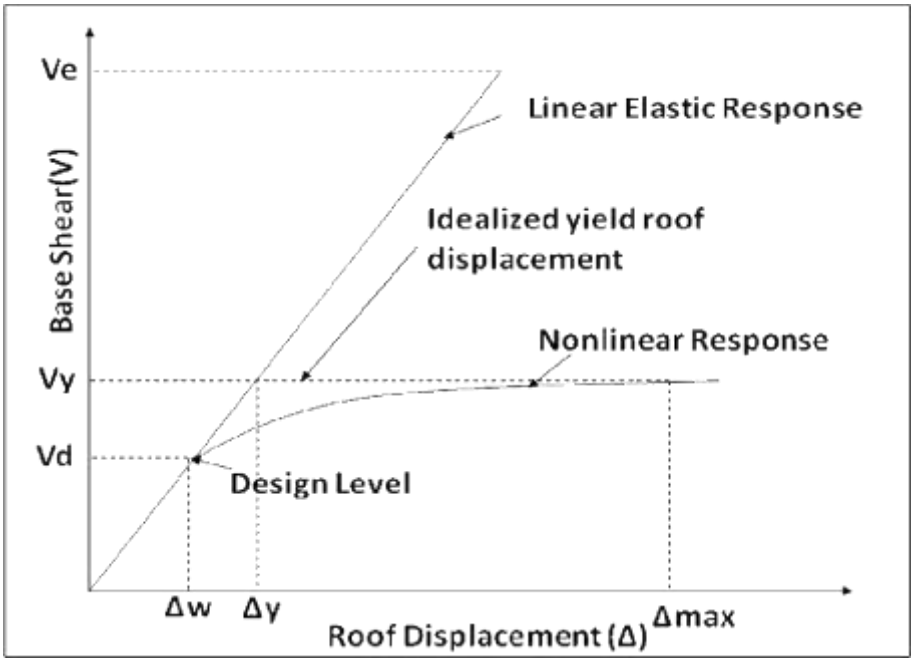

Figure 2.1: Force displacement responses of elastic and inelastic systems

2.3 Definition of R Factor and its Components

As previously discussed in section 2.1, R factors are essential seismic design tools, which defines the level of inelasticity expected in structural systems during an earthquake event. R factor reflects the capability of structure to dissipate energy through inelastic behavior. R factor is used to reduce the design forces in earthquake resistant design and accounts for damping, energy dissipation capacity and for over-strength of the structure.

Conventional seismic design procedures adopt force-based design criteria as opposed to displacement-based. The basic concept of the latter is to design the structure for a target displacement rather than a strength level. Hence, the deformation, which is the major cause of damage and collapse of structures subjected to earthquakes, can be controlled during the design. Nevertheless, the traditional concept of reducing the seismic forces using a single reduction factor, to arrive at the design force level, is still widely used. This is because of the satisfactory performance of buildings designed to modern codes in full-scale tests and during recent earthquakes.

In order to justify this reduction, seismic codes rely on reserve strength and ductility, which improves the capability of the structure to absorb and dissipate energy. Hence, the role of the force reduction factor and the parameters influencing its evaluation and control are essential elements of seismic design according to codes. (ATC,40) states that values assigned to the response modification factor (R) of the US codes (FEMA, 1997; UBC, 1997) are intended to account for both reserve strength and ductility. Some literatures also mention redundancy in the structure as a separate parameter.

The philosophy of earthquake resistant design is that a structure should resist earthquake ground motion without collapse, but with some damage. Consistent with this philosophy, the structure is designed for much less base shear forces than would be required if the building is to remain elastic during severe shaking at a site**.** Such large reductions are mainly due to two factors: (1) the ductility reduction factor (Rμ), which reduces the elastic demand force to the level of the maximum yield strength of the structure, and (2) the over strength factor, (**Ω**), which accounts for the over strength introduced in code-designed structures. Thus, the response reduction factor (R) is simply **Ω** times Rμ. See Figure 2-2.

$$R = R\mu \times \Omega \quad \text{.....2.1}$$

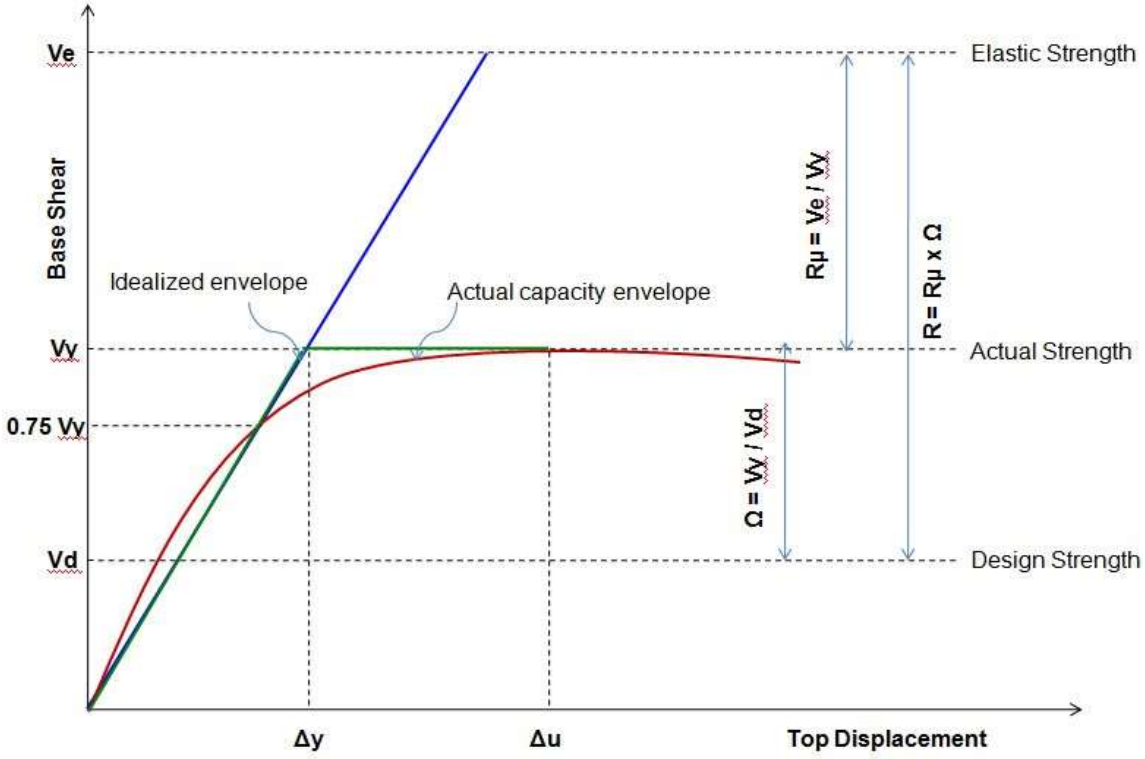

Figure 2.2: Relationship between force reduction factors (R), structural over strength (Ω), and ductility reduction factor (Rμ)

2.3.1 Ductility Reduction Factor (Rμ)

The ductility reduction factor (Rμ) is a factor which reduces the elastic force demand to the level of idealized yield strength of the structure and, hence, it may be represented as the following equation:

$$R\mu = V_e / V_y \quad \text{.....2.2}$$

Ve is the max base shear coefficient if the structure remains elastic. The ductility reduction factor (Rμ) takes advantage of the energy dissipating capacity of properly designed and well-detailed structures. Hence, primarily depends on the global ductility demand, μ, of the structure (μ is the ratio between the maximum roof displacement and yield roof displacement). (Newmark and Hall 1973, 1982) made the first attempt to relate Rμ with μ for a single-degree-of-freedom (SDOF) system with elastic-perfectly plastic (EPP) resistance curve. They concluded that for a structure of a natural period less than 0.2 second (short period structures), the ductility does not help in reducing the response of the structure. Hence, for such structures, no ductility reduction factor should be used. For moderate period structures, corresponding to

the acceleration region of elastic response spectrum T = 0.2 to 0.5 sec the energy that can be stored by the elastic system at maximum displacement is the same as that stored by an inelastic system. For relatively long-period structures of the elastic response spectrum, (Newmark and Hall 1973, 1982) concluded that inertia force obtained from an elastic system and the reduced inertia force obtained from an inelastic system cause the same maximum displacement. This gives the value of ductility reduction factor in a mathematical representation as;

$$R\mu = \mu \quad \text{.....2.3}$$

2.3.2 Structural Over strength (Ω)

Structural overstrength plays an important role in collapse prevention of the buildings. The overstrength factor (Ω) may be defined as the ratio of actual to the design lateral strength.

$$\Omega = V_y \ / \ V_d \quad \text{.....2.4}$$

Where V_y is the base shear coefficient corresponding to the actual yielding of the structure;
Vd is the code-prescribed un factored design base shear coefficient.

The inertia force due to earthquake motion, at which the first significant yield in a reinforced concrete structure starts, may be much higher than the prescribed un factored base shear force because of many factors such as (1) the load factor applied to the code-prescribed design seismic force; (2) the lower gravity load applied at the time of the seismic event than the factored gravity loads used in design; (3) the strength reduction factors on material properties used in design; (4) a higher actual strength of materials than the specified strength; (5) a greater member sizes than required from strength considerations; (6) more reinforcement than required for the strength; and (7) special ductility requirements, such as the strong column-weak beam provision. Even following the first significant yield in the structure, after which the stiffness of the structure decreases, the structure can take further loads. This is the structural over strength which results from internal forces distribution, higher material strength, strain hardening, member oversize, reinforcement detailing, effect of nonstructural elements, strain rate effects.

2.4 Overview of R Factor

The seismic force values used in the design of buildings are calculated by dividing forces that would be associated with elastic response by a response modification factor. Concept of R factor was proposed based on the fact that well detailed framing systems could sustain large inelastic deformation without collapse (ductile behavior) and develop lateral strength in excess of their design strength (often termed as reserve strength or over strength). Level of this reduction normally specified in code is based on the observation of the performance of different structural systems in previous earthquakes or during tests in laboratories. The R factor is assumed to represent the ratio of the forces that would develop under the specified ground motion if the framing system was to behave entirely elastically to the prescribed design forces at the strength level. (See Figure 2.2)

R factors are used in current building codes to estimate strength demands for structural systems designed using linear methods but responding in nonlinear manner. Their values are vital in the specification of design seismic loading. R factors were originally based on judgment and qualitative comparisons with known response of some of the framing systems. Now it has come a long way by actually quantifying it using nonlinear analysis tools and peak ground and spectral parameters.

Response modification factor (also termed as behavior factor) plays a key role in seismic design process. No other parameter in the design base shear equation impacts the design actions in a seismic framing system as does the value assigned to R.

As mentioned previously, structures are not designed to resist earthquake forces in their elastic range; instead, concepts of energy absorption in the inelastic range are used to reduce the elastic forces. Lower force levels are generated in the inelastic system, due to energy absorption by hysteresis (inelastic force-displacement response).

2.5 R Factor Calculation Methods

In the previous sections of this chapter, Response modification or Force reduction factor (R) was discussed in detail from the capacity point of view. In this section, reduction factor from demand perspective will be considered. The reduction factor 'demand' is defined as the ratio between the elastic ($Sa_{elastic}$) and the inelastic ($Sa_{inelastic}$) response spectral ordinates corresponding to a specific period T (ATC-19). (See Figure 2-3).

Force Reduction Factor = $Sa_{elastic}$ (T) / $S_{ainelastic}$ (T) ……..….2.6

Thus, it expresses the ratio of the elastic strength demand to the inelastic strength demand for a specified constant ductility μ.

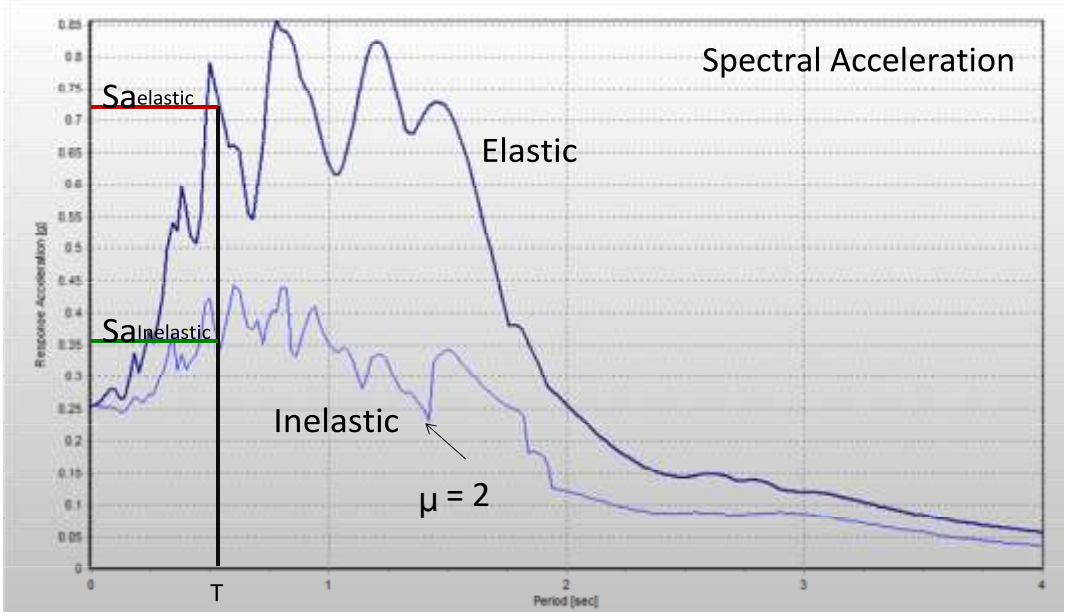

Figure 2.3: Elastic and inelastic acceleration response spectra

The response factor 'demand' represents the minimum reduction coefficient corresponding to a specific level of ductility obtained from inelastic constant ductility spectra and elastic spectra (See Figure 2.3). For a given period, the elastic spectral ordinate should be divided by the inelastic counterpart for a value of ductility expected for the structural system under consideration. Some of the observations in this regard are as follows:

- R factor is not constant but rather varies considerably with period.
- At very short periods, the R factor is almost unity.
- For low levels of ductility, the statically derived relationships of R=1, R=μ,
- And $R = \sqrt{2\mu - 1}$ hold quite well (Newmark and Hall, 1982), but are distinct from the actual R factors for higher ductility levels.

The relationship between displacement ductility and ductility-dependent R factor has been the subject of considerable researches. A few of most frequently used relationships are discussed below:

2.5.1 Newmark and Hall (1982)

In this early study, Rμ was determined to be a function of μ. It was observed that in the long period range, elastic and ductile systems with the same initial stiffness reached almost the same displacement. As a result, the response factor can be considered equal to the displacement ductility. This is referred to as 'equal displacement' region. For intermediate period structures, the ductility is higher than the response factor and the 'equal energy' approach may be adopted to calculate force reduction.

2.5.2 Krawinkler and Nassar (1992)

A relationship was developed for the force reduction factor derived from the statistical analysis of 15 western USA ground motions with magnitude between 5.7 and 7.7 (Krawinkler and Nassar, 1992). The influence of response parameters, such as yield level and hardening coefficient α, were considered. A 5% damping value was assumed. The equation derived is given as:

$$R_\mu = [c\ (\mu - 1) +]^{1/c} \quad \text{.....2.5}$$

$$C\ (T,\alpha) = \frac{T^a}{(1+T^a)} + \frac{b}{T} \quad \text{.....2.6}$$

Where c is a constant which is dependent on period (T) and α which is the strain hardening parameter of the hysteretic model and a and b are regression constants. Values of the constants in above equations were recommended for three values of hardening α as in Table 2.5 below:

Table 2.1: Model parameter constants for Krawinkler and Nassar

Hardening Value	Model Parameters	
α	A	B
0%	1.00	0.42
2%	1.01	0.37
10%	0.80	0.29

2.5.3 Miranda and Bertero (1994)

The equation for reduction factor introduced by (Miranda and Bertero 1994) was obtained from a study of 124 ground motions recorded on a wide range of soil conditions. The soil conditions were classified as rock, alluvium and very soft sites characterized by low shear wave velocity.

A 5% of critical damping was assumed. The expressions for the period-dependent force reduction factors Rμ are given by:

$R_\mu = \frac{\mu-1}{\Phi} \pm 1$ ……2.7

where Φ is calculated from different equations for rock, alluvium and soft sites

as shown below:

$\Phi = 1+\frac{1}{10T-\mu T} - \frac{1}{2T}\exp[-1.5(lnT-0.6)^2]$ for rock site…….....2.8

$\Phi = 1+\frac{1}{12T-\mu T} - \frac{1}{5T}\exp[-2(lnT-0.2)^2]$ for alluvium site……....2.9

$\Phi = 1+\frac{1}{3T-\mu T} - \frac{3T1}{4T}\exp[-3\left(\ln(\frac{T}{T1})-0.25\right)^2]$ for soft site……2.10

Where; T corresponds to the period at which the relative velocity of a linear system with 5% damping is maximum within the entire period range, T_1 is the predominant period of the ground motion, and μ is the displacement factor.

2.5.4 Vidic et al. (1994)

The reduction coefficients Rμ calculated by (Vidic 1994) were approximated by a bilinear curve. In the short period range, the reduction factor increases linearly with the period from 1.0 to a value that is almost equal to the ductility factor. In the remaining part of the period range the reduction factor is constant. To calculate the reduction factor, a bilinear response model and a stiffness degrading 'Q-model' were employed. In this work, the standard records from California (USA) and Montenegro-1979 (Yugoslavia) were chosen as being representative for 'standard' ground motion, i.e. severe ground motion at moderate epicentral distance, with a duration ranging between 10 and 30 seconds and predominant period between 0.3 and 0.8 seconds. The proposed formulation of reduction factor, for special strong motion features, is:

$R_\mu = c_1(\mu-1)^{CR\frac{T}{To}+1}$ when T < T0……2.13

$R_\mu = c_1(\mu-1)^{CR+1}$ when T ≥T0……2.14

where T_0 is the period dividing the period range into two portions. It is related to

the predominant period of the ground motion T_1 by means of:

$T_0 = c_2 \mu^{c_T}$ ……..…2.15

The coefficients c_1, c_2, c_R and c_T in the above equations depend on the hysteretic behavior, either bilinear or with degrading stiffness, and damping, e.g. time dependent or independent. The values of the model parameters are outlined in Table 2.6 below.

Table 2.2: Model parameter constants for Vidic et al.

Model	Damping	C_1	C_2	C_R	C_T
Bilinear	Mass-proportional	1.35	0.75	0.95	0.20
Bilinear	Instantaneous stiffness proportional	1.10	0.75	0.95	0.20
Q-model	Mass-proportional	1.00	0.65	1.00	0.30
Q-model	Instantaneous stiffness proportional	0.75	0.65	1.00	0.30

2.6 R factor based on Peak Ground Parameters

Another method of calculating force reduction factor was introduced by (A.J.Kappos 1992) which considers peak ground parameters, either in terms of acceleration, velocity or displacement depending on type of structure and its period. It considers both, the actual structural response and actual ground motion, giving a coupled response by considering both demand and supply. The reduction factor is thus defined as the ratio between the peak ground acceleration of the record causing ultimate limit state and the peak ground acceleration of the record causing yield limit state.

Force Reduction Factor = PGA causing ultimate limit state / PGA causing yield limit state

Velocity and displacement based peak ground parameters can also be used in place of acceleration, but will depend on the period of the structure being assessed. For long period structure, using displacement based peak ground parameter is a better approach. Short period structures are sensitive to acceleration, intermediate period structures to velocity and long period structures are sensitive to displacement.

2.6.1 Response Parameters

The evaluation of the deformation quantities Δu and Δy from action-deformation relationships is not always straightforward. (Park 1988) tried to define yield and ultimate deformation based

on force deformation relationship in order to quantify global ductility of structural systems. These definitions for yield and ultimate deformation are presented in following sections.

2.6.2 Yield Deformations

Yield points in reinforced concrete structures are often not well defined because of nonlinearities associated with cracking of concrete and formation of plastic hinges in beams, columns and joints. Various definitions for yield deformations have been proposed as summarized below (Park, 1988):

a) Deformation corresponding to first yield.
b) Deformation corresponding to the yield point of an equivalent elasto-plastic system with the same elastic stiffness and ultimate load as the real system.
c) Deformation corresponding to the yield point of an equivalent elasto-plastic system with the same energy absorption as the real system.
d) Deformation corresponding to the yield point of an equivalent elasto-plastic system with reduced stiffness computed as the secant stiffness at 75% of the ultimate lateral load of the real system.

2.6.3 Ultimate Deformations

Definitions for ultimate deformations are as follows (Park, 1988):

i. Deformation corresponding to a limiting value of strain.

ii. Deformation corresponding to the apex of the load-displacement relationship.

iii. Deformation corresponding to the post-peak displacement when the load carrying capacity has undergone a small reduction (often taken as 10%-15%).

iv. Deformation corresponding to fracture or buckling.

Ductile structures usually have post-peak load strength and their load deformation curves do not exhibit abrupt reduction in resistance, especially for MRFS.

2.7 Relationship Between Limit States and IDA

The definition of yield and ultimate deformation, as explained in section 2.6.1, can be employed on both pushover curve and IDA plot. So, the definition of yield and ultimate deformation will be used on IDA plot. The deformation corresponding to the yield point of an equivalent elasto-plastic system with reduced stiffness computed as the secant stiffness at 75% of the ultimate lateral load of the real system is more realistic for reinforced concrete because it accounts for the reduction of structural stiffness due to cracking (park 1998) and used in this study. The initial stiffness is evaluated as the secant stiffness at 75% of the ultimate strength from incremental dynamic analysis (IDA plots). Projection of the intersection of this secant with elastic–perfectly-plastic idealization, on the IDA plot gives the yield point as illustrated in Figure 2.4.

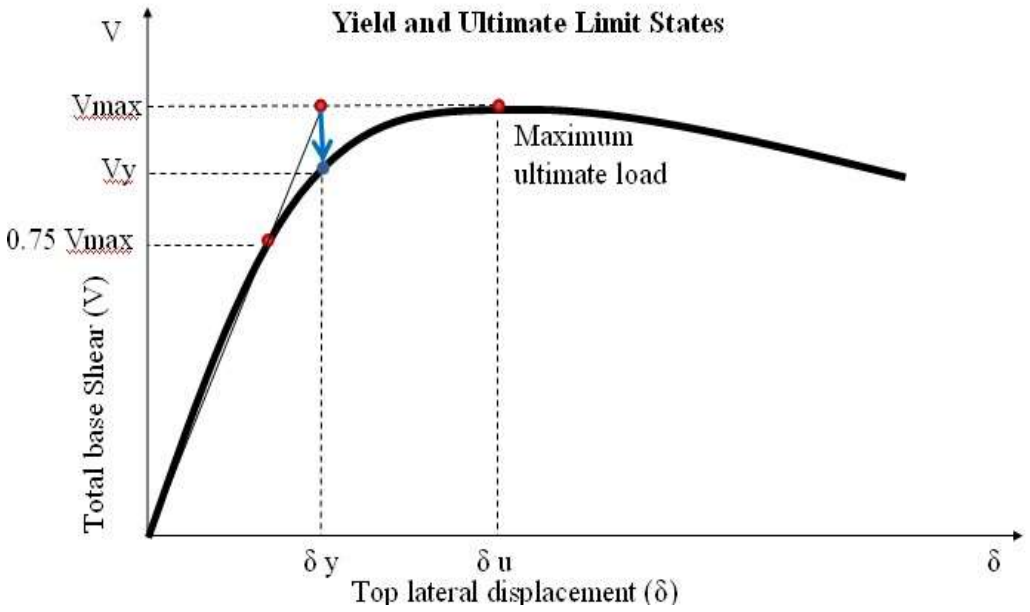

Figure 2.4: Limit states definition to be used.

CHAPTER 3 MODELING ANALYSIS AND DESIGN

In this chapter, a description of the configuration of the study buildings. Member sizes and material properties used in the design are described. It also defines the seismic loading parameters, capacity design principles and detailing rules used for the design for the design of the models according to ES EN.

3.1 Modeling

In this section, models of the building are created using ETABS 2016.2.1, which is the latest version of CSI ETABS structural analysis and design software. For modeling the frames, the minimum section sizes are used which fulfills the minimum serviceability as per the requirements of ES EN: 1992-2015.

A total of Sixteen (16) building models are analyzed and designed for different combinations of ground acceleration, soil type and ductility classes for the completion of the objectives of this research. The typical floor plans for models and the data necessary to analyze the models are summarized below. All the models selected are regular in elevation and the range of elevations are shown in figure 3.2.

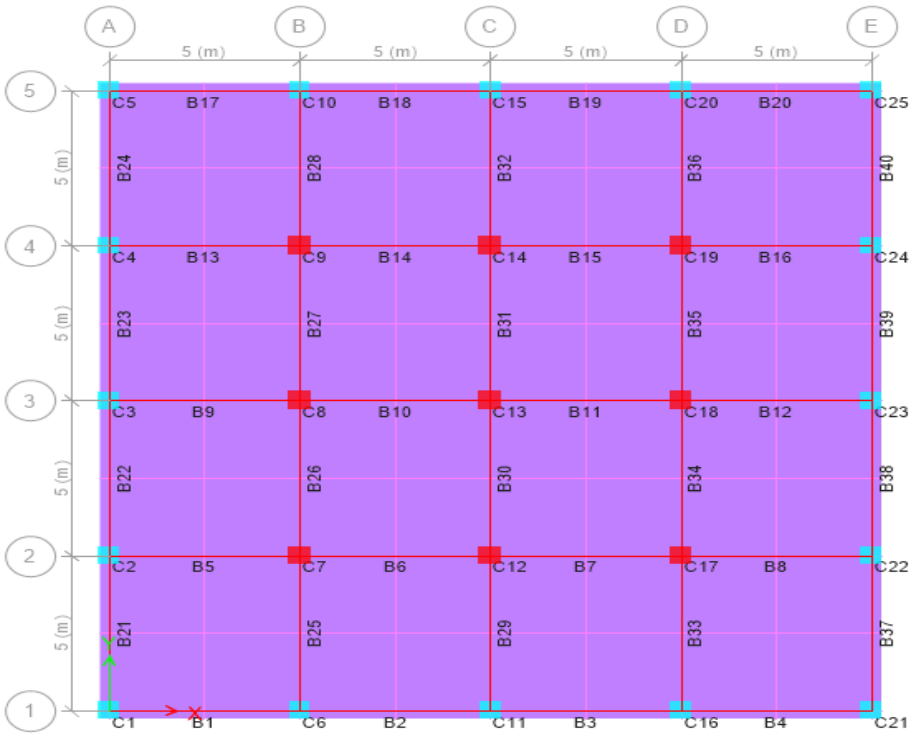

a)

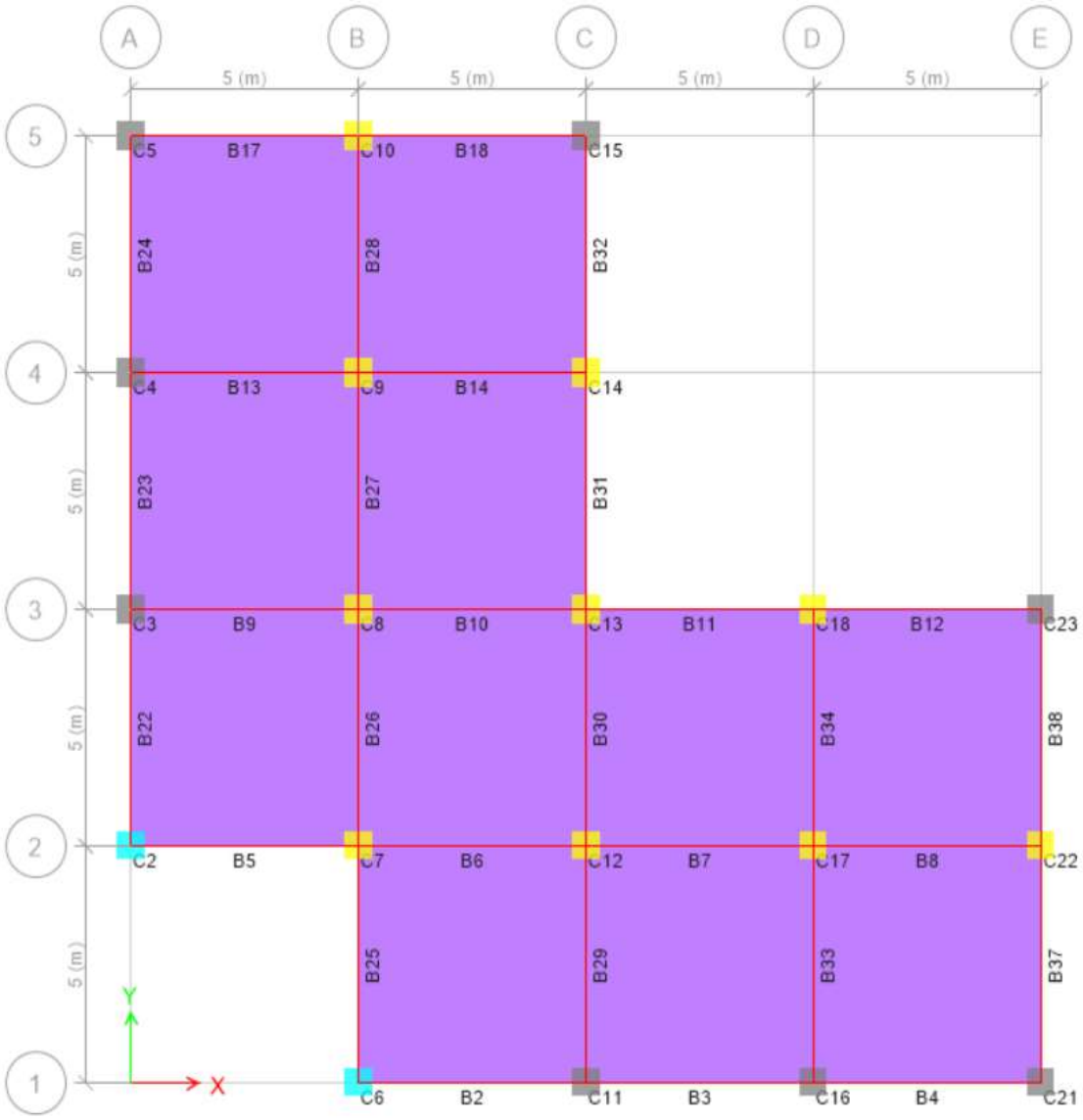

b)

Figure 3.1: Plan view of the models a) regular b) irregular models

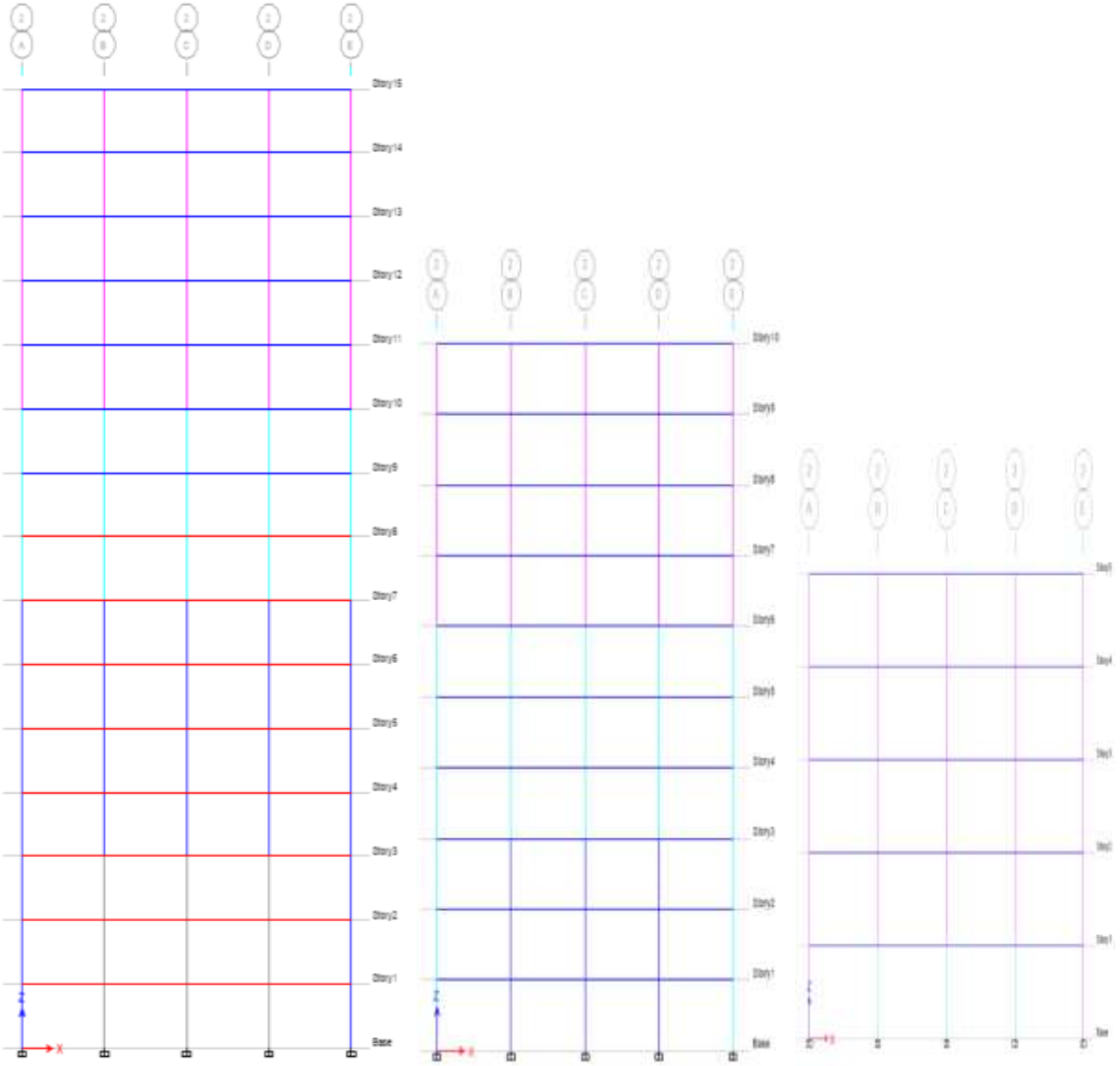

15 story *10 story* *5 story*

Figure 3.2: Elevation view of the models

Table 3.1: Types of Models and their designation

Non-Linear 2D models						
Story	Ductility Class	Ag	Ground Type	Plan Regularity	Behavior Factor(q)	Designation
5	DCM	0.15	A	Regular	3.9	DCM 5
10						DCM 10
15						DCM 15
10	DCM	0.1	A	Regular	3.9	DCM 0.1
		0.15				DCM 0.15
		0.2				DCM 0.2
10	DCM	0.15	A	Regular	3.9	DCM A
			B			DCM B
			C			DCM C
3D models						
Story	Ductility Class	Ag	Ground Type	Plan Regularity	Behavior Factor(q)	Designation
5	DCM	0.15	A	Regular	3.9	DCM 5 favorable
	DCH				5.85	DCH 5 favorable
10	DCM	0.15	A	Regular	3.9	DCM 10 favorable
	DCH				5.85	DCH 10 favorable
	DCM	0.2	C	Regular	3.9	DCM 10 unfavorable
	DCH				5.85	DCH 10 unfavorable
	DCH	0.2	C	Irregular	5.175	DCH 10 Plan Irregular

Favorable: - Models under good situation (subjected to moderate seismic action, supported on hard ground type)

Unfavorable: - model under worst situation subjected to higher seismic action and supported on loss ground type)

Table 3.2: Materials and importance class used for the analysis and design of the models.

Concrete	C25/30 for 10 and 15 story models C 20/25 for 5 story models
Reinforcement bar	S400 for longitudinal reinforcement S300 for shear reinforcement
Importance class of structure	II (Ordinary buildings)

The reason for fixing the above material and parameters is to avoid the effect of the variation of these variables. Thus, to evaluate the cases under the same conditions. For further comparison of results, the buildings were designed for two different levels of ductility requirements which are Ductility Class Medium and Ductility Class high. In modeling the structure, it was considered that the properties of bending and shear of elastic rigidity on primary elements correspond only to 50% of the stiffness of non-cracking elements to take account the cracking effect. For the seismic design situation, it is necessary to adjust the size / stiffness of earthquake-resistant elements according to the value of the seismic action corresponding to each ductility demand with the aim of verifying the relevant limit states. So, in this context, to all models, it was done an iterative process to obtain the final structural definition.

3.2 Loads and Load Combinations

In this research the loads applied on the structures are dead load, live load and seismic loads. The load combinations are created as per (ES EN 1998: -2015). A total of 34 load combinations are considered for all models and the maximum action effects are used for analysis and design of the buildings. The dead loads considered in this project are the self-weight of the structure and additional dead load of 3kN/m^2 to consider floor finish and partition wall loads. The live load is taken from the structural function of the buildings and is chosen as 3kN/m^2 assuming the floor is used for office.

3.2.1 Load Combinations

The following load combinations are used

$DL + LL$ …….3.5

$1.35DL + 1.5LL$…….3.6

$DL + 0.3LL \pm EQX1 \pm 0.3EQY1$……...3.7

$DL + 0.3LL \pm EQX1 \pm 0.3EQY2$……...3.9

$DL + 0.3LL \pm EQX2 \pm 0.3EQY1$……...3.10

$DL + 0.3LL \pm EQX2 \pm 0.3EQY2$……...3.11

$DL + 0.3LL \pm 0.3EQX1 \pm EQY1$…….3.12

$DL + 0.3LL \pm 0.3EQX1 \pm EQY2$…….....3.13

$DL + 0.3LL \pm 0.3EQX2 \pm EQY1$…….……3.14

$DL + 0.3LL \pm 0.3EQX2 \pm EQY2$…….……3.16

3.3 Accounting for Imperfections

Global imperfection can be accounted during the analysis stage as Equivalent Horizontal force (EHF) or during the design stage as eccentricity (ECC). The most convenient way to account for global imperfection is to consider it as an ECC in design of isolated vertical members. This method is available in ETABS 2016 and SAP2000 v19 for design of structures based on (EC2 2004) and used in this research.

The inclination value is calculated as:

$\theta_i = \theta_o \alpha_h \alpha_m$ ……..……...……..……3.17

θ_o = the basic value given as 0.005 (1/200)

$\alpha_m = 1$

$\alpha_h = \frac{2}{\sqrt{L}}$; $2/3 \leq \alpha_h \leq 1$, L = actual length of the vertical member, L_0=effective length

The resulting geometric imperfection moments, Mi2 and Mi3, will be added to analysis first order moments in a single direction at a time:

$$M_{i2} = e_{i2} N_{ed} \quad \text{.....3.18}$$

$$M_{i3} = e_{i3} N_{ed}$$

The eccentricity due to imperfection will be calculated as:

$$e_i = \theta_i L_0 / 2 \quad \text{.....3.19}$$

3.4 Behavior Factor

For purposes of defining the value of behavior coefficient, it is necessary to classify the structural system and define their regularity in plan and height. If the structure is not defined by regular in height, the reference values of behavior coefficient must be reduced by 20%. The lateral force resisting mechanism of the models used in this research is frame system thus, the values in table 3.5 are used for analysis.

The energy dissipation capacity of the structure is considered mainly through the ductile behavior of its elements by performing a linear analysis based on a reduced response spectrum, called design spectrum. This reduction is accomplished by introducing the behavior factor q. The value of behavior factor is defined by the following equation.

$$q = q_o . k_w \quad \text{.....3.20}$$

Where qo is the basic value of the behavior factor, dependent on the type of the structural system and on its regularity in elevation

kw is the factor reflecting the prevailing failure mode in structural systems with walls.

Table 3.3: Behavior factors used for the analysis.

Structure type	DCM	DCH
2D and 3D frame systems	3*1.3=3.9	4.5*1.3=5.85
3D plan irregular frame systems	3*1.15 = 3.45	4.5*1.15 = 5.175

3.5 Analysis Verification and 2nd Order Effects

The application of ES EN: 1998-2015 on design of structures subjected to seismic action is intended to ensure three objectives: 1). safeguarding human lives; 2). limit structural damage; 3). important structures for civil protection remain operational. In this context, it is necessary that structures are designed for non-occurrence of local or global collapse to a seismic level with small probability of occurrence, designated as design seismic action, and is controlled the damage level in the same structure for a seismic action with minor intensity and higher probability of occurrence than the design seismic action. The damage should not correspond to disproportionately high costs when compared to the structure itself. These two requirements are accomplished, if the two limit states are verified:

1. **Ultimate limit states:** For ultimate limit states verifications, Interstory drift sensitivity coefficient should be evaluated as follows.

   If $\theta \leq 0.10$ second order effects can be ignored otherwise 2nd order effects have to be considered. But The value of the coefficient θ shall not exceed 0,3.

   $$\theta = \frac{P_{tot}.\, dr}{V_{tot}.\, h} \leq 0.1 \quad \text{.....3.21}$$

   Where;

   θ = Interstory drift sensitivity coefficient

   P_{tot} = total gravity load at and above the story considered in the seismic design situation

   V_{tot} = total seismic story shear at and above the story considered

   h = interstory height

   dr = design interstory drift, evaluated as the difference of the average lateral displacement's ds at the top and bottom of the story under consideration. *ds* correspond to the elastic displacement obtained from the analysis for the seismic design situation amplified by the value of the behavior coefficient in that direction.

2. **Damage limit state:** The "damage limitation requirement" is considered to be satisfied, if drift limits in the following table are satisfied.

Table 3.4: Maximum relative displacement between floors according to the material of non-structural elements.

Non-structural elements with brittle materials fixed to the structure	Non-structural ductile elements	Absence or fixing of non-structural elements to the structure
$d_r v \leq 0.005h$	$d_r v \leq 0.0075h$	$d_r v \leq 0.010h$

ν is the reduction coefficient whose value is 0,4 for importance class IV and V and 0,5 for importance class I and II.

3.6 Analysis of Buildings

After modeling and performing the preliminary design of the structure to the vertical loads, equivalent static analysis is performed for all the models described in the previous sections. After performing linear static analysis, the corresponding ultimate and damage limit state requirements of the code are checked and respected. Thus, a summary of this task is presented in the tables below. In the case where it was found that θ exceeds 0.2, explicit 2nd orders analysis is done using ETABS 2016.2.1.

The size / stiffness of the elements was obtained by a process of iteration as the demand of the ductility classes for each model and optimized sections are obtained keeping the satisfaction of the limits provided in the design codes. In all cases, the sections are selected to full fill all the capacity design requirements. All of the following design information's are checked being in the required limit. Longitudinal reinforcement, shear reinforcement, beam column capacity, joint shear capacity, torsional reinforcement, P-M failure, shear failure. Capacity Design

As a design tool, the capacity design approach is widely recognized in the field of earthquake engineering. Resulting from nonlinear response and energy absorption ability (R > 1.5), structures subjected to linear analyses with reduced seismic design forces require use of the capacity design approach.

The main energy dissipating elements in the lateral force resisting system are designed and detailed according to the capacity design approach to ensure stable response behavior under strong seismically induced inelastic lateral deformations. The remaining structural elements that do not particularly contribute to such a behavioral response are designed and detailed as non-ductile structural components. Through an effective design and detailing of the main

energy dissipating structural components, inelastic lateral deformations are forced to occur in those elements. By utilizing the approach as such, a capacity designed structure is able to ensure greater seismically generated ground motions than those specified by design levels.

The aim of design is to control the inelastic seismic response. (M.N. Fardis, 2009) states that Capacity design can be achieved through;

1. Structural configuration and relative sizing of members to ensure a beam – sway mechanism,
2. Detailing of plastic hinge regions (beam ends, base of columns and walls) to sustain inelastic deformation demands. Plastic hinge regions are detailed for deformation (ductility) demands.

In capacity design of buildings;

- Avoid weak column / strong beam frames
- Avoid Soft-story collapse mechanism through proper structural configuration

Provide strong column/weak beam frames, with beam sway mechanisms, involves plastic hinging at all beam ends either plastic hinging at column bottoms, or rotations at the foundation.

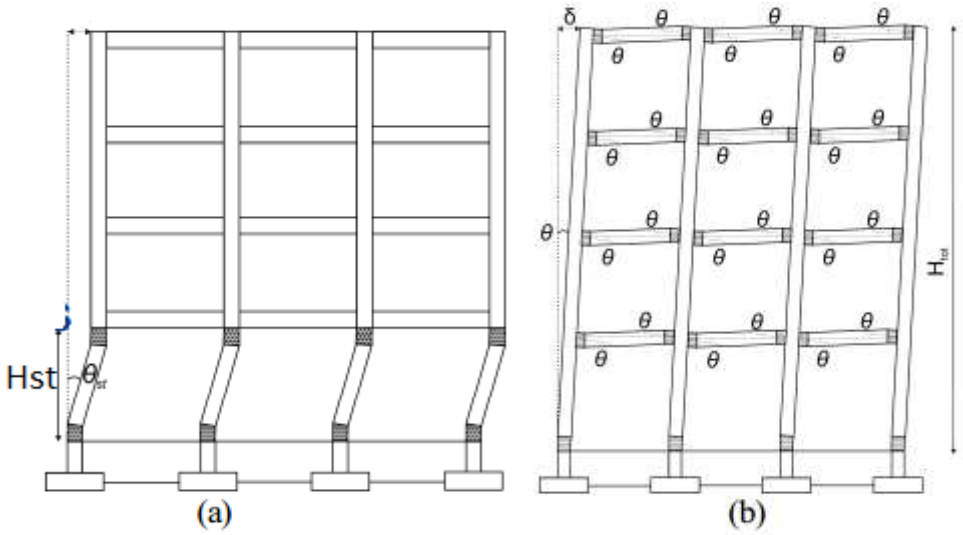

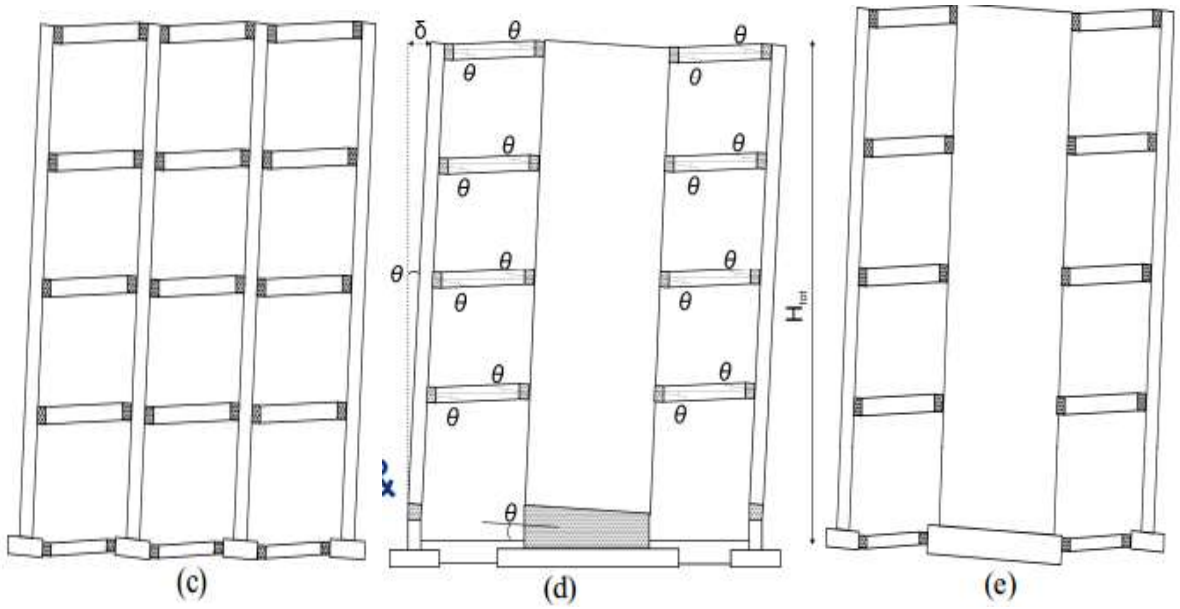

Figure 3.3: (a) soft story mechanism in weak column/strong beam frame, (b,c) beam-sway mechanism in strong column/weak beam frame, (d,e) beam – sway mechanism in wall system (M.N. Fardis 2009).

In capacity design the fulfillment of strong column/weak beam capacity design rule is maintained with over strength factor γ_{Rd} on beam strengths. Sum of column resistances is > 1.3 sum of beam resistances for each node which is stated in equation 3.23.

$$\Sigma M_{RC} \geq \gamma_{RD} \Sigma M_{RB} \quad \text{.....3.23}$$

The recommended value for the overstrength facror in the code is γRd =1.3 for frames and frame equivalent dual system.

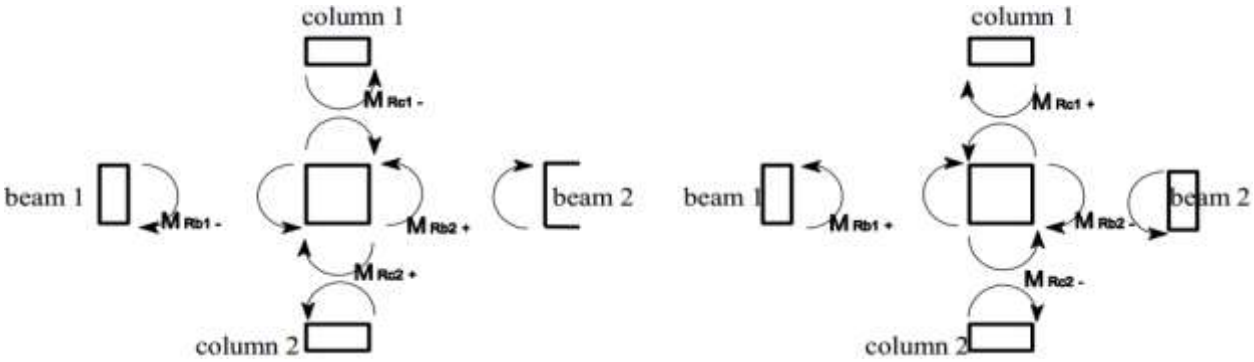

Figure 3.4: Beam and column flexural capacity at a joint in capacity design rule (M.N. Fardis 2009).

3.6.1 Design Action Effects

The design values of bending moments and axial forces are obtained from the analysis of the structure for the seismic design situation by considering second order effects when it was found necessary. The design values of shear forces of primary seismic beams, columns, are determined as follows.

1. **Beams**

The design shear forces for beams are determined in accordance with the capacity design rule, on the basis of the equilibrium of the beam and this is implemented in the current version of ETABS used for this research (CSI Concrete frame design manual 2017).

a) The transverse load acting on it in the seismic design situation and

b) End moments Mi,d (with i=1,2 denoting the end sections of the beam), corresponding to plastic hinge formation for positive and negative directions of seismic loading. The plastic hinges should be taken to form at the ends of the beams or (if they form there first) in the vertical elements connected to the joints into which the beam ends frame.

$$M_{i,d}=\gamma_{RD*}M_{Rb,I*}\min\left(1,\frac{\sum Mrc}{\sum Mrb}\right) \quad \text{.....3.24}$$

where

γ_{Rd} is the factor accounting for possible over strength due to steel strain hardening, which in the case of DCM beams may be taken as being equal to 1.0;

$M_{Rb,I}$ is the design value of the beam moment of resistance at end i in the sense of the seismic bending moment under the considered sense of the seismic action;

ΣM_{Rc} and ΣM_{Rb} are the sum of the design values of the moments of resistance of the columns and the sum of the design values of the moments of resistance of the beams framing into the joint, respectively. The value of ΣMRc should correspond to the column axial force(s) in the seismic design situation for the considered sense of the seismic action.

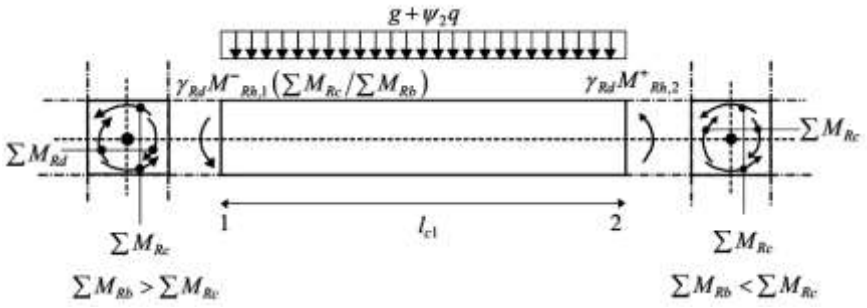

Figure 3.5: Capacity Design Shear Force for beams

2. Columns

In primary seismic columns the design values of shear forces shall be determined in accordance with the capacity design rule, on the basis of the equilibrium of the column under end moments Mi,d (with i=1,2 denoting the end sections of the column), corresponding to plastic hinge formation for positive and negative directions of seismic loading. The plastic hinges should be taken to form at the ends of the beams connected to the joints into which the column end frames, or (if they form there first) in the columns. End moments Mi,d may be determined from the following expression:

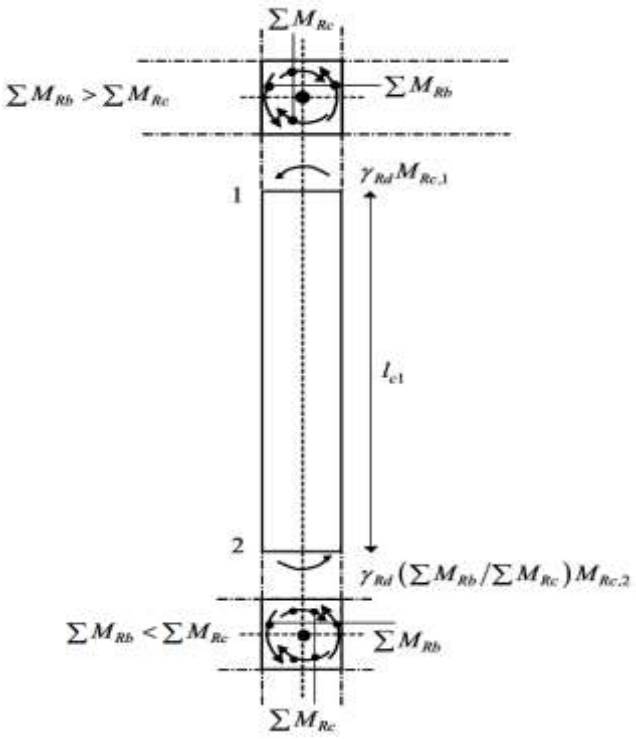

Figure 3.6: Capacity Design Shear Force for columns

$$M_{i,d} = \gamma_{RD} * M_{Rc,I} * \min\left(1, \frac{\sum Mrb}{\sum Mrc}\right) \ldots\ldots\ldots\ldots\ldots\ldots\ldots\ldots\ldots\ldots\ldots\ldots\ldots\ldots\ldots\ldots\ldots\ldots 3.25$$

Where;

γ_{Rd} is the factor accounting for over strength due to steel strain hardening and confinement of the concrete of the compression zone of the section, taken as being equal to 1.1 for DCM;

$M_{Rc,i}$ is the design value of the column moment of resistance at end i in the sense of the seismic bending moment under the considered sense of the seismic action;

ΣM_{Rc} and ΣM_{Rb} are as defined above.

To ensure local and global ductility of the structure, (ES EN 1998:1-2015) considers the following calculation rules for real capacity given in Eq. 3.23.

It should be prevented the formation of brittle failure mechanisms or mechanisms undesirable, such as shear failure of resistant elements or concentration of plastic hinges in columns of a single story. To this end, design values should be obtained by equilibrium conditions considering resistant values at adjacent sections and a γ_{RD} factor whose value varies from element to element and the ductility class of the structure. Eq. (3.26) should be checked for all nodes between primary or secondary beams and primary columns of frame systems or frame equivalent systems with two or more floors. The condition must be checked in two orthogonal planes of flexion for both senses of the action.

To calculate the bending moment resistant of beams the slab reinforcement parallel to the beams located in effective width of the flange should be considered.

$$\Sigma M_{RC} \geq 1.3 \Sigma M_{RB} \ldots\ldots\ldots\ldots\ldots\ldots\ldots\ldots\ldots\ldots\ldots\ldots\ldots\ldots\ldots\ldots\ldots\ldots\ldots\ldots\ldots\ldots\ldots\ldots 3.26$$

ΣM_{RC} sum of resistant bending moments of columns connected to node.

ΣM_{RB} sum of resistant bending moments of beams connected to node.

3.7 Design Outputs

In the design of the buildings the following have been checked and kept in the required limit as per (ES EN 1998:1-2015) design code.

1. Damage limitation, under the damage limitation earthquake (50% of design seismic action), using 50% of uncracked gross section stiffness is checked for all models.
2. For (ULS) verifications, interstory drift has been checked and Member verification for the ultimate limit state (ULS) in bending under the design seismic action with elastic spectrum reduced by the behavior factor q are checked during moment curvature analysis in chapter four of this paper.
3. In frames fulfillment of strong column / weak beam capacity design rule, with over strength factor greater than 1.3 and sample column to beam capacity ratios from DCH 10 favorable models are shown in Appendix C of this paper.
4. Capacity design of members and joints in shear is done using the outputs from ETABS vs 2016.2.1
5. Detailing rules of each ductility classes, detailing of plastic hinge regions, on the basis of the value of the curvature ductility factor that corresponds to different ductility classes are evaluated and the sample evaluations are presented in Appendix D of this paper.

CHAPTER 4 NON-LINEAR ANALYSIS AND EVALUATION OF BEHAVIOR FACTOR

In this chapter, modeling and generation of nonlinear hinge properties, types of hysteresis models, procedures of the nonlinear analysis techniques used for this research, verification of the software using experimental results. In addition, parametric study on behavior factor, the summery of the results of each models used in this study and seismic performance comparison of structures designed for different ductility classes are discussed in detail.

4.1. Modeling of Nonlinear Plastic Hinges

In this section, the details of how material nonlinearity was accounted in ETABS models is presented. First, the options of modeling nonlinearity and the reason for the chosen method implemented in the final models are discussed. The models used to create nonlinear moment-curvature relationships for the members that were expected to be in the plastic range are presented next. Structural damage limit states typically defined in performance-based design for reinforced concrete structures built in areas of high seismic hazard are described and used to create idealized moment-curvature curves. Finally, the actual properties of the nonlinear plastic hinges used in the structural models are summarized.

4.2. Background of Modeling Material Nonlinearity in ETABS

The background of how the version of ETABS used for this thesis allows modeling of material nonlinearity is described in this section, including the relevant limitations and requirements. In ETABS, material nonlinearity can be modeled by link elements or discrete, lumped plasticity hinges (CSI Reference Manual, 2017). Link elements are additional members added to the structure that must be independently defined from the structure's frame and area elements. They are suitable for modeling base isolation and supplemental damping, in addition, links can provide nonlinearity in multiple degrees of freedom using just a single element. Hinges, on the other hand, are better suited for static nonlinear (pushover) analysis because the hinges can be modeled with strength loss and hinge state at each step of analysis can be observed graphically. Link elements should be modeled with monotonically increasing force-deformation response,

which cannot be graphically observed. Additionally, the distribution of plasticity can be easily modeled through the application of multiple hinges along the member's length.

For this thesis, the chosen method to model nonlinearity is through discrete flexural plastic hinges because it is commonly used in academia and practical design. The modeling of link elements would take a substantial amount of additional time, and for the purposes of the analyses performed, it was determined that hinges were adequate and more efficient to model. In addition, because the hinge state can be plotted and viewed graphically, which the latter cannot be done for link elements, modeling hinges provides an advantage with valuable insight into the structure's response to loading.

The types of hinges that can be applied to frame members include uncoupled moment, torsion, axial, shear and coupled axial with moment interaction (PMM) hinges. The degrees of freedom that are not assigned as a hinge remain elastic. Any combination of the different types of hinges can be applied at the same location, and any number of discrete hinges can be used to distribute plasticity along a member, if desired. However, modeling several hinges greatly increases the computational cost and thus increases analysis run-time, so it is not always appropriate to use several hinges on each member if the structural model is large (Bolander, Julie Christine, 2014). In the case of the structures under investigation in this thesis, very large models with many elements and several nonlinear analyses were performed, so the minimum number of hinges was used to model plasticity.

The location of a hinge is specified as a relative distance along the member, chosen by the user. It is important to ensure that the location of the hinges is representative of where the moment demands are greatest so that the hinges will be activated appropriately and the structure will perform as expected and realistically. To be consistent with the intended first-mode, strong-column weak-beam hinge mechanism. Plastic hinges were assigned at the ground level for columns and at each end (i.e. beam-column faces) of all beams. Since everything below grade is expected to remain elastic, hinges are not modeled beneath the ground level.

Hinge properties can be determined using the default ETABS hinges, or they can be completely user-defined. The default hinge properties in ETABS are based on (FEMA 356, 1997) guidelines, which are material-dependent. Since the hinges are also dependent on the cross-section properties of the element it is assigned to, the properties cannot be viewed until after the hinge is applied to an element and becomes a "generated" hinge. Also, once generated, the

hinge properties cannot be modified. Thus, in order for the program to automatically define the hinge properties, the user must make sure the section is correctly modeled, including all steel reinforcing and material properties. However, the version of ETABS used does not have the ability to account for the difference between confined and unconfined concrete regions because hoop/tie transverse reinforcing cannot be modeled analytically. Thus, the generated hinge properties based on the default FEMA guidelines are not accurate for reinforced concrete sections that are designed to provide ductility through adequate confinement.

User-defined hinge properties can also be used and are based on plastic force displacement (F-D), for axial and shear degrees of freedom, or moment-rotation (M-θ), for bending and torsion moment degrees of freedom, relationships. User-defined properties can be based on the default FEMA properties and modified, or they can be fully user-defined. Fully user-defined properties allow for symmetric F-D/ M-θ backbone curves, or the curves can be different in the negative and positive directions. To define the plastic deformation curve, several points must be input into ETABS. Figure 4.1 (a) shows the points on the plastic deformation curve and while the shape shown is typically used for pushover analysis, any shape can be defined as long as they comply with the following point definitions.

Point A is always the origin and cannot be changed. From Point A to Point B, all deformation is linear and occurs inside the frame element. Point B represents yielding, but in the ETABS version used, the hinges are rigid-plastic, so the deformation at B is always defined as zero, as shown in Figure 4.1 (b). Thus, no deformation occurs in the hinge up to Point B and only plastic deformation beyond B will be exhibited by the hinge. For a typical pushover analysis, Point C should be defined as ultimate capacity and Point D represents residual strength. For other purposes, a positive slope can be defined from C to D and/ or D to E. For any shape of backbone curve, Point E represents total failure. Beyond E, the hinge will drop the load to zero force/ moment as shown in the figure 4.1. Additionally, the moment-rotation backbone curves were chosen to be symmetric, such that the absolute value of each point coordinate in the negative direction is the same as the positive direction coordinate

In addition to the five points required for defining the plastic deformation backbone curve, the user has the option of specifying the deformation values at the Immediate Occupancy (IO), Life Safety (LS), and Collapse Prevention (CP) levels used for performance-based design. These measures are used only as recorders for obtaining analysis results at the defined points,

and do not affect the structure's behavior. As such, they can be used to measure other points of interest and are not required to be specified.

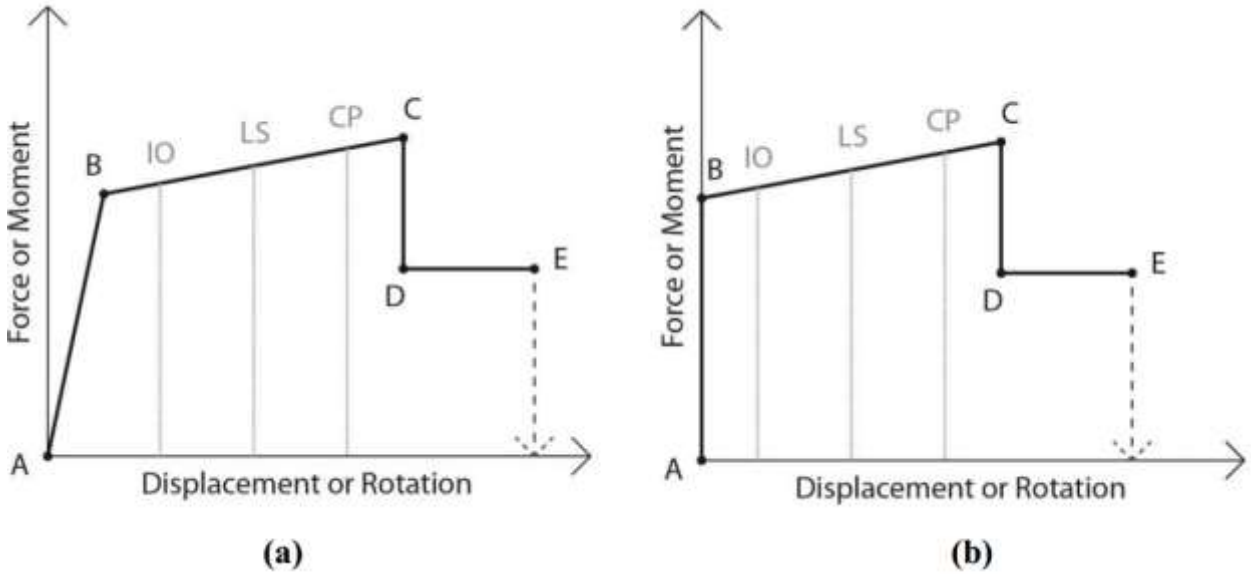

Figure 4.1: a) Plastic deformation backbone curve and b) Actual rigid-plastic deformation curve used for hinges

Fully user-defined hinges were used to model material nonlinearity for the structures under investigation because the default hinges were not able to accurately account for confinement without the transverse steel modeled. Since all hinges intended for use in this thesis are purely flexural hinges, the bending moment-rotation relationships were obtained for each element.

4.3. Moment-Curvature Analysis Models and Generation

The moment-curvature relationships of structural elements are critical to define their hysteresis response and ensure an accurate nonlinear structural analysis of the building. The development of moment-curvature relationships for the structural members is performed on SAP200 Section Designer. The program uses the strain compatibility approach to analyze reinforced concrete sections under constant axial loads and their corresponding moment-curvature relationships are developed through section evaluations under various strain conditions. Section Designer evaluates a reinforced concrete section by representing the actual cross-section by a series of thin layers with the assumption of each layer in the cross-section under uniform stress and strain. As different material properties can be specified to the program, it is crucial to define the material properties for concrete and reinforcing steel. In order to effectively generate

moment curvature relationships using Section Designer, the unconfined concrete, confined concrete and reinforcing steel properties need to be appropriately defined.

Within the seismic design of reinforced concrete members, regions exhibiting potential plastic hinges must be thoroughly detailed for ductility. The adequate ductility of reinforced concrete members is necessary to ensure that effective moment redistribution between members can occur, and most importantly, cyclic loading caused by seismic activity will not cause collapse to the members of the structure. In the design for ductility in plastic hinge regions of reinforced concrete members, the most important design consideration is for the provision of sufficient transverse reinforcement. The presence of transverse reinforcement is crucial in providing confinement to the compressed concrete, thereby preventing the buckling of longitudinal bars as well as preventing failure due to shear. Research conducted on tests developed for reinforced concrete subjected to uniaxial compressive loading and confined by transverse reinforcement has shown that suitable arrangements of transverse reinforcement results in significantly increasing the strength and ductility of concrete (Mander et al., 1988).

4.3.1. Confined Concrete Model

The accurate development of stress-strain behavior for confined concrete is crucial in developing reliable moment-curvature relationships with respect to the available ductility from reinforced concrete members containing transverse reinforcement. As the appropriate stress-strain curves and moment-curvature relationships are established, an element by element behavioral response is acquired in order to appropriately model structural elements with reasonable plastic rotational capacities simulating those exhibited by the members of the actual structure.

4.3.1.1. Mander Confined Concrete Model

In describing the stress-strain relationship of confined concrete, several constitutive models were investigated to appropriately select the determining confined concrete model to be used for structural members throughout the height of the building. Among the constitutive models of confined concrete models made available for analysis in SAP2000, the Mander Confined Concrete Model is used for the purpose of this work. Based on an equation suggested by Popovics (Mander et al., 1988), the proposed stress-strain model for confined and unconfined concrete under monotonic loading is illustrated in Figure 4.2.

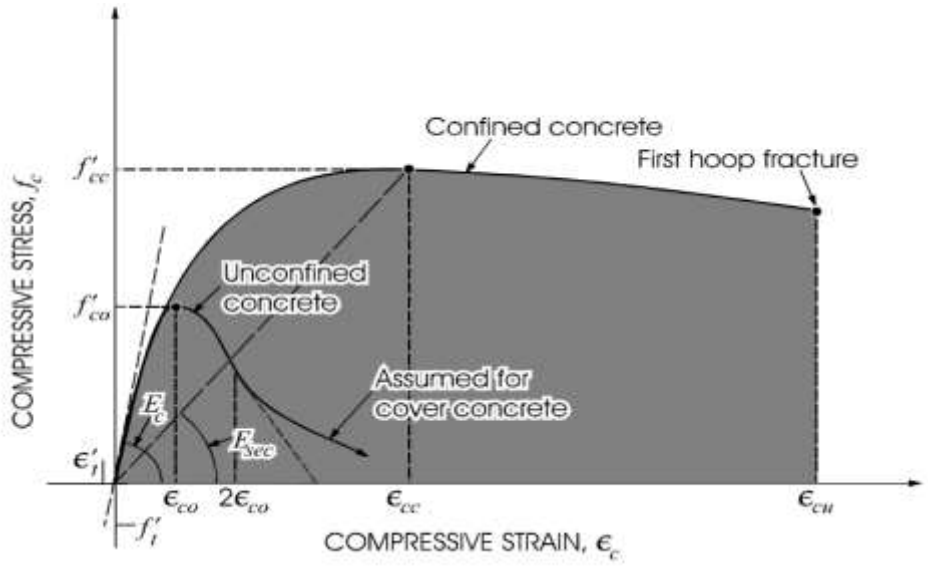

Figure 4.2: Mander Stress-Strain Model (Mander et al., 1988),

4.4. Hysteretic Hinge Behaviour and Models

In a dynamic analysis, hysteresis loops are described by a hysteresis model and its corresponding rules, which define the load reversal paths within the hysteresis loops. These hysteresis loops depend on material properties and reflect the force-deformation characteristics of structural members as they are subjected to cyclic loading. The four hysteretic options available in ETABS 2016 are isotropic, kinematic, Takeda, and pivot. The default option is isotropic hysteresis.The following descriptions of the hysteresis types are based on information from the (CSI Analysis Reference Manual, 2017).

4.4.1. Isotropic Hysteresis Model.

This model is, in a sense, the opposite of the kinematic model. Plastic deformation in one direction “pushes” the curve for the other direction away from it, so that both directions increase in strength simeltaniously.

Unloading and reverse loading occur along a path parallel to the elastic line until the magnitude of the action in the reverse direction equals that of backbone curve at the same amount of deformation in the reverse direction, and then continues along a horizontal secant to the back bone curve.

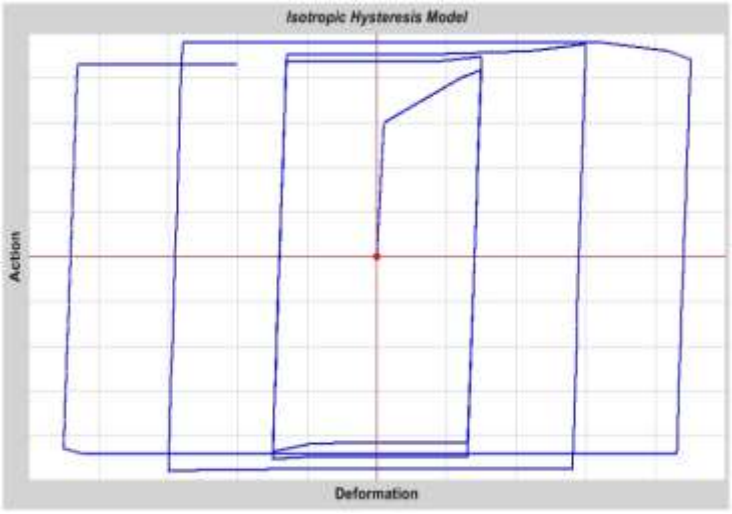

Figure 4.3: Isotropic Hysteresis Model under Increasing Cyclic Load

4.4.2. Kinematic Hysteresis Model.

The Multilinear Kinematic Model, based on the kinematic hardening behavior commonly observed in metals, presents a nonlinear force-deformation relationship under monotonic loading provided by a multilinear curve described by a set of user-defined points, as seen in Figure 4.4.

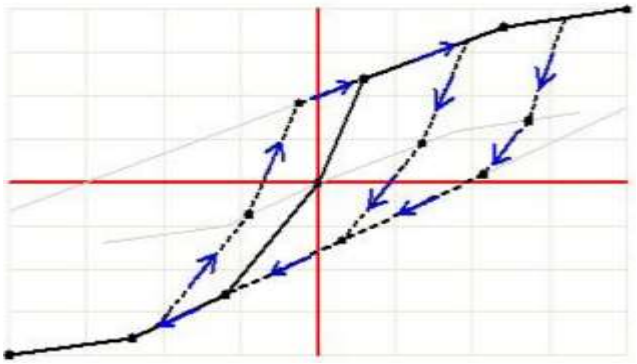

Figure 4.4: Kinematic Plasticity Property Type for Uniaxial Deformation

As shown in the Figure 4.4, the first slope on either side of the origin is elastic and the remaining portions of the curve define plastic deformation. Upon reversals of deformation, the hysteresis path follows the two elastic segments of the curve from either side of the origin before initiating plastic deformation in the reverse direction. Once initiated, plastic deformation in one direction of loading "pulls" with it the curve for the reverse direction of loading.

4.4.3. Takeda Hysteresis Model

The hysteresis model developed by Takeda et al. (1970) is based on the experimental behavioral observation on a number of medium-size reinforced concrete members subjected to lateral load reversals with light to medium amount of axial load. The Takeda model includes stiffness changes at flexural cracking and yielding by using a multilinear skeleton force-deformation relationship.

The Multilinear Takeda Model is identical to the Multilinear Kinematic Model in the specification of properties and portrays close similarities to cyclic load behavior. The distinguishable factor between the two models lies in the Multilinear Takeda Model using a degrading hysteretic loop, as seen in Figure 4.5.

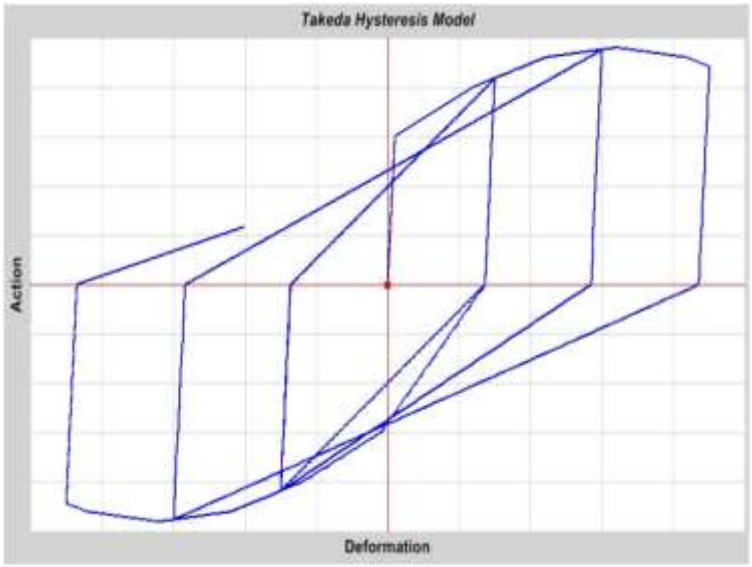

Figure 4.5: Takeda Plasticity Property Type for Uniaxial Deformation

The behavior of the Multilinear Takeda Model differs from that of the Multilinear Kinematic Model particularly in the unloading path, as seen in Figure 4.5. When crossing the horizontal axis, the Multilinear Takeda Model curve follows a secant path to the backbone force deformation relationship upon unloading for the reversed direction.

4.4.4. Pivot Hysteresis Model

This model is similar to the Takeda model, but has additional parameters to control the degrading hysteretic loop. It is particularly well suited for reinforced concrete members, and is based on the observation that unloading and reverse loading tend to be directed toward specific

points, called pivots points, in the action-deformation plane. The most common use of this model is for moment-rotation. This model is fully described in Dowell, Seible, and Wilson (1998).

The Takeda and pivot hysteresis models are commonly used to represent the behavior of reinforced concrete. And hence this hysteresis model is used in this research.

This hysteretic model is based on the unloading and reversed loading paths portraying the tendency to be directed to specific points in the force-deformation plane. These specific points are termed pivot points that are defined according the following:

♦ α1: locates the pivot point for unloading to zero from positive force

♦ α2: locates the pivot point for unloading to zero from negative force

♦ β1: locates the pivot point for reverse loading from zero toward positive force

♦ β2: locates the pivot point for reverse loading from zero toward negative force

♦ η: determines the amount of degradation of the elastic slopes after plastic deformation model

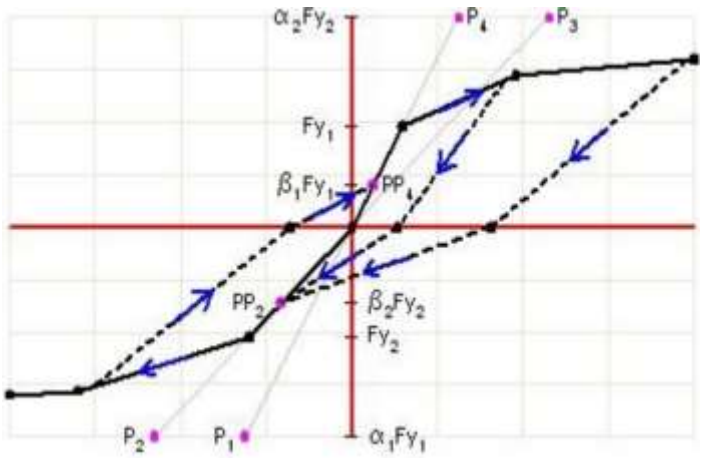

Figure 4.6: Pivot Hysteresis Model Parameters

4.5. Non-linear Analysis and Computation of Behavior Factor

4.5.1. Static Push Over Analysis

Nonlinear static pushover analysis is used to determine the nonlinear behavior of the building structures. In this simplified method, a capacity curve is obtained which shows the relation of base shear and roof displacement. This curve represents the behavior of the building structure under increasing base shear forces. As the capacities of the members of the lateral force resisting system exceed their yield limits during the increasing of the base shear forces, the slope of the force-deformation curve will change, and hence the nonlinear behavior can be represented. Thus, upon the application of pushover load cases, member forces are calculated for each step and the stiffness of the members whose capacities are exceeded is changed according to the hinge properties in the next step of the analysis. This process ends when the structure becomes unstable.

In this research displacement-controlled pushover analysis is used to establish initial conditions and global limit states of the models for nonlinear direct integration time history analysis and it is used to verify and control the outputs of nonlinear direct integration time history analysis.

The following general sequence of steps is involved in performing nonlinear static pushover analysis using ETABS 2016.2.1.

1. Create a model just like you would for any other analysis.

2. Define frame hinge properties and assign them to the frame elements.

3. Define any Load Patterns and static and dynamic Load Cases that may be needed for concrete design of the frame elements, particularly if default hinges are used. But user defined hinge properties are used in this research.

4. Run the Load Cases needed for design.

5. If any concrete hinge properties are based on default values to be computed by the program, you must perform concrete design so that reinforcing steel is determined.

6. Define the Load Patterns that are needed for use in the pushover analysis, including: Gravity loads and other loads that may be acting on the structure before the lateral seismic loads are applied.

7. Define the nonlinear static Load Cases to be used for pushover analysis, including: A sequence of one or more cases that start from zero and apply gravity and other fixed loads using load control. One or more pushover cases that start from this sequence and apply lateral pushover loads. These loads should be applied under displacement control.

The monitored displacement is usually at the top of the structure and will be used to plot the pushover curve.

8. Run the pushover Load Cases.

9. Review the pushover results: Plot the pushover curve, the deflected shape showing the hinge states, and print or display any other results you need.

10. Revise the model as necessary and repeat the steps.

4.5.2. Non-linear Time History Dynamic Analysis Method

Time-history analysis is a step-by-step analysis of the dynamical response of a structure to a specified loading that may vary with time. Time-history analysis is used to determine the dynamic response of a structure to arbitrary loading. The dynamic equilibrium equations to be solved are given by:

$$ku(t) + Cu'(t) + Mu''(t) = r(t) \quad \text{.....4.4}$$

where K is the stiffness matrix; C is the damping matrix; M is the diagonal mass matrix; u, u', and u" are the displacements, velocities, and accelerations of the structure; and r is the applied load.

There are two types nonlinear time history Analysis's

- Non-linear modal time history analysis (FNA).
- Non- linear direct integration time history analysis

4.5.2.1. Non-linear modal time history analysis (FNA)

The Fast-Nonlinear Analysis (FNA) method is extremely efficient, particularly for structural systems which are primarily linear elastic but which have a limited number of predefined nonlinear elements. However, there is no limit on the number of nonlinear elements that can be considered, provided that adequate modes are obtained. This is best done using a sufficient number of Ritz vectors. For the FNA method, all nonlinearity is restricted to the Link/Support elements. This includes hinges that are modeled as Links (CSI Reference Manual, 2017).

4.5.2.2. Non- linear direct integration time history analysis

In this method direct integration of the full equations of motion is done without the use of modal superposition. While modal superposition is usually more accurate and efficient, direct integration does offer the following advantages (CSI Reference Manual, 2017):

• Full damping that couples the modes can be considered

• Impact and wave propagation problems that might excite a large number of modes may be more efficiently solved by direct integration

• All types of nonlinearity can be included in a nonlinear direct integration analysis.

In this research non-linear direct integration time history analysis is chosen because it is better to account all kinds of nonlinearity available ETABS and discrete hinge properties cannot be used for FNA.

In this research incremental direct integration time history analysis is used for construction the capacity curve to determine the behavior factor of each models through continuously scaling up the ground motion until global limits of the models.

Incremental dynamic analysis, also termed dynamic pushover, is a nonlinear time history analysis method that can be utilized to estimate structural capacity under earthquake loading. It provides a continuous picture of the system response, from elasticity to yielding and finally to collapse. Several nonlinear time history analyses are undertaken and the response from these analyses is plotted. The resulting plots, termed IDA (Incremental Dynamic Analysis) plots, give an indication of the system performance at all levels of excitation in a manner similar to the load displacement curve from static pushover.

The following general sequence of steps is involved in performing incremental nonlinear dynamic time history analysis using ETABS 2016.2.1.

1. Create a model just like you would for any other analysis.
2. Define frame hinge properties and assign them to the frame elements.
3. Define any Load Patterns and static and dynamic Load Cases that may be needed for concrete design of the frame elements, particularly if default hinges are used. But user defined hinge properties are used in this research.
4. Run the Load Cases needed for design.
5. If any concrete hinge properties are based on default values to be computed by the program, you must perform concrete design so that reinforcing steel is determined.
6. Define the Load Patterns that are needed for use in nonlinear direct integration time history analysis.
7. Conduct a nonlinear time history analysis of a structure for specific acceleration record by using the lowest intensity scaling factor and get maximum roof displacement and corresponding base shear. This gives one point on IDA plot.
8. Increase the intensity of the scaling factor for the ground motion and repeat this iteration process until creating enough points on the IDA plot to give a complete spectrum of structural response. The scale factors have to be selected so as to have a continuous smooth capacity curve.
9. Stop the analysis when the base shear value drops below the ultimate limit state and construct the capacity curve that is used to compute behavior factor, using the results of the load cases used in the analysis.

4.5.3. Ground Motions and Analysis Parameters

Ethiopia exists in seismicity area and has been prone to many damaging earthquakes in the past. But it is known that, not enough ground motion records from previous earthquakes are available which can be suitable for the use of this research. Thus, matched ground motions of the time history curves available in ETABS are used for the incremental nonlinear direct integration time history analysis.

Three matched ground motions Elcentro, Holiste and LACC-NOR are selected to generate the capacity curves which are used to compute behavior factor. The response spectrum and matched time history curves are shown in following figures.

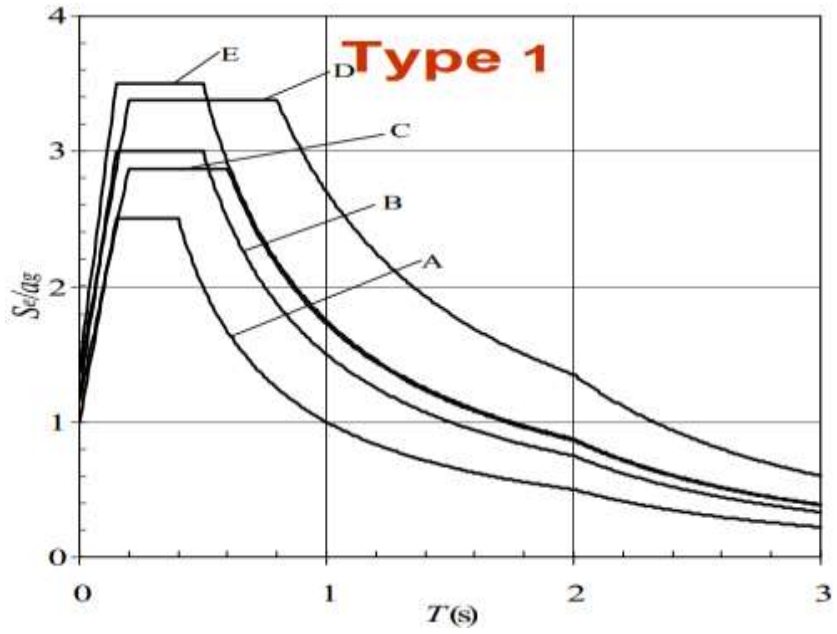

Figure 4.7: Recommended horizontal elastic spectra for the standard ground (5% damping)

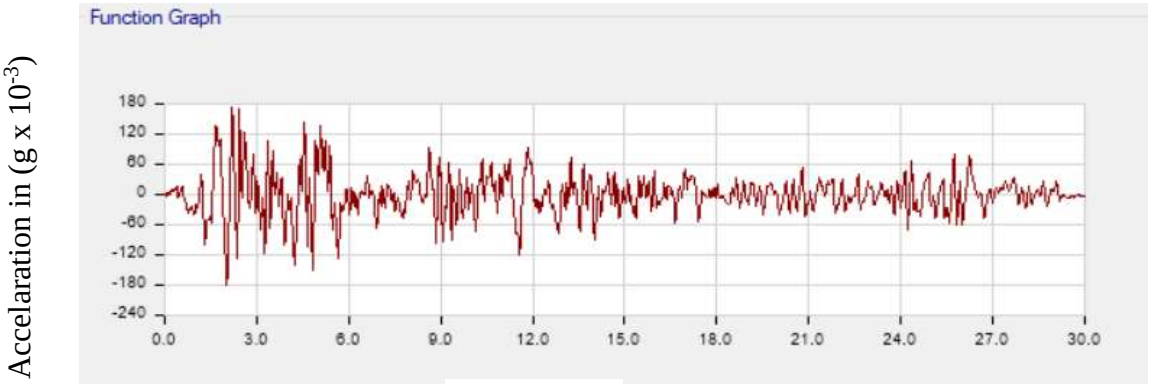

Figure 4.8: Matched Elcentro ground motion

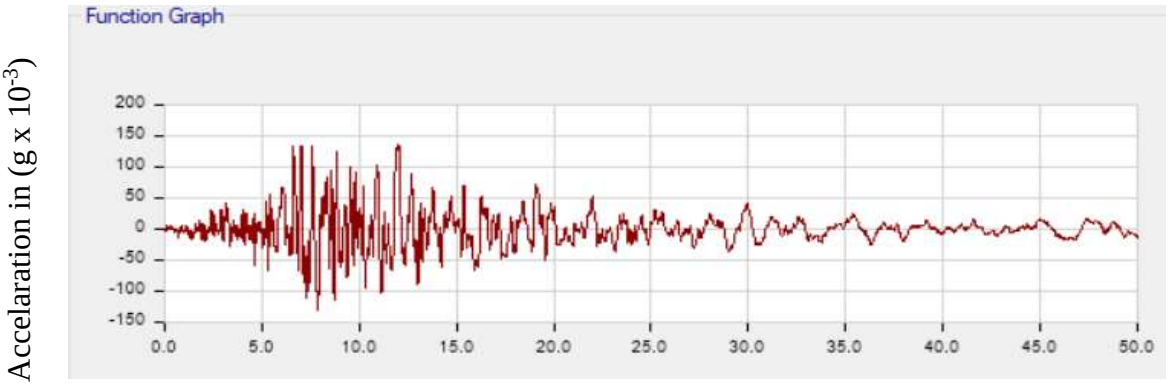

Figure 4.9: Matched Holiste ground motion

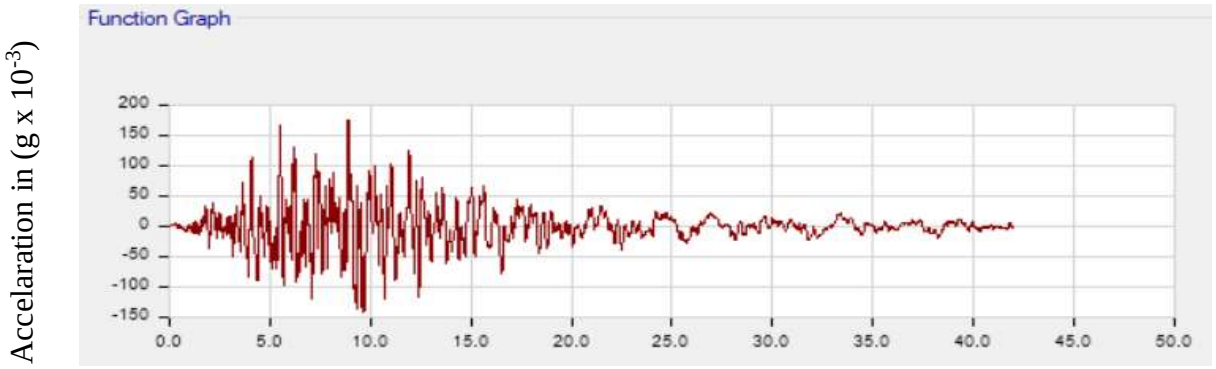

Figure 4.10: Matched LACC-NOR ground motion.

4.6. Verification of ETABS for Non-linear Analysis using Experimental Results

The experimental frame was developed and tested by *Vecchio and Emara (1992)* and the frame was loaded to a lateral displacement of 155 mm and then unloaded to a net lateral load of zero (Serhan Guner, 2010). The loading, geometry and cross-sectional detail of the frame as used in the experiment is shown in figure 4.11 below.

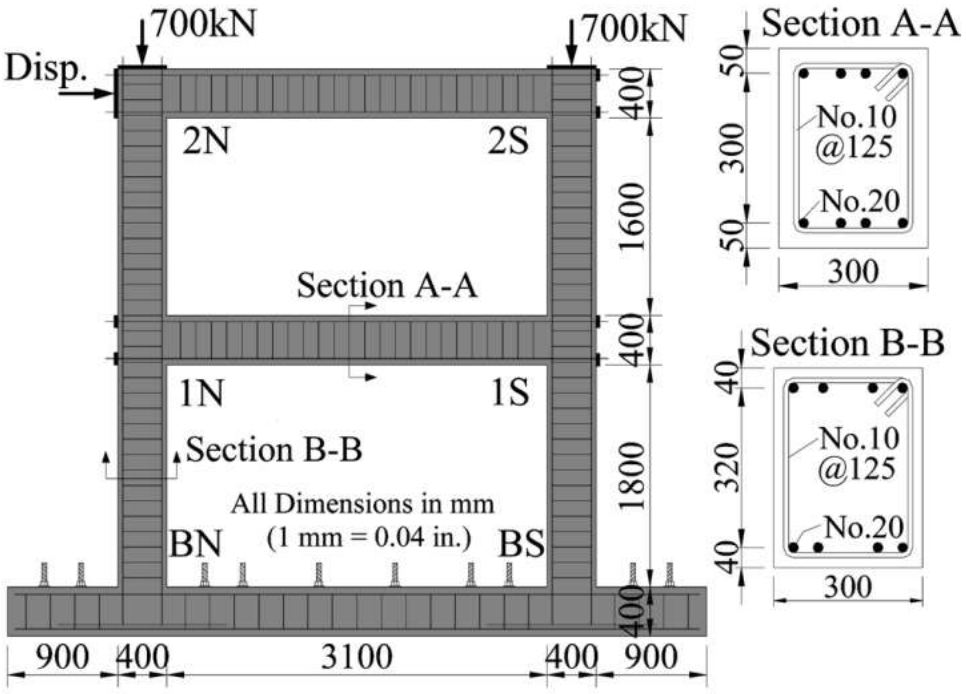

Figure 4.11: Structural details of Vecchio and Emara (1992) frame.

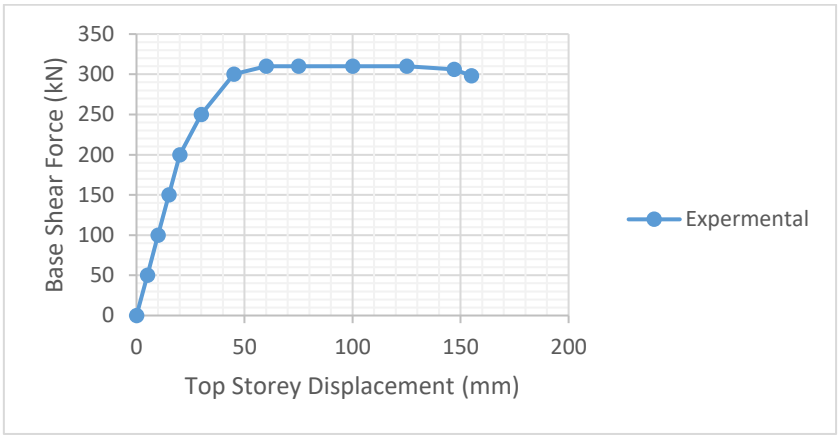

Figure 4.12: Experimental capacity curve

4.6.1. Moment Curvature Data for Beam and Column Sections of The Experimental Frame

The moment curvature of the sections was done using SAP2000 section designer.

Table 4.1: Moment curvature relation for beam

	Point	M	Ɵ	m/sf	Ɵ/sf
Beam	A	0	0.0000	0.000	0.000
	B	152.1	0.0010	1.000	0.000
	C	216.2	0.0373	1.421	0.036
	D	30.42	0.0373	0.200	0.036
	E	30.42	0.0746	0.200	0.074

Table 4.2: Moment curvature relation for Column

	Point	M	Ɵ	m/sf	Ɵ/sf
Column	A	0	0.0000	0.000	0.000
	B	235.5	0.0021	1.000	0.000
	C	236.5	0.0270	1.004	0.037
	D	47.1	0.0270	0.200	0.037
	E	47.1	0.0541	0.200	0.078

Pushover analysis and incremental nonlinear time history analysis using Elcentro ground motion were performed in ETABS Vs 16.2.1 by modelling the experimental frame with the default hinge (DH) and using user defined Hinge (UDH). And the results of analysis's are as shown in the figures and tables below. In user defined hinges the curve is generated using SAP 2000 section designer and the type of hysteresis used in this research is pivot hysteresis model as discussed in the previous sections.

4.6.2. Comparison of Experimental and Analytical Results

Push over (UDH)	
Dis Placement (mm)	Base Shear (kN)
0.001	0
18.909	208.760
27.852	263.078
37.296	286.716
58.358	303.562
91.296	312.541
142.449	321.008

Push over (DH)	
Dis Placement (mm)	Base Shear (kN)
0.001	0
20.001	220.8207
22.348	246.7354
32.997	306.6056
33.728	307.9561
53.728	318.1368
70.304	326.6784
70.301	261.6477

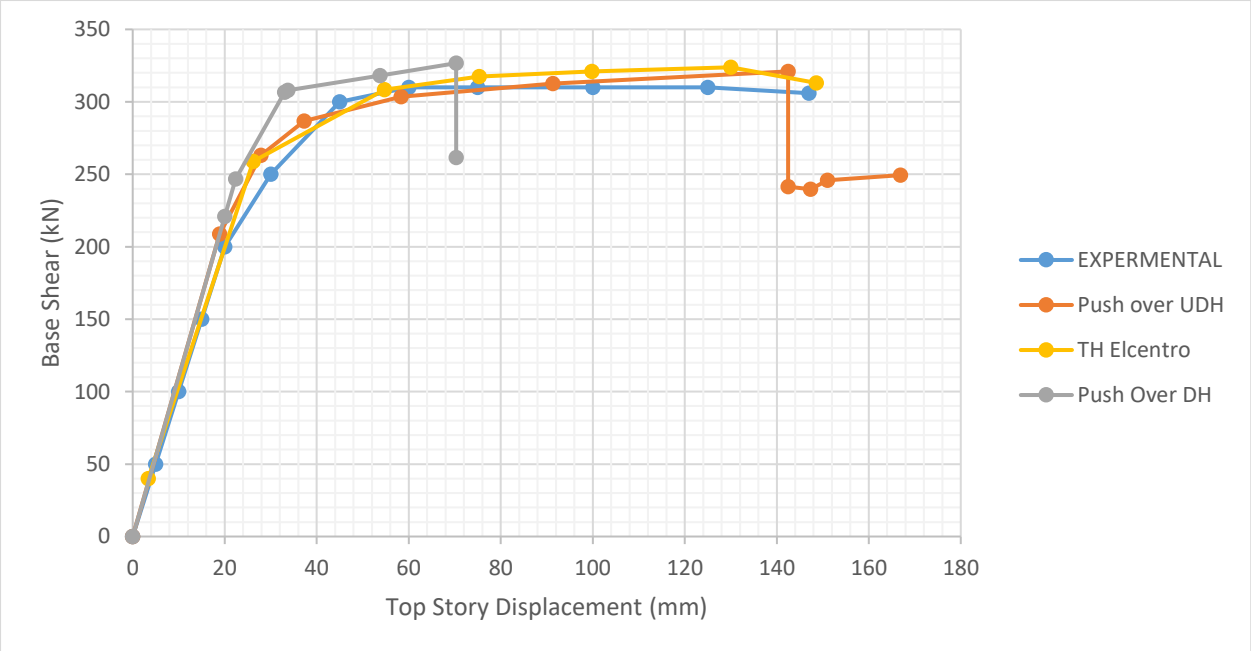

Figure 4.13: Capacity curves of Experimental, push over and time history analysis

Table 4.3: Comparison of experimental and ETABS VS 16.2.1 Analytical Outputs.

	Experimental	Push over (DH)	Push over (UDH)	TH Elcentro
Max Base shear (kN)	310	326	321	323.84
Max Top displacement (mm)	147	70.3	142.45	148.6

As we can see from the above results when user defined hinge properties are properly used, the variation of between experimental and ETABS VS 16.2.1 Analytical outputs were small enough but the use of default hinge properties of the software can't consider the effect of confinement of stirrups properly. Thus, when default hinges are used, the deformation capacity of the frame is undermined as compared to the experimental outputs. Generally, the results of the software with user defined hinges were found to be acceptable. And thus, this software with user defined hinges is used for all nonlinear Analysis conducted in this thesis.

4.7. Calculation of Behavior Factor from Non-linear Analysis

In the force based seismic design, the force is extracted from spectra based on linear behavior together with the use of a reduction factor that modifies the linear system to an equivalent one to account approximately for the nonlinear effects. This force reduction factor or response modification factor (often called q-factor or R-factor) has an important role in the estimation of design force of a structure. Its value depends on the parameters that directly affect the energy dissipation capacity of the structure: ductility, added viscous damping and strength reserves coming from its redundancy and the over strength of individual members. An appropriate definition of the R-factor is based on a ductility dependent component, an over strength-dependent component, and a redundant dependent component as shown in Figure.

$$q = \frac{Ve}{Vd} = \frac{Ve}{Vy}\,\frac{Vy}{V1}\,\frac{V1}{Vd} = R\mu\ R\rho\ R\Omega = R\mu \mathrm{Rs} \quad \ldots\ldots 4.5$$

Where, Ve, Vy, V1 and Vd correspond to the structure's elastic response strength, the idealized yield strength, the first significant yield strength and design base shear (design strength), respectively. RS is an overall over-strength factor defined as the ratio between the real lateral strength of the structure and the design lateral strength. The ductility factor Rμ is the ratio of

the elastic base shear to the real lateral strength of the structure. This ductility factor is a measure of the global inelastic response of the structure and is expressed as a function of the displacement ductility.

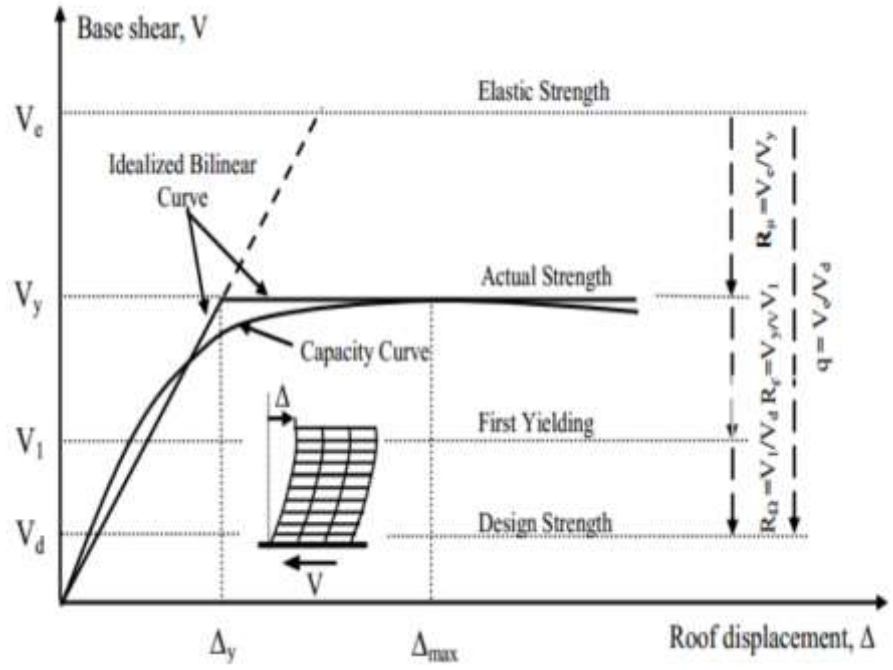

Figure 4.14: Capacity curve of a structure

In the case of using pushover analysis the relation expressing the global behavior of the structure is the capacity curve, which is a base shear versus roof displacement relation obtained under monotonic increasing lateral loads. The force-displacement response curve obtained from pushover analysis is generally idealized by a bilinear elastic–perfectly plastic response curve, as shown Figure 4-14.

Ductility Factor

Ductility of a structure, or its members, is the capacity to undergo large inelastic deformations without significant loss of strength or stiffness. Ductility is a very important property, especially when the structure is subjected to seismic loads. High ductility allows a structure to undergo large deformations before it collapses resulting in the dissipation of large amount of energy. It is represented by the ratio of maximum absolute displacement to its idealized yield displacement expressed as follows.

$$R\mu = \frac{\Delta max}{\Delta y} \quad \text{.....4.6}$$

Where, Rμ is the ductility factor, Δu (△max) is the ultimate deformation at failure and Δy is the yield deformation. Yield deformation is obtained from idealized bilinear pushover curve. It can be expressed in terms of displacements, rotations (for members) and curvatures (for members).

Over strength Factor:

The structure has finally reached its strength and deformation capacity. The additional strength beyond the design strength is called the over strength. Most structures display considerable over strength. Sequential yielding of critical regions, material over strength, strain hardening, capacity reduction factors are the sources of over strength (Ω).

$$R\Omega = \frac{V1}{Vd} \quad \text{.....4.7}$$

Where, V_1 first significant yield strength and Vd is the design base shear.

Redundancy Factor

Redundant is usually defined as exceeding what is necessary or naturally excessive. Building should have a high degree of redundancy for seismic load resistance. More redundancy in the structure leads to increased level of energy dissipation and more over strength. Generally, over strength, redundancy and ductility together contribute to act that an earthquake resistant structure can be designed for much lower force than is implied by the strong shaking

$$Rp = \frac{Vy}{V1} \quad \text{.....4.8}$$

Generally, from above expression the relation of both the formula proposed by American codes and in Euro-code 8 is shown as equation 4.9

$$q = R = q_o \frac{\alpha u}{\alpha 1} = R\mu\, R\rho\, R\Omega = R\mu\, Rs \quad \text{.....4.9}$$

where, $R_\rho = \alpha u/\alpha 1$ is the redundancy factor

Rs= $R\rho\, R\Omega$ is overstrength factor including redundancy and

q_o = Rμ RΩ is the basic behavior factor.

4.8. Failure Mechanism

Under the application of Time history loads the members in a structure initially remain elastic up to a certain moment that is the maximum moment of resistance of a fully yielded section. Any further increase of moment will cause the beam to rotate with little increase in load. The rotation occurs at that particular moment. So, these expected locations of damage caused by a yielded zone having large inelastic rotation capacity at constant restraining moment are called plastic hinges. The combination of inelastic hinges at the ends of beams and columns which formed in a frame eventually makes it unstable and causes its collapse, hence called collapse mechanism.

Structural performance limits:

The performance levels are defined based on the structure type and its intended functions. According to, (ATC-40, 1996) the performance limits can be grouped into two categories: global/structural limits and local/element/component limits.

The global limits typically include requirements for the vertical load capacity, lateral load resistance and lateral drift. For example, the various performance levels in (ATC-40, 1996) are specified in terms of the maximum inter-story drift ratio as shown (Table 4-4).

Table 4.4: Deformation limits for different performance levels, as per ATC-40

Performance level				
	Immediate Occupancy	Damage Control	Life safety	Structural Stability
Maximum inter-story drift ratio	0.01	0.01-0.02	0.02	$0.33V_i/P_i$

Among these performance levels, the Structural Stability level corresponds to the ultimate limit state of the frame, which can be used for obtaining q for a selected frame. The maximum total inter-story drift ratio in the i^{th} story should not exceed 0.33Vi/Pi,

Where,

Vi - is the total lateral shear force demand in the i^{th} story and

Pi -is the total gravity load acting at that story.

The local performance levels are typically defined based on the displacement, rotation or curvature responses of different elements (beams, columns, shear walls, floors, etc.). The limits on the response of structural elements, such as beams and columns, are many times governed by non-structural and component damages as well. For example, the 'local' deformation limits specified by (ATC-40, 1996) in terms of plastic hinge rotations of beam elements and column elements for reinforced concrete frame see in Table (4.-5 and 4-6) respectively.

Table 4.5: Plastic rotation limits for RC beams controlled by flexure, as per FEMA356

$\frac{p_{top}-p_{bot}}{p_{bal}}$	Transverse Reinforcement	$\frac{V}{b_w d\sqrt{f'c}}$	Immediate Occupancy (IO)	Life Safety (LS)	Collapse Prevention (CP)
≤ 0	C	≤ 3	0.005	0.02	0.025
≤ 0	C	≥ 6	0.005	0.01	0.02
≥ 0.5	C	≤ 3	0.005	0.01	0.02

C indicates transverse reinforcement meets the criteria for ductile detailing.

Table 4.6: Plastic rotation limits for RC columns controlled by flexure, as per FEMA356

$\frac{N}{Af'c}$	Transverse Reinforcement	$\frac{V}{b_w d\sqrt{f'c}}$	Immediate Occupancy (IO)	Life Safety (LS)	Collapse Prevention (CP)
≥ 0.4	C	≤ 3	0.003	0.012	0.015
≥ 0.4	C	≥ 6	0.003	0.01	0.012

C indicates transverse reinforcement meets the criteria for ductile detailing.

These limits are for flexural failures of an element. Therefore, to use these limits, one should ensure that the failure of a member (structure) is governed by flexural demands, and shear failure, does not take place before these rotational limits are reached. The shear detailing provisions specified in Euro code 2 ensures that shear failure does not initiate before the formation of flexural plastic hinges at member ends. On the basis of this background information, it is decided to consider an ultimate limit state based on flexural failure at both local and global levels in this paper.

The mode of failure in the form of sequence, location of hinge and number of plastic hinges in as the time history load is scaled up in sequence was done and the formation of hinges confirms the capacity design.

4.9. The Performance Limit States of The Structure

As mentioned earlier in Sect 4.8 two performance limits are considered in nonlinear analysis. The first one corresponds to structural stability limit. This limit state is defined at global structure (in terms of lateral load resistance) as well as at the story level (in terms of the maximum inter-story-drift ratio). The second limit is based on plastic hinge rotation capacities that are obtained for each member depending on its cross-sectional geometry.

4.9.1. Story Drift

Figure 15 and figure 16 shows inter story drift ratio for 10 story models at the collapse point. From this information, one can know which model has maximum inter story drift ratio and which model has best performance in terms of story drift. The expected performance level of a given structure is evaluated by comparing the drift of the frame with the limit drift as shown in the tables below.

Therefore, it is important to accurately quantify the story drift in order to have a clear image of the damage on the frames and the performance level of the frames.

Inter-story drifts ratio: Inter-story drift ratio is defined as the ratio of relative horizontal displacement of two adjacent floors and corresponding story height (h).

Inter-story drift ratio (IDR) $= \Delta / h = (\Delta_i - \Delta_{i-1}) / h$ Where, Δi = displacement at i th story and h = each story height.

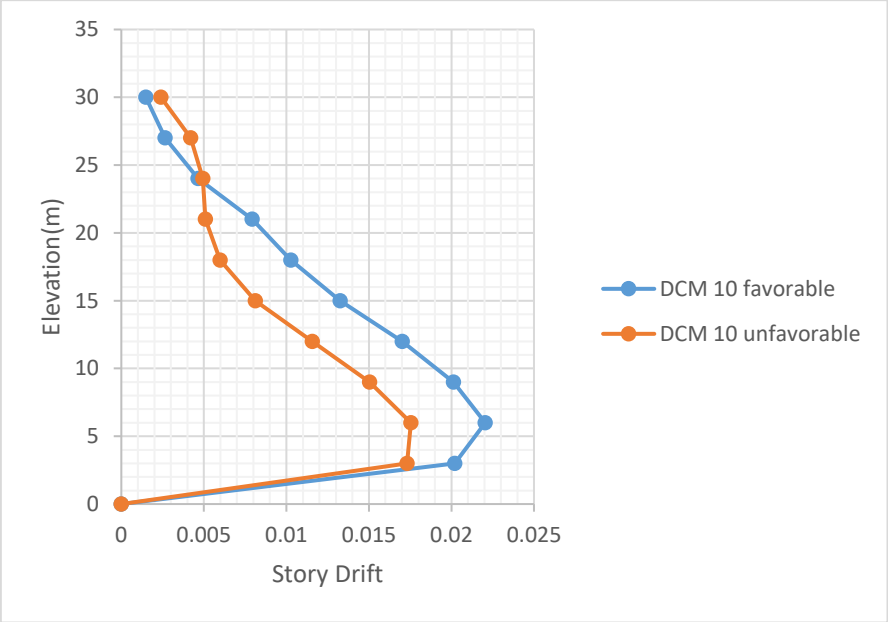

Figure 4.15: Maximum IDR for DCM10 favorable and unfavorable models

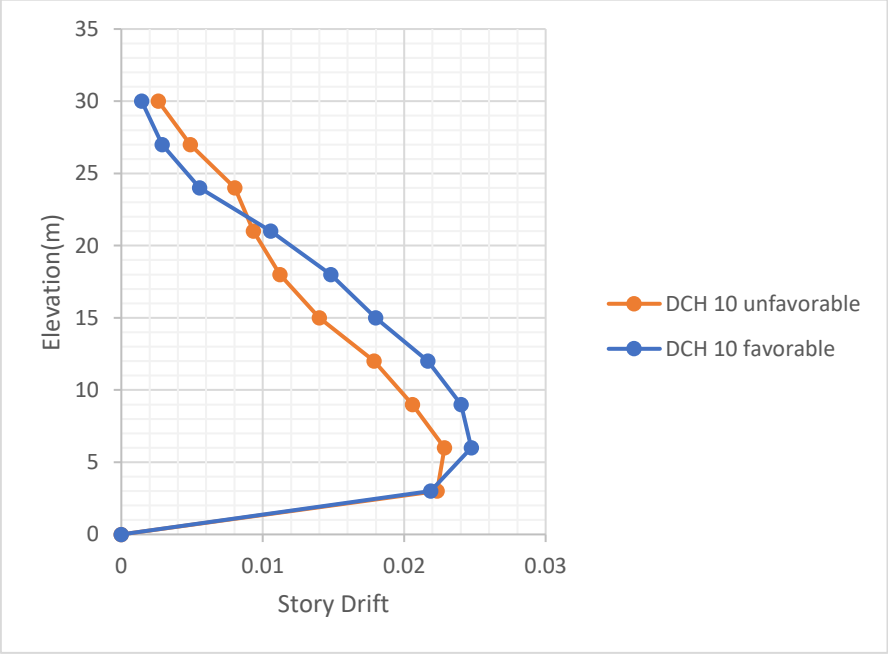

Figure 4.16: Maximum IDR for DCH10 favorable and unfavorable models

4.10. Parametric Study on Behavior Factor

Behavior factor is affected by a number of factors related to the structural configuration (geometry), the soil type on which the structure is supported, ductility class, the input excitation and the final member sections and reinforcements used by the designer. In this research the

most know and critical factors that affect the behavior factor are investigated. These are peak ground acceleration, soil type and story height. In order to explore the effects of variation of this parameter on the behavior factor, a parametric study was conducted and summarized below. To minimize the effect of other factors related to the design, it is used the optimized design sections respecting all the requirements of capacity design and detailing rules under the pain of obtaining the final sections for all models.

4.10.1. Parameters Description

Buildings are analyzed and designed by varying parameters i.e., story height (number of story), input excitation (peak ground acceleration) and soil types to see the effect of the variables on the behavior factor. Table 4-7 shows the parameters which were varied along with their range of values.

Table 4.7: parameters and models used in the parametric study

Parameters	peak ground acceleration (a_g m/s^2)	story height (m)	soil type
Ranges	0.10	5 story	A
	0.15	10 story	B
	0.20	15 story	C

In this section, a total of nine models were subjected to nonlinear analysis to examine the effects of variation of different parameters on behavior factor and to draw comparison. The models are selected to be two dimensional and analyzed using nonlinear static push over analysis so as to minimize the total runtime and as this is used only to identify unfavorable conditions for three dimensional models. The design results of these 2D models are taken from 3D linear static models and the ductility class of the models were selected to be medium ductility. And in the study of each parameters, other parameters are fixed to be constant so as to easily notice the independent effects of each parameters on behavior factor. Accordingly, a 10-story model on ground type A is subjected to different ground excitation and the result is provided on figure 4.17. Similarly, a 10-story model is subjected to ground acceleration a_g = 0.15, under different ground type to see the effect of the soil and the result is shown on figure 4.18. Ground type A and ground acceleration a_g = 0.15 are used to study the story height variations on the behavior factor and the result is provided on figure 4.18.

4.10.2. Analysis and Results

As it was done for other models' stability and drift requirements the code was checked and the hinge properties of the models which are based on the design results of the frames were calculated using SAP 2000.

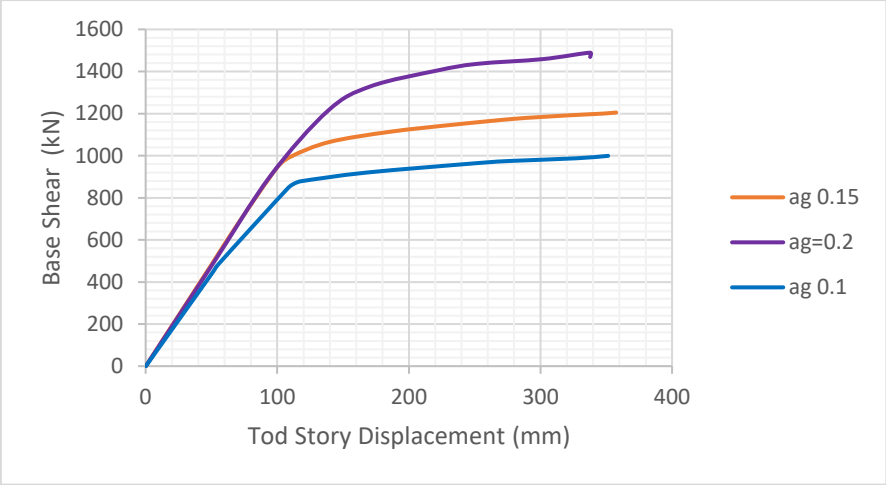

Figure 4.17: Capacity curve varying peak ground accelerations (10 stories and soil type A)

Table 4.8: Behavior factor for corresponding input ground accelerations

Ag	Δy (mm)	Δu (mm)	Vd (kN)	Vu (kN)	Rμ	Rs	q calculated	q code value
0.1	140	350	350	1000	2.500	2.857	7.143	3.9
0.15	130	350	556	1200	2.692	2.158	5.811	3.9
0.2	175	337	698	1420	1.926	2.034	3.918	3.9

Where; Δy is the yield deformation, Δu is ultimate deformation, Vd is the design base shear, Vu is the ultimate base shear capacity, Rμ is ductility factor and Rs is overstrength factor including redundancy.

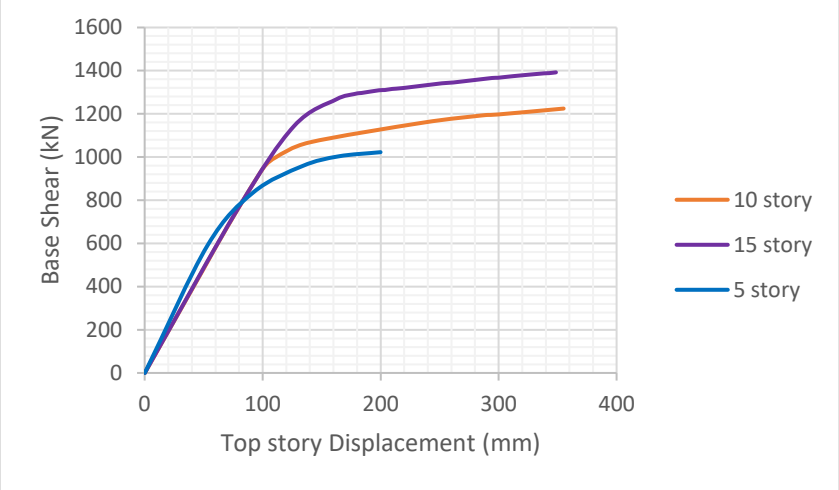

Figure 4.18: Capacity curve for different story heights (a_g = 0.15 and soil A)

Table 4.9: Behavior factor for corresponding number of stories

Story	Δy (mm)	Δu (mm)	Vd (kN)	Vu (kN)	Rμ	Rs	q calculated	q code value
5 story	75	200	460	1022	2.667	2.222	5.925	3.9
10 story	140	348	556	1200	2.486	2.158	5.365	3.9
15 story	175	337	678	1400	1.926	2.065	3.976	3.9

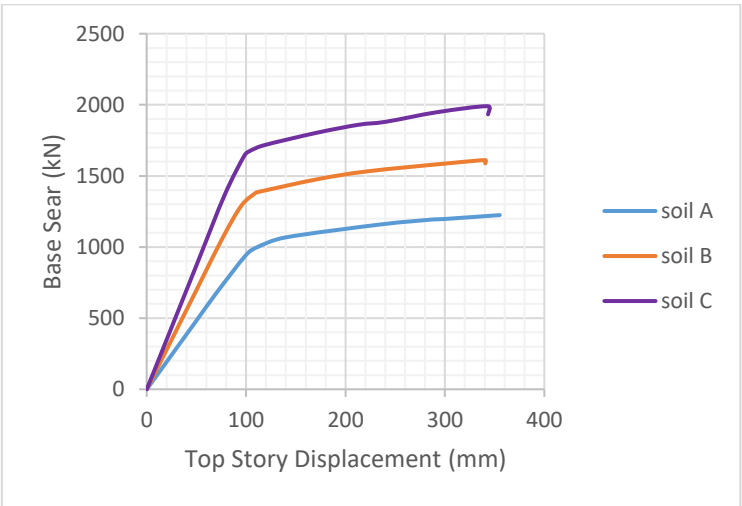

Figure 4.19: Capacity curve for different ground type (10 stories and a_g = 0.15)

Table 4.10: Behavior factor for corresponding Soil Type

soil Type	Δy (mm)	Δu (mm)	Vd (kN)	Vu (kN)	Rμ	Rs	q calculated	q code value
A	130	355	556	1224	2.731	2.201	6.012	3.9
B	125	340	823	1610	2.720	1.956	5.321	3.9
C	125	343	1110	1989	2.744	1.792	4.917	3.9

Generally, as presented above there are some favorable conditions that the structure can perform well and there are some unfavorable conditions where the structure is obliged to perform less. As the parametric study indicates the parameters selected (ag, story height and soil type) were found significant and affects behavior factor considerably. Thus, behavior factor decreased, as supporting soil becomes loose, as story height increases and as the peak ground acceleration increases.

4.11. 3D Incremental Time History Analysis Results and Behavior Factor

3D incremental dynamic analysis method involves subjecting a structural model to one or more ground motion records. Each record is then scaled to multiple levels of intensity, thus producing one or more load displacement curves.

Once the significant parameters that affects behavior factor are determined using 2D pushover analysis, subsequent 3D non-linear time history analysis were performed for different models under favorable and unfavorable conditions following the steps discussed in section 4.5.2.2 using a server machine. A large number of nonlinear time history analysis were performed to come up with the capacity curves of each models which were used for the calculation of behavior factor and the results obtained from the Analysis are organized as follows.

4.11.1. Analysis Results and Behavior Factor for Regular Frames Under Favorable and Unfavorable Conditions

a. Five story Models

In this part the capacity of 3D 5 story building models which were designed for both ductility class medium and high were investigated under a matched Elcentro, Holiste and LACC-NOR ground motions. These models were initially designed for favorable conditions only under moderate ground acceleration (ag=0.15) and firm ground condition (soil type A).

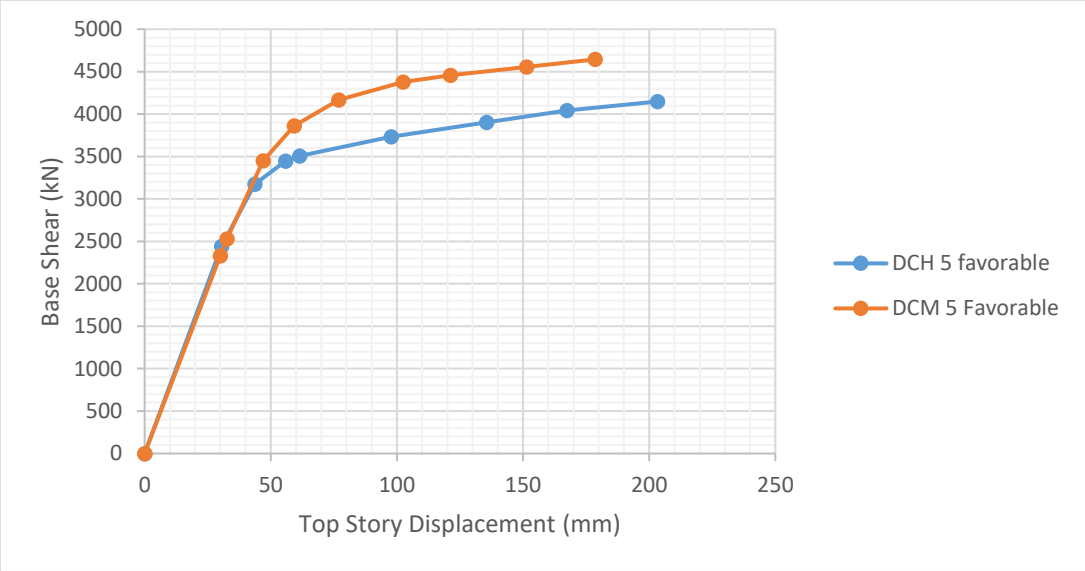

Figure 4.20: Capacity curve for DCH 5 and DCM 5 using Elcentro ground motion under favorable conditions.

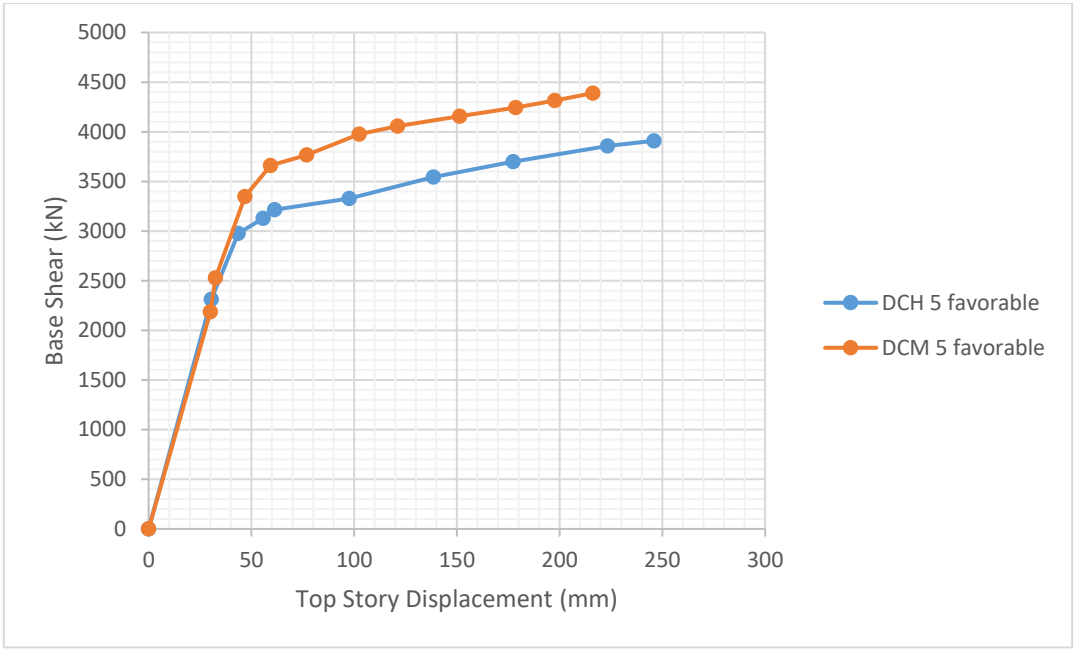

Figure 4.21: Capacity curve for DCH 5 and DCM 5 using Holiste ground motion under favorable conditions.

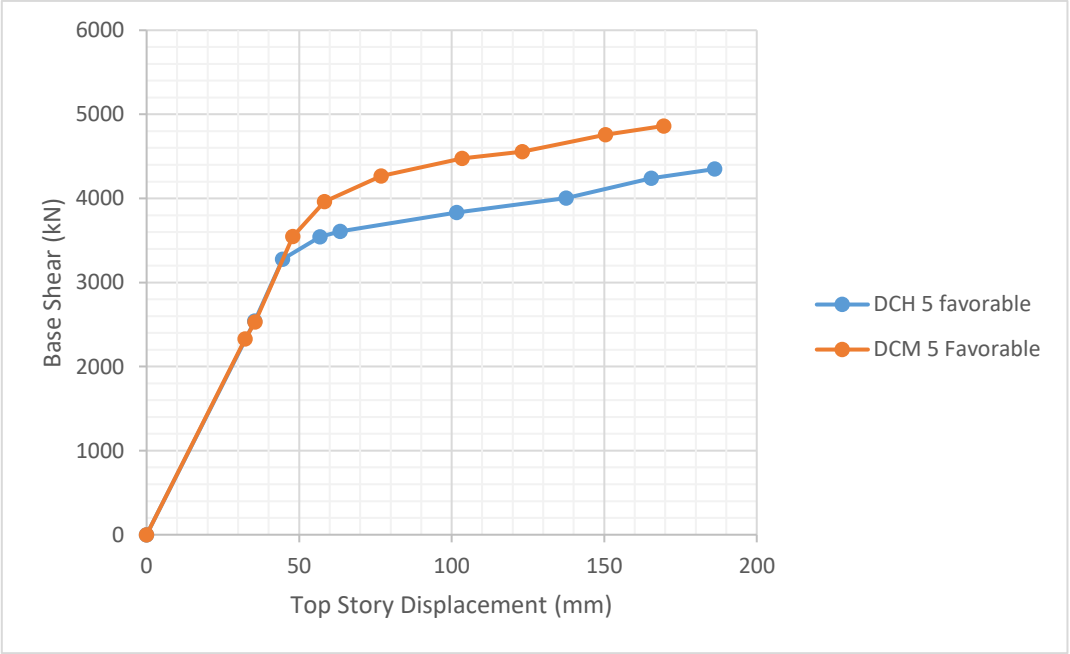

Figure 4.22: Capacity curve for DCH 5 and DCM 5 using LACC-NOR ground motion under favorable conditions.

Table 4.11: Behavior factor for DCM 5 and DCH 5 favorable models

Ground Motion	Model	Δy (mm)	Δu (mm)	Vd (kN)	Vu (kN)	Rμ	Rs	q calculated	q code value	q* code value
Elcentro	DCH 5 favorable	75.00	203.31	1215.00	4147.92	2.71	3.41	9.25	5.85	7.02
	DCM 5 favorable	65.00	178.60	1820.00	4640.00	2.75	2.55	7.01	3.90	4.68
Holiste	DCH 5 favorable	80.00	245.86	1215.00	3909.18	3.07	3.22	9.89	5.85	7.02
	DCM 5 favorable	72.00	216.23	1820.00	4389.35	3.00	2.41	7.24	3.90	4.68
LACC-NOR	DCH 5 favorable	75.00	186.26	1215.00	4349.32	2.48	3.58	8.89	5.85	7.02
	DCM 5 favorable	68.00	169.60	1820.00	4862.60	2.49	2.67	6.66	3.90	4.68
Average	DCH 5 favorable	76.67	211.81	1215.00	4135.47	2.76	3.40	9.34	5.85	7.02
	DCM 5 favorable	68.33	188.14	1820.00	4630.65	2.75	2.54	6.97	3.90	4.68

Where; Δy is the yield deformation, Δu is ultimate deformation, Vd is the design base shear, Vu is the ultimate base shear capacity, Rμ is ductility factor and Rs is overstrength factor including redundancy.

q calculated: - is the calculated behavior factor using the capacity curves obtained from incremental dynamic time history analysis.

q code value: -is the value of factored behavior factor in our code considering human factors

q* code value: -is the value of behavior factor to be used if a special quality plan is employed in the design procurement and construction of the building (Theoretical value)

As we can see from the results above the models for both ductility classes under favorable conditions performs well and the calculated behavior factor was even far from the theoretical behavior factor in the code. The calculated average value of DCH 5 favorable was 25% higher than the theoretical value of the code and calculated average value of DCM 5 favorable was 33% higher than the theoretical value of the code. The behavior factor calculated from the average of the results of matched ground motions were relatively comparable to the value of behavior factor from individual matched ground motions. Thus, only Elcentro ground motion was used in the subsequent studies as 3D incremental time history analysis critically required a server machine and huge amount of run time.

b. Ten story Models

In this part, the capacity of 3D 10 story building models which were designed for both ductility class medium and high were investigated only under Elcentro ground motion for the reason that the server machine used in this research was available for a short period. These models were subjected to favorable and unfavorable conditions. Models named as Favorable were initially designed for moderate ground acceleration (ag=0.15) and firm ground (soil type A) and models named as unfavorable were designed for worst ground acceleration (ag=0.2) and loose ground condition (soil type C). In the design stage of these models, bigger frame sections were required for unfavorable models as a result of grater base shear for both ductility classes to satisfy ultimate limit state requirements.

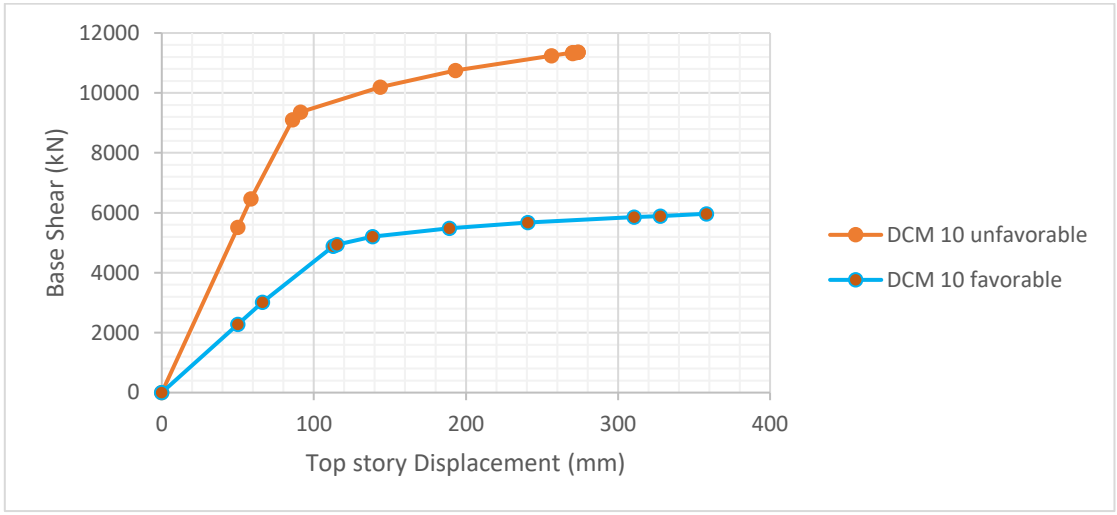

Figure 4.23: Capacity curve for DCM 10 favorable and unfavorable models subjected to Elcentro ground motion.

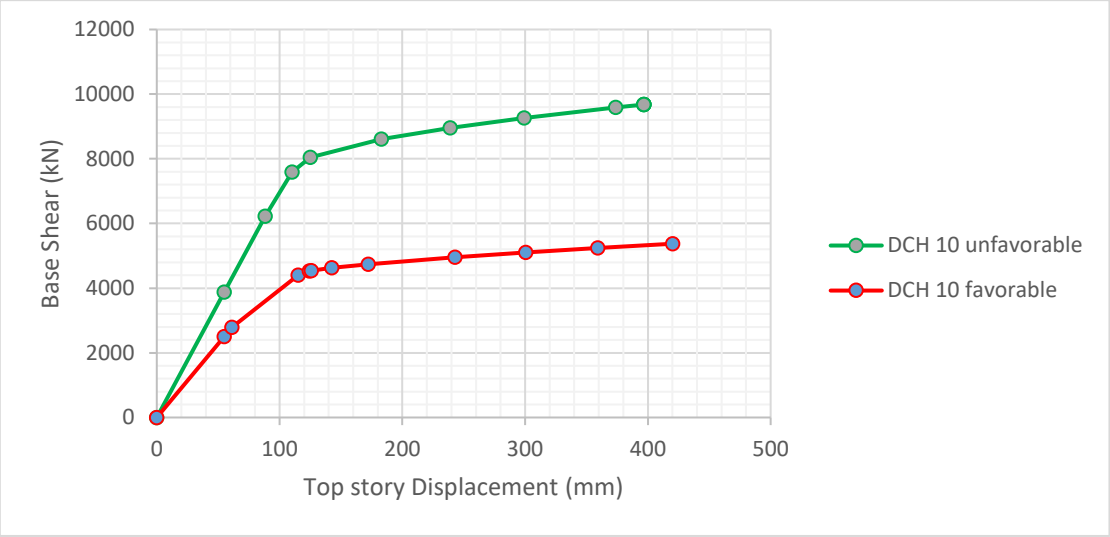

Figure 4.24: Capacity curve for DCH 10 favorable and unfavorable models subjected to Elcentro ground motion.

The following sections provide and discuss the results of calculated q-factor of the models used in this study under favorable and unfavorable conditions. Generally, the calculated q-factor demonstrates the effect of ground acceleration, supporting ground type, ductility class assigned to the structure and the design itself. In figures (4.25 and 4.26) The design value of q-factor specified by (ES EN 1998:1-2015) is represented by a solid vertical line and the theoretical value in the code is represented by dashed vertical line (q values from the code are also specified in Table 4.12 as q and q* for regular Frames).

Table 4.12: Behavior factor for DCM 10 and DCH 10 favorable and unfavorable models

Model	Δy (mm)	Δu (mm)	Vd (kN)	Vu (kN)	Rμ	Rs	q calculated	q code value	q* code value
DCM 10 favorable	140.0	358.0	2221.0	5967.0	2.56	2.69	6.87	3.90	4.68
DCM 10 unfavorable	120.0	275.0	5500.0	11350.0	2.29	2.06	4.73	3.90	4.68
DCH 10 favorable	160.0	420.0	1666.0	5417.0	2.63	3.25	8.54	5.85	7.02
DCH 10 unfavorable	150.0	396.0	3490.0	9600.0	2.64	2.75	7.26	5.85	7.02

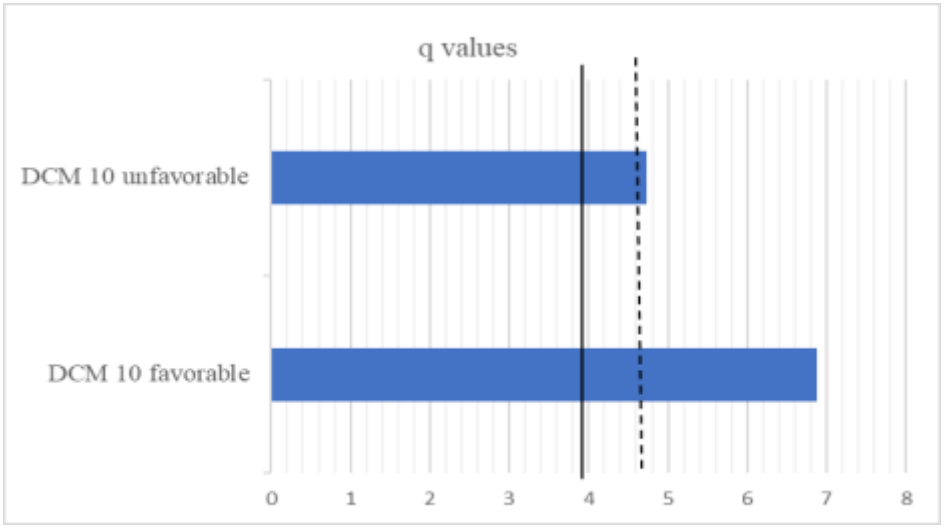

Figure 4.25: Behavior factor for DCM10 favorable and unfavorable models.

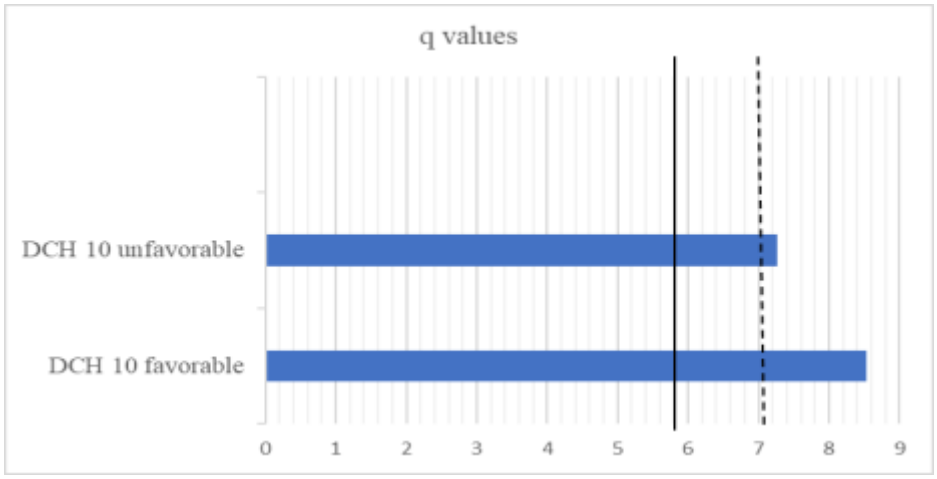

Figure 4.26: Behavior factor for DCH10 favorable and unfavorable models

As shown in Table 4.12 the behavior factor for unfavorable models were found to be slightly above the theoretical behavior factor value of the code. This shows us as long as the structure is properly designed following capacity design principles and detailed respecting the detailing rules for each ductility class discussed in chapter 3 of this research. Thus, a good performance of a structure and the expected behavior factor even under unfavorable situations can be achieved through proper design and detailing. On the other hand, the behavior factor for models under favorable conditions were relatively higher than the theoretical behavior factor values of the code and this shows us behavior factor can be slightly increased for models subjected to favorable conditions. In addition, because models under unfavorable conditions were initially designed for greater base shear and as a result bigger sections were used, models under unfavorable conditions exhibits larger base shear capacity than models under favorable

conditions but their over strength factor was still below the models under favorable conditions. Generally, the performance of models under favorable conditions were found to be higher than the models under unfavorable conditions.

4.11.2. Analysis Results and Behavior Factor for Plan Irregular Frame Under Unfavorable Conditions

As one of the objectives of this study is to examine the behavior factor provision of our code for plan irregular multi bay multistory moment resisting frames, a 3D 10 story plan irregular moment resisting frame as shown in figure 3.1b was initially analyzed using linear time history analysis under Elcentro ground motion and designed following the capacity design principles discussed before. The model was designed for high ductility class for ag=0.2 and ground type C to see the combined effect of plan irregularity and unfavorable conditions. Subsequently, the hinge properties of the frame are assigned and the frame is subjected to a nonlinear time history analysis under Elcentro ground motion and the results are presented underneath.

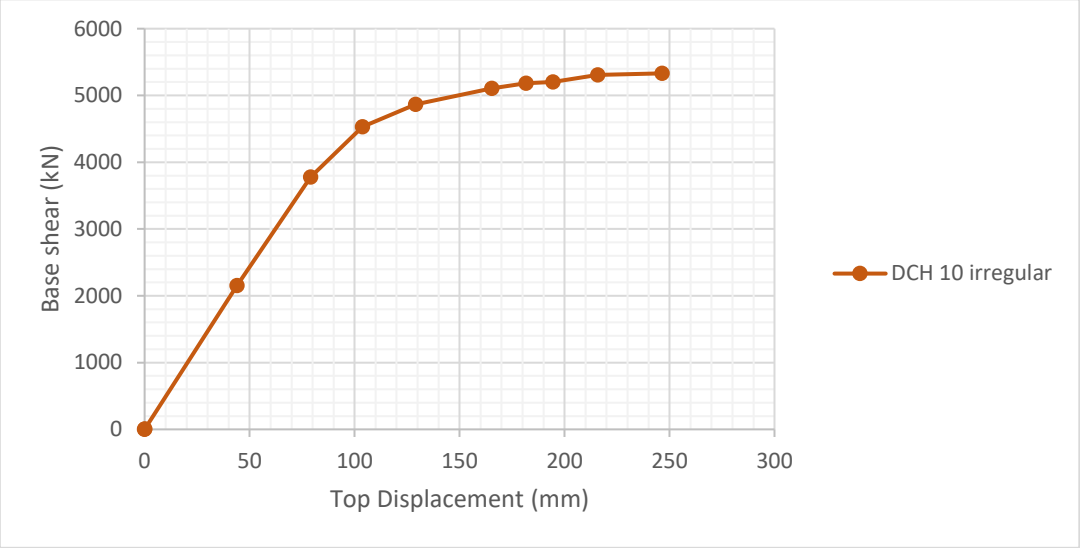

Figure 4.27: Capacity curve for DCH 10 irregular model subjected to Elcentro ground motion.

Table 4.13: Behavior factor for DCH 10 irregular model

Model	Δy (mm)	Δu (mm)	Vd (kN)	Vu (kN)	Rμ	Rs	Q calculated	q code value	q* code value
DCH 10 irregular	115	246.45	3015.5	5202.7	2.14	1.72	3.70	5.175	6.21

The behavior factor calculated for this model was found to be lesser than the design value of behavior factor provided in ES EN 1998:1-2015 (the result is also shown using a bar chart in figure 4.28 and the vertical solid line represents the code design q factor). The calculated behavior factor (q=3.7) is 28.5% lesser than the design behavior factor in the code (q=5.175) which is a critical problem. so, in such cases the expected seismic performance of plan irregular structures under unfavorable conditions is not satisfied and the value of behavior factor provided in EC8 (ES EN 8) is overestimated. Thus, behavior factor values provided in our code should be modified in such a way that this value can be achieved even in extreme scenarios.

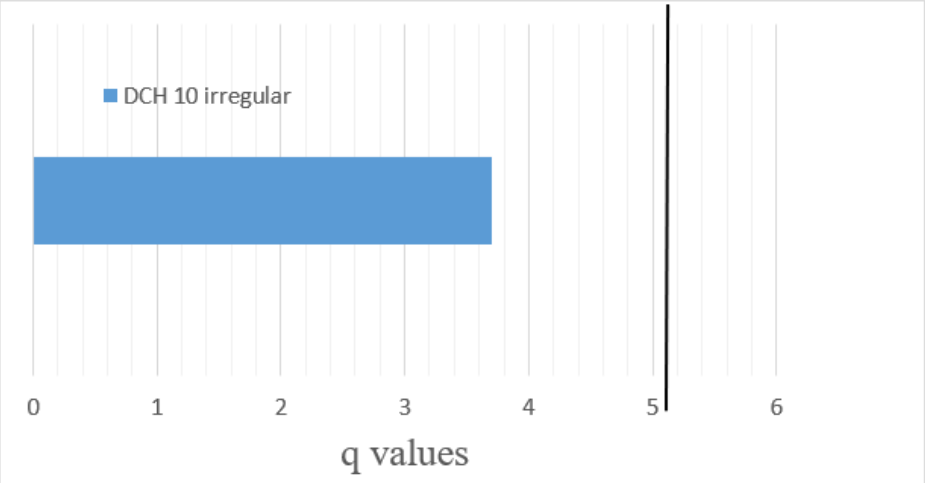

Figure 4.28: Behavior factor for DCH 10 irregular model

4.12. Seismic Performance Comparison of Structures Designed for Different Ductility Classes

As the specific objective of this study is to compare the performance of structures designed for different ductility classes, the performance of 5 story models subjected to favorable conditions and 10 story modes subjected to favorable and unfavorable conditions were compared and the comparison is discussed following the results in the figures bellow.

The capacity curve made by scaling up the time history load cases of Elcentro ground motion is shown in figures (4.29 through 4.31) and the results are from the capacity curves used for the calculation of behavior factor in previous sections.

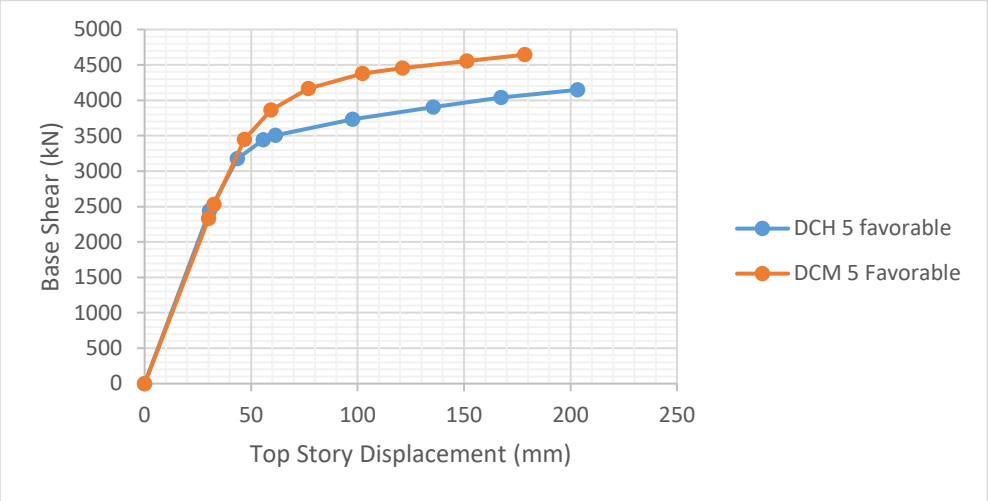

Figure 4.29: Capacity curve for DCM 5 and DCH 5 favorable models subjected to Elcentro ground motion.

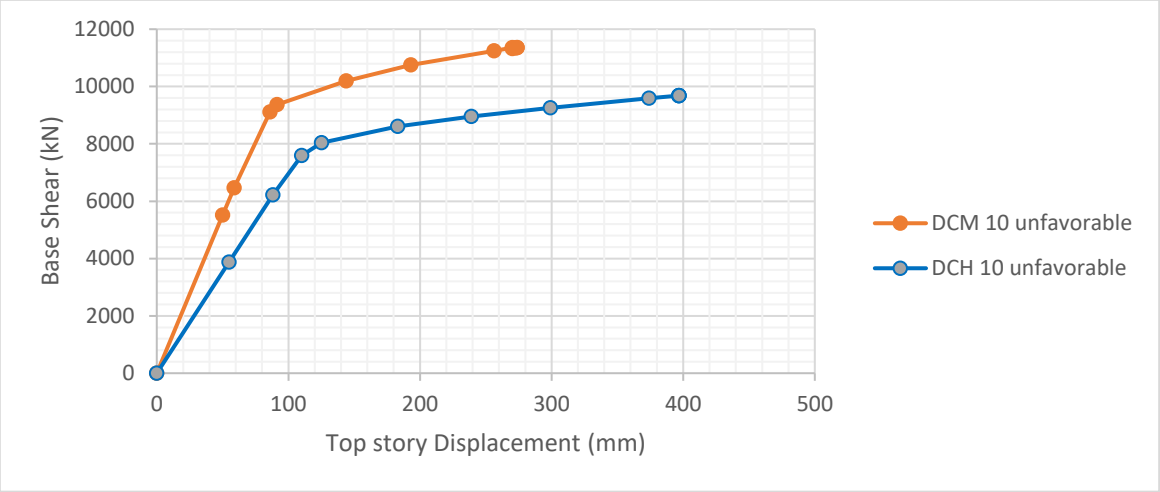

Figure 4.30: Capacity curve for DCM 10 and DCH 10 un favorable models subjected to Elcentro ground motion.

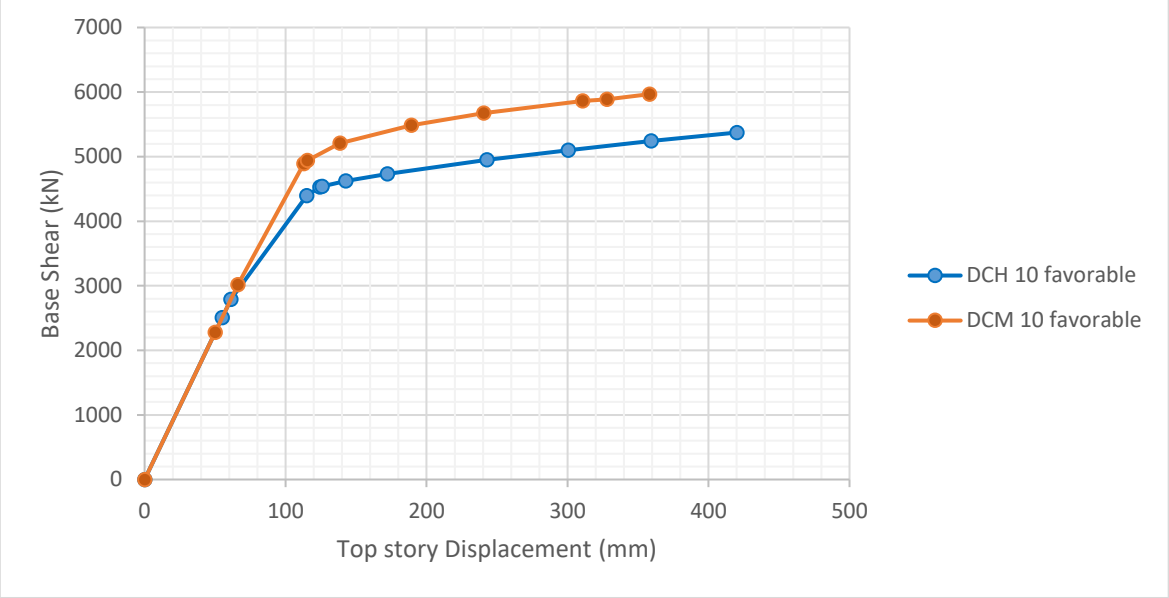

Figure 4.31: Capacity curve for DCM 10 and DCH 10 favorable models subjected to Elcentro ground motion.

The story drifts result at the collapse point of the selected models for performance comparison are shown in the following figures and the limits are already checked in section 4.10.

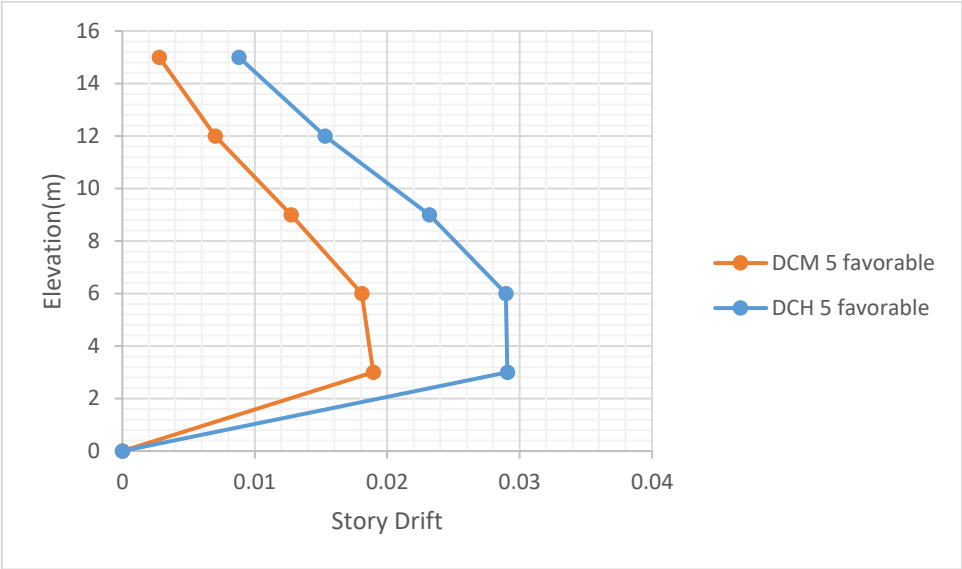

Figure 4.32: Maximum drift for DCH 5 and DCM 5 favorable models

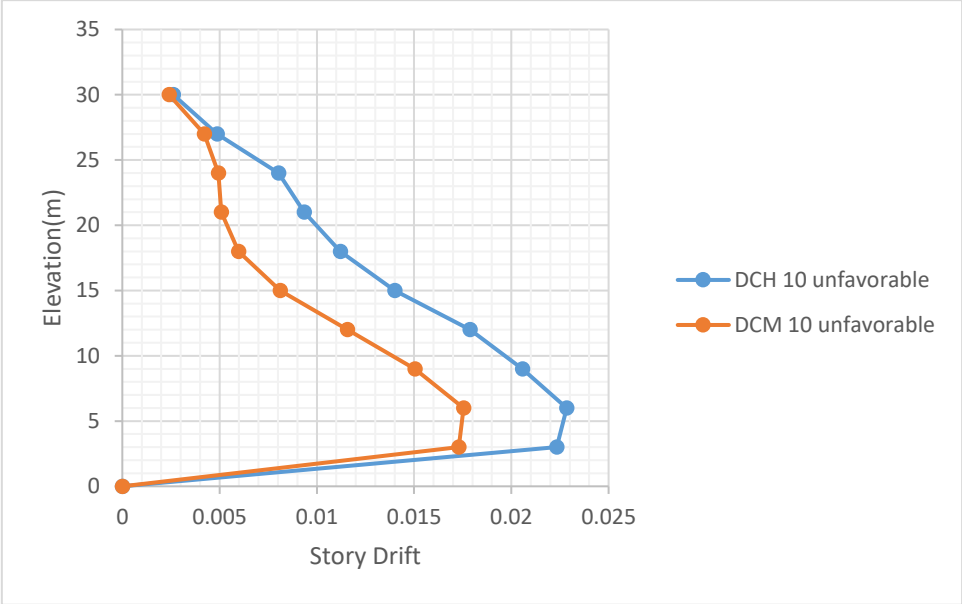

Figure 4.33: Maximum drift for DCH 10 and DCM 10 unfavorable models

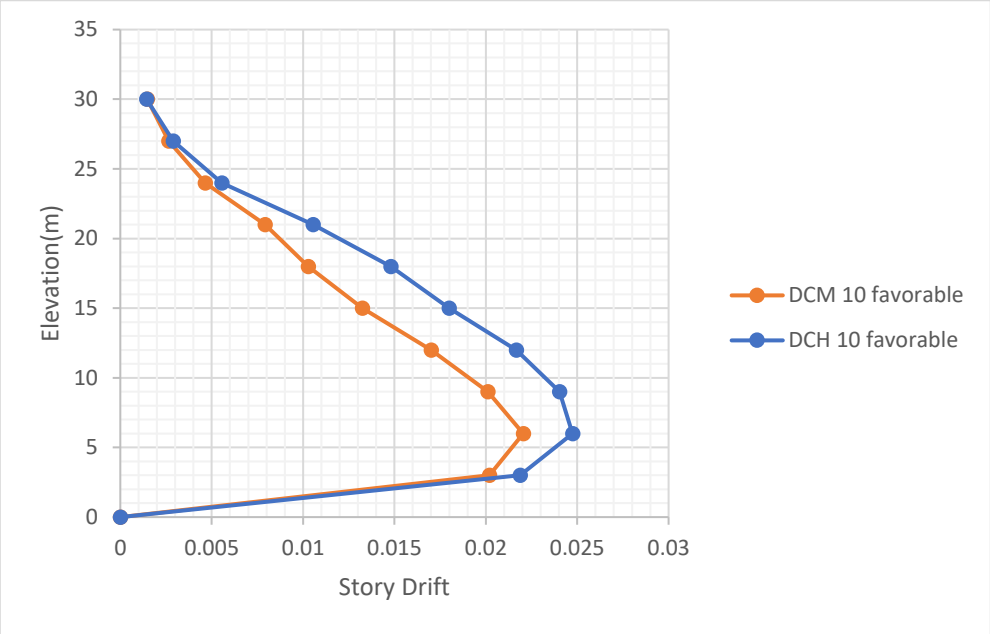

Figure 4.34: Maximum drift for DCH 10 and DCM 10 favorable models

As shown in the figures (4.29 through 4.31), the deformation capacity of DCH 5 favorable was 12.14% higher than DCM 5 favorable, the deformation capacity of DCH 10 favorable was 14.2% higher than DCM 10 favorable and the deformation capacity of DCH 10 unfavorable was 30.5% higher than DCM 10 unfavorable. Thus, in all cases the performance in terms of ductility (deformation capacity) of structures designed for ductility class high was found to be

better than structures designed for ductility class medium. Along with this, as the percentage shows the ductility capacity of the structures designed for high ductility was higher in case of unfavorable situation. So, in cases were the structure was designed under favorable conditions both structures can perform well with slight variation. On the other hand, the base shear capacity of DCM 5 favorable 10.6% higher than DCH 5 favorable, the base shear capacity of DCM 10 favorable 9.2% higher than DCH 10 favorable and the base shear capacity of DCM 10 unfavorable 15.24% higher than DCH 10 unfavorable. Thus, the difference in base shear capacity of the structures designed for these two ductility classes were more visible in case of unfavorable condition. Generally, the overall seismic performance can be compared using behavior factor as it is a measure of energy dissipation capacity of the structures, hence the performance of structures designed for ductility class high was found to be better than structures designed for ductility class medium.

As shown in figures (4.32 through 4.34), the story drift of structures designed for medium ductility is found lesser than structures designed for ductility class high. This shows as the performance of structures designed for ductility class medium in drift resistance, are better than structures designed for ductility class high. But the story drift for all models designed for both ductility classes were found to be with in the limit of (ATC 40, 1996) requirements as it is checked in section 4.9.

CHAPTER 5 CONCLUSION AND RECOMMENDATION

5.1 Conclusion

Conclusions derived based on this thesis study, are presented as follows.

- Practically, the behavior factor (q) provided in (ES EN 1998:1-2015) depends on types of structure, ductility type and regularity requirement. However, this value is kept constant for multistory, multi-bay frame structures. This study has obtained different values, both in the parametric study using push over analysis and 3D incremental time history analysis. Thus, behavior factor is not a unique value for all multi-bay multistory RC frames under the same ductility class rather its value depends on different factors such as seismic location, ground type, the number of stories, regularity of the frame, the modeling type and the final design sections and reinforcements that the designer uses (redundancy and overstrength).
- As obtained in the parametric study and in the calculation of behavior factor for DCH 5, DCM 5, DCH 10 and DCM 10 favorable models, the value of behavior factor recommended by (ES EN 1998:1-2015) for moment resisting frames subjected to favorable conditions (i.e. low seismic area, firm ground condition and low-rise frames) was found to be underestimated. Thus, behavior factor used in design can be increased without adverse effect on seismic performance. This observation is constrained by the limited number of models used in this research and uncertainties not considered in modelling such as foundation modelling and inclusion of infill walls.
- As observed in DCH 10 $_{\text{unfavorable}}$ and DCM 10 $_{\text{unfavorable}}$ models, the value of behavior factor for regular RC multi-bay multi story moment resisting frame structures even under extreme scenarios (unfavorable conditions) can be achieved as long as the design is done using capacity design principles of the code and respecting the detailing rules of each ductility class.
- The result found in the determination of behavior factor for plan irregular model combined with unfavorable conditions showed that, the value of behavior factor given in the code (ES EN 1998:1-2015) for plan irregular buildings was found to be overestimated. Thus, this value of the code should be reexamined using large number

of models and modified in such a way that the expected energy dissipation capacity of this structures can be achieved.

- As the seismic performance of structures designed for different ductility classes was investigated in this study, in terms of deformation capacity, structures designed for high ductility class performs well better than structures designed for medium ductility class, since the detailing rules for ductility class high is tighter. And in terms of base shear capacity, structures designed for medium ductility class were found to be better than structures designed for high ductility, because for these types of structures, bigger sections and larger amount of longitudinal reinforcement bar specially in beams were used. In addition, because bigger sections were used in structures designed for medium ductility as a result of greater base sear, the drift resistance of structures, designed for medium ductility were found to be better than structures designed for high ductility. The maximum drift value of structures designed for medium ductility was with in life safety performance limit while the maximum story drift for high ductility structures was with in collapse prevention performance limit as per (ATC 40,1996). Generally, as the overall seismic performance of the structures can be compared using behavior factor (a measure of energy dissipation capacity), structures designed for high ductility class were found to be better. Along with this, it is possible to conclude that the performance of structures designed for both ductility classes under favorable conditions (low-rise structures located on low seismic area and supported on firm ground) are comparable, and the selection between the ductility classes will be determined by economic terms while seismic performance will govern in cases of unfavorable conditions.
- Regarding the nonlinear analysis techniques used in this research, the results of push over analysis specifically for plan irregular model varies as the control joint is changed and the result of push over analysis using the center of rigidity as a control point was found to be different from the results of incremental nonlinear time history analysis. Thus, Incremental dynamic analysis, also termed as dynamic pushover, was better specially in the presence of irregularities and much nonlinearity as it provides a continuous picture of the system response, from elasticity to yielding and finally to collapse. In addition, because the load has to be applied in the direction of principal axis where the controlling response of the structure is detected, push over analysis cannot be applied in that direction as there is no option to adjust the direction of load

application in the current version of ETABS. Thus, nonlinear time history analysis was found to be better as the direction of load application can be easily adjusted by the user.

- As it can be concluded from the results of failure mechanism of the planner frame used to show the formation of plastic hinges (i.e. location and sequence), edge and corner base columns were more susceptible to nonlinear rotation. Thus, the critical length of those columns should be detailed more tighter in order to achieve better deformation capacity.

5.2 Recommendation for Future Work

The research work presented in this thesis is evaluation of behavior factor for RC regular and plan irregular moment-resisting frame buildings. And further possible research areas are recommended hereunder:

- Evaluation of behavior factor for irregular structures (both in plan and in elevation) using nonlinear analysis.
- In this thesis the effect of soil structure interactions and infill walls were not included. Therefore, it is required to study the evaluation of behavior factor considering the effect of these factors.
- Since this research is done only for moment resisting frames, the evaluation of behavior factor for dual and wall systems is recommended.
- Moreover, as behavior factor is a central measure of seismic performance, it is better to check the provision of the code through a repetitive research using a large number of models and conditions by a research team in the university.

REFERENCE

ES EN (1998:1-2015). Design of Structures for Earthquake Resistance, Part-1: General Rules, Seismic Actions and Rules for Buildings. Ministry of Urban Development, Housing and Construction, 2015, Ethiopia.

Kashyap N. Patel and Jignesh A. Amin (2017). Performance Based Assessment of Seismic Response Factor for SMRF Staging Elevated Water Tank, ICRISET, 2017.

ATC 40 (1996). Seismic Evaluation and Retrofit of Concrete Buildings: Vol. 1. Applied Technology Council, 1996, USA.

Newmark, NM. and Hall, WJ. (1982). Earthquake Spectra and Design, EERI Monograph Series, 1982, Oakland. EERI.

ATC 19 (1978). Seismic Evaluation and Retrofit of Concrete Buildings: Vol. 1. Applied Technology Council, 1978, USA.

Krawinkler, H. and Nassar, A. (1992). Seismic Design Based on Ductility and Cumulative Damage Demands and Capacities, Nonlinear Seismic Analysis of Reinforced Concrete Buildings, 1992, New York, USA.

Eduardo Miranda Vitelmo V.Bertero (1994) Evaluation of strength factor for earth quick resistant design. Earthquake Spectra, 1994, Vol. 10, No. 2, pp. 357-379, Okland, USA

Tomaz Vidic,Peter Fajfar,Matej Fischinger (1994) Constant Inelastic spectra: Strength and displacement. Earth quick Spectra, 1994, Vol.23, pp. 507-521, Okland, USA

Vamvatslos, D. & Cornell,A.C. (2001). Incremental dynamic analysis. Earth quick Spectra, 1994, Vol.31, pp. 491-514, Okland, USA

Kappos, A.J (1992). Seismic damage indices for R/C buildings: Evaluation of concept and procedures. Progress in structural engineering and material, 1992, Vol.1, pp 78-87

Park, R. (1988). Ductility evaluation from laboratory and analytical testing Vol &VIII. Proceedings of the 9th world conference on earthquake engineering, Tokyo, Japan.

EC2 (2004). Design of concrete structures - Part 1: General rules and rules for buildings, European Committee for Standardization (CEN), 2004, Brussels.

M.N. Fardis (2009). Design of Structures for Earthquake Resistance. Technical Chamber of Greece – Hellenic Concrete Section Japan Society of Civil Engineers, 2009, Athens, Greece.

Bolander, Julie Christine (2014). Investigation of Torsional Effects on Thirteen-Story Reinforced Concrete Frame-Wall Structure Modeled in ETABS and SAP2000 Using Linear and Nonlinear Static and Dynamic Analyses, UC San Diego Electronic Theses and Dissertations,2014, San Diego

Federal Emergency Management Agency FEMA (1997), "Pre-standard and Commentary for the Seismic Rehabilitation of Buildings" (FEMA 356), 1997, Washington.

Mander J.B., Priestly, M.J.N., and Park, R. (1988). Theoretical Stress-Strain Model for Confined Concrete, ASCE Journal of Structural Engineering, Vol. 1 pp 83-94, 1998, USA

Serhan Guner (2010). Pushover Analysis of Shear Critical Frames: Verification and Application. ACI structural journal, 2010, USA

APPENDIXES

Appendix A: Design Sections and Reinforcements for Sample Models.

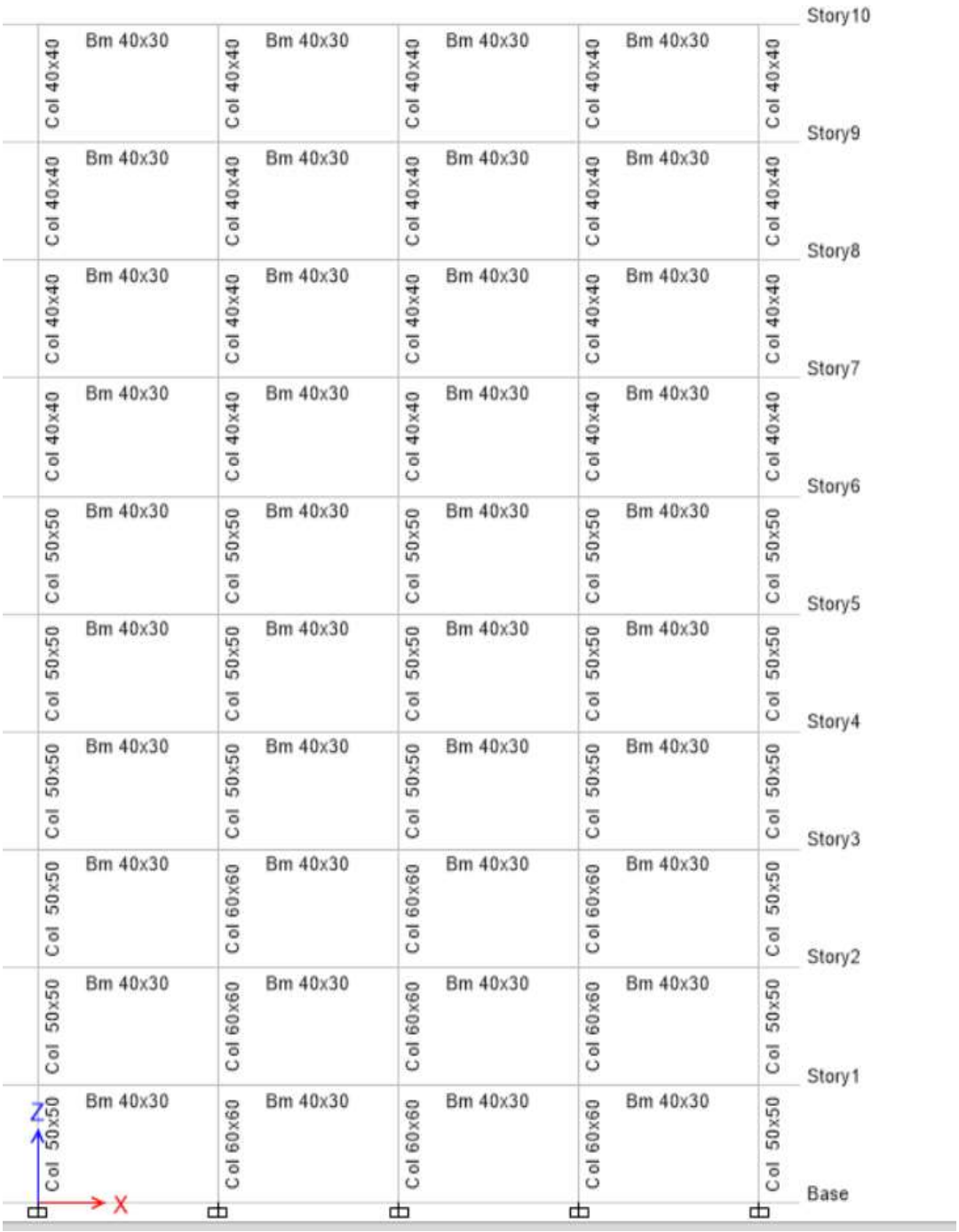

Figure Appendix 1: Sample design sections of DCM 10 and DCH 10 favorable models along axis-2

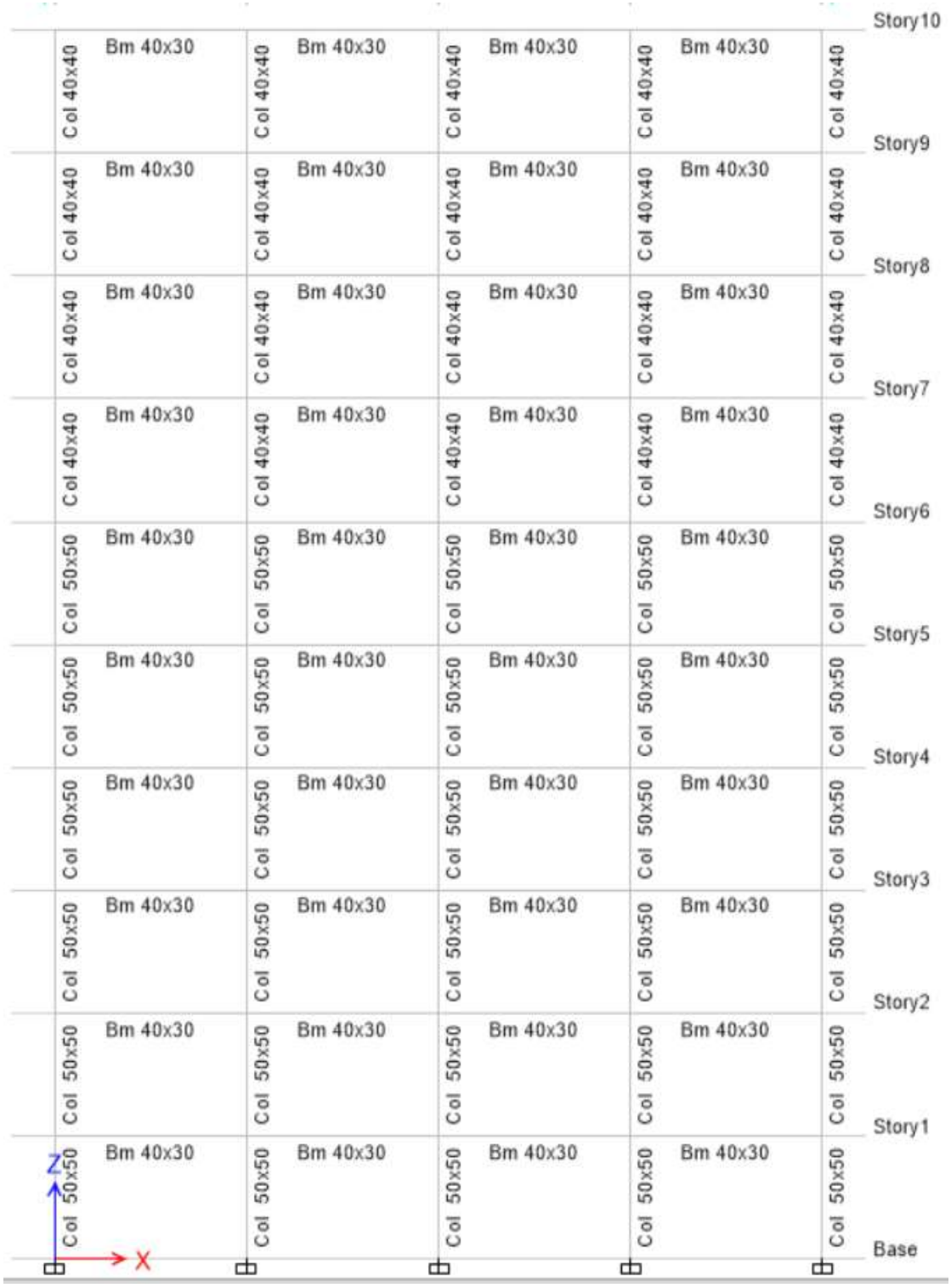

Figure Appendix 2: Sample design sections of DCM 10 and DCH 10 favorable models along axis-1

Table Appendix 1: sample Design sections and Reinforcements of beams for DCM 10 favorable along axis 2

Axis	Story	Joint	SECTION (mm)	Longitudinal Rebar		stirrup
				Top	Bot	
Axis 2	story 10	A	400X300	4Φ16	2Φ16	Φ8 C/C 100
		B	400X300	4Φ16	2Φ16	Φ8 C/C 100
		C	400X300	4Φ16	2Φ16	Φ8 C/C 100
		D	400X300	4Φ16	2Φ16	Φ8 C/C 100
		E	400X300	4Φ16	2Φ16	Φ8 C/C 100
	story 9	A	400X300	4Φ16	2Φ16	Φ8 C/C 100
		B	400X300	4Φ16	2Φ16	Φ8 C/C 100
		C	400X300	4Φ16	2Φ16	Φ8 C/C 100
		D	400X300	4Φ16	2Φ16	Φ8 C/C 100
		E	400X300	4Φ16	2Φ16	Φ8 C/C 100
	story 8	A	400X300	6Φ16	3Φ16	Φ8 C/C 100
		B	400X300	6Φ16	3Φ16	Φ8 C/C 100
		C	400X300	6Φ16	3Φ16	Φ8 C/C 100
		D	400X300	6Φ16	3Φ16	Φ8 C/C 100
		E	400X300	6Φ16	3Φ16	Φ8 C/C 100
	story 7	A	400X300	6Φ16	3Φ16	Φ8 C/C 100
		B	400X300	6Φ16	3Φ16	Φ8 C/C 100
		C	400X300	6Φ16	3Φ16	Φ8 C/C 100
		D	400X300	6Φ16	3Φ16	Φ8 C/C 100
		E	400X300	6Φ16	3Φ16	Φ8 C/C 100
	story 6	A	400X300	5Φ20	4Φ16	Φ8 C/C 100
		B	400X300	5Φ20	4Φ16	Φ8 C/C 100
		C	400X300	5Φ20	4Φ16	Φ8 C/C 100
		D	400X300	5Φ20	4Φ16	Φ8 C/C 100
		E	400X300	5Φ20	4Φ16	Φ8 C/C 100
	story 5	A	400X300	6Φ20	5Φ16	Φ8 C/C 100
		B	400X300	6Φ20	5Φ16	Φ8 C/C 100

		C	400X300	6Φ20	5Φ16	Φ8 C/C 100
		D	400X300	6Φ20	5Φ16	Φ8 C/C 100
		E	400X300	6Φ20	5Φ16	Φ8 C/C 100
	story 4	A	400X300	6Φ20	5Φ16	Φ8 C/C 100
		B	400X300	6Φ20	5Φ16	Φ8 C/C 100
		C	400X300	6Φ20	5Φ16	Φ8 C/C 100
		D	400X300	6Φ20	5Φ16	Φ8 C/C 100
		E	400X300	6Φ20	5Φ16	Φ8 C/C 100
	story 3	A	400X300	6Φ20	5Φ16	Φ8 C/C 100
		B	400X300	6Φ20	5Φ16	Φ8 C/C 100
		C	400X300	6Φ20	5Φ16	Φ8 C/C 100
		D	400X300	6Φ20	5Φ16	Φ8 C/C 100
		E	400X300	6Φ20	5Φ16	Φ8 C/C 100
	story 2	A	400X300	6Φ20	5Φ16	Φ8 C/C 100
		B	400X300	6Φ20	5Φ16	Φ8 C/C 100
		C	400X300	6Φ20	5Φ16	Φ8 C/C 100
		D	400X300	6Φ20	5Φ16	Φ8 C/C 100
		E	400X300	6Φ20	5Φ16	Φ8 C/C 100
	story 1	A	400X300	6Φ16	3Φ16	Φ8 C/C 100
		B	400X300	6Φ16	3Φ16	Φ8 C/C 100
		C	400X300	6Φ16	3Φ16	Φ8 C/C 100
		D	400X300	6Φ16	3Φ16	Φ8 C/C 100
		E	400X300	6Φ16	3Φ16	Φ8 C/C 100

Table Appendix 2: Sample design sections and Reinforcements and axial force ratios of base columns for DCM 10 favorable model

Axis	Longitudinal Rebar	Stirrup	Axial force (kN)	Section (mm)	N/Ag*Fcd
Center	12Φ20	Φ8 C/C 150	-3160	600x600	0.527
Edge	8Φ20	Φ8 C/C 150	-1810	500x500	0.434
Corner	8Φ20	Φ8 C/C 150	-1507	500x500	0.362

Appendix B: Hinge properties for sample models

Table Appendix 3: Sample hinge properties of beams for DCM 10 favorable model along axis 2

Axis 2	point	M (kNm)	k	Lpl (m)	m/sf	Θ/sf
beam st 9-10	A	0.000	0.000	0.150	0.000	0.000
	B	99.280	0.008	0.150	1.000	0.000
	C	126.710	0.358	0.150	1.276	0.053
	D	25.342	0.358	0.150	0.255	0.053
	E	25.342	0.717	0.150	0.255	0.105
beam st 1,7,8	A	0.000	0.000	0.150	0.000	0.000
	B	145.380	0.009	0.150	1.000	0.000
	C	160.000	0.280	0.150	1.101	0.041
	D	32.000	0.280	0.150	0.220	0.041
	E	32.000	0.559	0.150	0.220	0.081
beam st 6	A	0.000	0.000	0.150	0.000	0.000
	B	186.720	0.010	0.150	1.000	0.000
	C	208.600	0.242	0.150	1.117	0.035
	D	41.720	0.242	0.150	0.223	0.035
	E	41.720	0.485	0.150	0.223	0.070
beam st 2-5	A	0.000	0.000	0.150	0.000	0.000
	B	231.460	0.010	0.150	1.000	0.000
	C	260.480	0.218	0.150	1.125	0.031
	D	52.096	0.218	0.150	0.225	0.031
	E	52.096	0.436	0.150	0.225	0.062

Table Appendix 4: Sample hinge properties of base columns for DCM 10 favorable model

Axis 2	Point	M (kNm)	k	Lpl (m)	m/sf	Θ/sf
col center	A	0.000	0.000	0.250	0.000	0.000
	B	768.330	0.009	0.250	1.000	0.000
	C	793.120	0.099	0.250	1.032	0.022
	D	158.624	0.099	0.250	0.206	0.022
	E	158.624	0.197	0.250	0.206	0.045
col edge	A	0.000	0.000	0.250	0.000	0.000
	B	326.960	0.016	0.250	1.000	0.000
	C	327.410	0.097	0.250	1.001	0.020
	D	65.482	0.097	0.250	0.200	0.020
	E	65.482	0.194	0.250	0.200	0.040
col corner	A	0.000	0.000	0.250	0.000	0.000
	B	283.570	0.014	0.250	1.000	0.000
	C	283.700	0.094	0.250	1.000	0.020
	D	56.740	0.094	0.250	0.200	0.020
	E	56.740	0.188	0.250	0.200	0.040

Appendix C: Beam column capacity ratios of the sample models

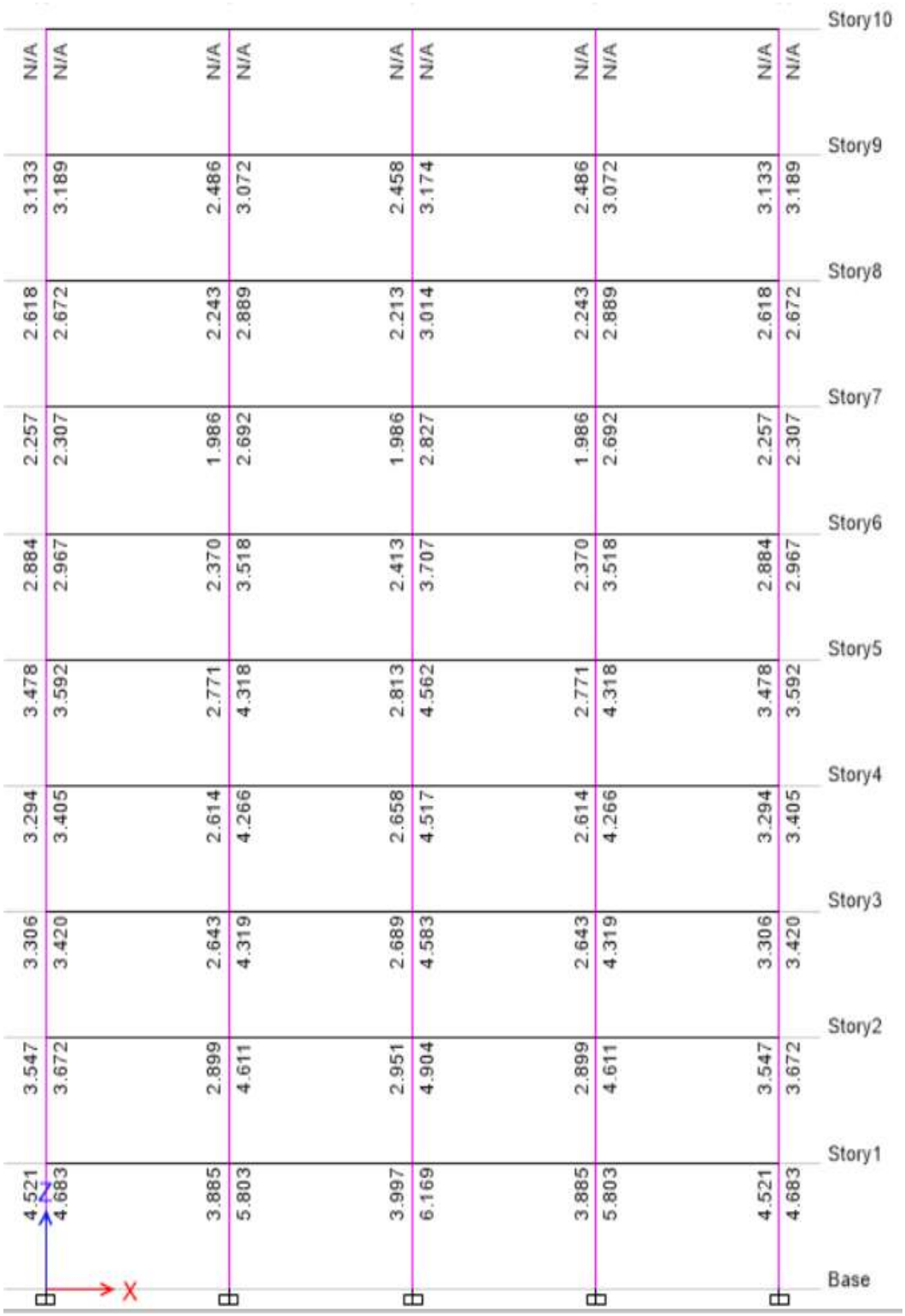

Figure Appendix 3: Sample column to beam capacity ratios for DCM 10 favorable model along axis 1

Appendix D: Detailing Rules and Evaluation of detailing parameters for sample models

In this section the detailing and dimensioning rules of primary seismic beams and primary seismic columns from EC 2 and EC 8 are presented in the tables 3.14 and 3.15 for each ductility classes. Based on the detailing rules in table 3.14 and 3.15 sample detailing of beams and columns and the evaluation according to the requirements are presented in Appendix D for DCM and DCH models.

Table Appendix 7: Detailing & dimensioning of primary seismic beams (secondary as in DCL)

	DCH	DCM	DCL
"critical region" length	1.5hw	Hw	
Longitudinal bars (L):			
ρmin, tension side	$\frac{0.5\,fctm}{fyk}$		$\frac{0.26\,fctm}{fyk}, 0.13\%$ (0)
ρmax, critical regions (1)	$\rho' + \frac{0.0018\,f_{cd}}{\mu_\phi \varepsilon_{sy}, d f_{yd}}$ (1)		0.04
As, min, top & bottom	2Φ14 (308mm2)	-	
As, min, top-span	As, top supports/4		
As, min, critical regions bottom	0.5As, top (2)		-
As, min, supports bottom	As, bottom span/4(0)		
$\frac{dbL}{hc}$ bar crossing interior joint (3)	$\frac{\frac{6.25(1+0.8\nu d)}{\rho'}\frac{fctm}{fyd}}{1+0.75\frac{\rho'}{\rho\max}}$	$\frac{\frac{7.5(1+0.8\nu d)}{\rho'}\frac{fctm}{fyd}}{1+0.5\frac{\rho'}{\rho\max}}$	-
$\frac{dbL}{hc}$ bar anchored at exterior joint (3)	$\le 6.25(1+0.8\nu d)\frac{fctm}{fyd}$	$\le 7.5(1+0.8\nu d)\frac{fctm}{fyd}$	-
Transverse bars (w):			
(i) outside critical regions			

spacing sw≤	0.75d		
ρw ≥ $\frac{0.08\,fcd(Mpa)}{2\,fyk(Mpa)}$ (0)	$\frac{0.08\,fcd(Mpa)}{2\,fyk(Mpa)}$ (0)		
(ii) in critical regions:			
dbw≥	6mm		
spacing sw≤	6dbL, *hw/4*, 24dbw, 175mm	8dbL, *hw/4*, 24dbw, 225mm	-
Shear design:			
VEd, seismic (4)	$1.2\frac{\sum M_{Rb}}{l_{cl}} \pm Vo.g + \varphi 2q_{(4)}$	$\frac{\sum M_{Rb}}{l_{cl}} \pm Vo.g + \varphi 2q_{(4)}$	From the analysis for the "seismic design"

Table Appendix 8: Detailing & dimensioning of primary seismic columns (secondary as in DCL)

	DCH	DCM	DCL
Cross-section sides, hc, bc ≥	0.25m; $\frac{hv}{10}$ if $\theta = \frac{P\delta}{Vh} > 0.1_{(1)}$		
"critical region" length (L)≥	1.5max(hc,bc), 0.6m, $\frac{lc}{5}$	max(hc,bc), 0.6m, $\frac{lc}{5}$	-
Longitudinal bars (L):			
ρmin	1%		$\frac{0.1Nd}{\text{Ac fyd}}$, 0.2% (0)
ρmax	4% (0)		
dbL≥	8mm		
bars per side ≥	3		2
Spacing between restrained bars	≤150mm	≤200mm	-
distance of unrestrained to nearest restrained bar	≤150mm		
Transverse bars (w):			

Outside critical regions:			
dbw≥	6mm, $\frac{d\,bL}{4}$		
Spacing sw ≤	20dbL, min (hc, bc), 400mmm		
sw in splices ≤	12dbL, 0.6 min (hc, bc), 240mm		
Within critical regions:(2)			
dbw≥ (3)	6mm, $0.4\frac{fyd}{fywd}\frac{1}{2}dbl$	6mm, $\frac{d\,bL}{4}$	
sw≤ (3), (4)	6dbL, $\frac{bo}{3}$, 125mm	8dbL, $\frac{bo}{3}$,175mm	-
ωwd≥ (5)	0.08	-	
αωwd≥ (4), (5), (6), (7)	$30\,\mu\phi * \nu\,d\,\varepsilon_{sy}, \frac{d\,bc}{bo}$ -0.035	-	
In critical region at column base:			
ωwd≥	0.12	0.08	ωwd≥
αωwd≥ (4), (5), (6), (8), (9)	$30\,\mu\phi\,\nu\,d\,\varepsilon_{sy}, \frac{d\,bc}{bo}$ -0.035		-
Capacity design check at beam-column joints: (10)	$1.3\sum M_{Rb} \le \sum M_{Rc}$ No moment in transverse direction of column		-
Verification for Mx-My-N:	Truly biaxial, or uniaxial with (Mz/0.7, N), (My/0.7, N)		
Axial load ratio νd=NEd/Acfcd	≤ 0.55	≤ 0.65	*Axial load ratio* νd=NEd/Acfcd
Shear design:			
VEd seismic (11)	$1.3\frac{\sum M_{Rc}\,ends}{lcl}$ (11)	$1.1\frac{\sum M_{Rc}\,ends}{lcl}$ (11)	VEd seismic (11)
$V_{Rd,max}$ seismic (12), (13)	As in EC2: $V_{Rd,max} = 0.3(1-\frac{f_{ck}}{250})$ min [1.25;(1+νd);2.5(1-νd)]$b_{wo}\,z\,f_{cd}\sin 2\theta$, with $1 \le \cot\theta \le 2.5$		
$V_{Rd,s}$ seismic (12), (13), (14)	As in EC2: $V_{Rd,s} = b_w\,z\,\rho_w\,f_{ywd}\cot\theta + \frac{N_{Ed}(h-x)}{lcl}$ with $1 \le \cot\theta \le 2.5$		

Appendix D1 Sample Detailing of Beam and Column and its Evaluation

In this section sample detailing of beams and columns and the evaluation according to the requirements are presented for DCM and DCH models. And the samples are taken from DCM 10 favorable and DCH 10 favorable models.

1. Medium Ductility Class

a) Beam detailing

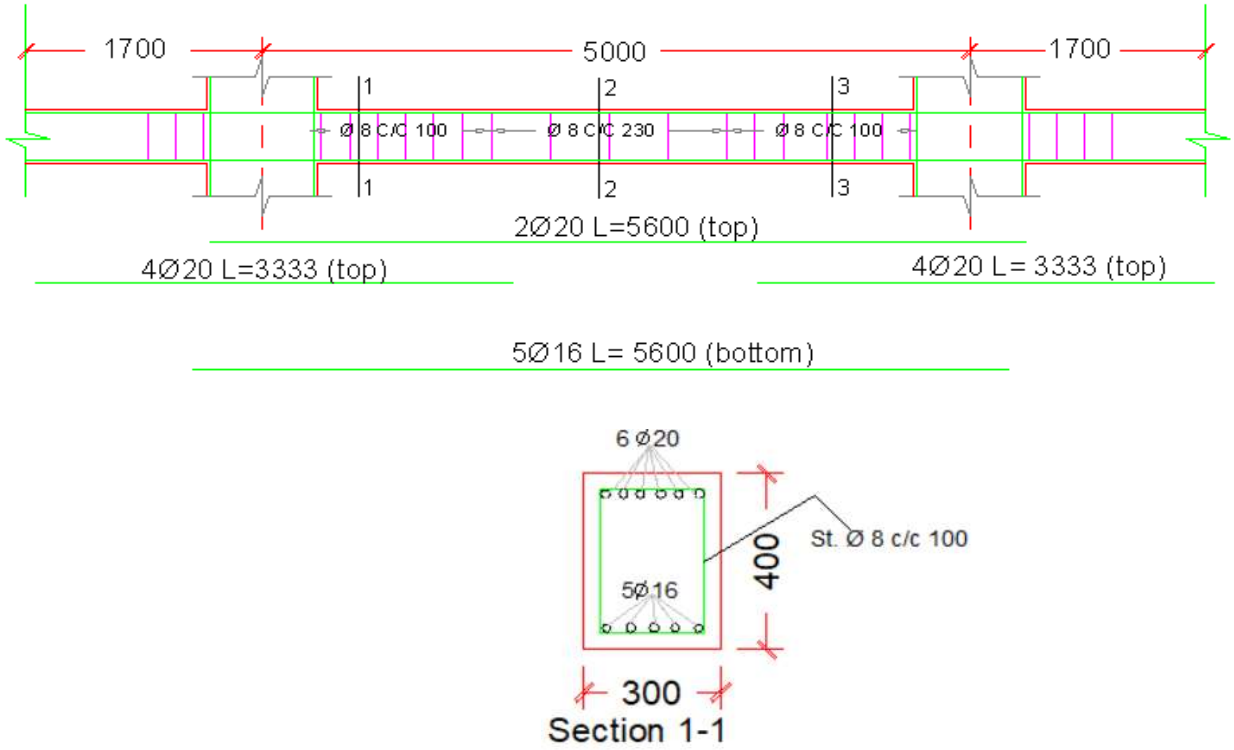

Figure Appendix 4*:* Sample detailing of a beam in DCM 10 favorable model

Table Appendix 5*:* Detailing requirement check for a beam in DCM 10 favorable model

Parameter	Limit requirement	Provided from design out put	Remark
Critical region length	h_w =600mm	600mm	Ok
ρ_{min}, tension side	0.003625	0.0084	Ok
ρ_{max}, critical regions (1)	0.0178	0.0158	Ok
$A_{s,\,min}$, top & bottom	308mm^2	628 mm^2	Ok
$A_{s,\,min}$, top-span	449 mm^2	628 mm^2	Ok
$A_{s,\,min}$, critical regions bottom	889 mm^2	1001 mm^2	Ok
$A_{s,\,min}$, supports bottom	942 mm^2	1001 mm^2	Ok
$\frac{dbL}{hc}$ - bar crossing interior joint (3)	< 0.0675	0.333	Ok
$\frac{dbL}{hc}$ - bar anchored at exterior joint (3)	< 0.0855	0.0333	Ok
Transverse bars (w):			
ii) Outside critical region			
spacing sw≤	267.75mm	230mm	Ok
$\rho w > \frac{0.08\,fcd(Mpa)}{2\,fyk(Mpa)}$ (0)	0.001	0.0092	Ok
ii) In critical regions			
dbw≥	6mm	8mm	Ok
spacing sw≤	150mm	100mm	Ok

b) Column detailing

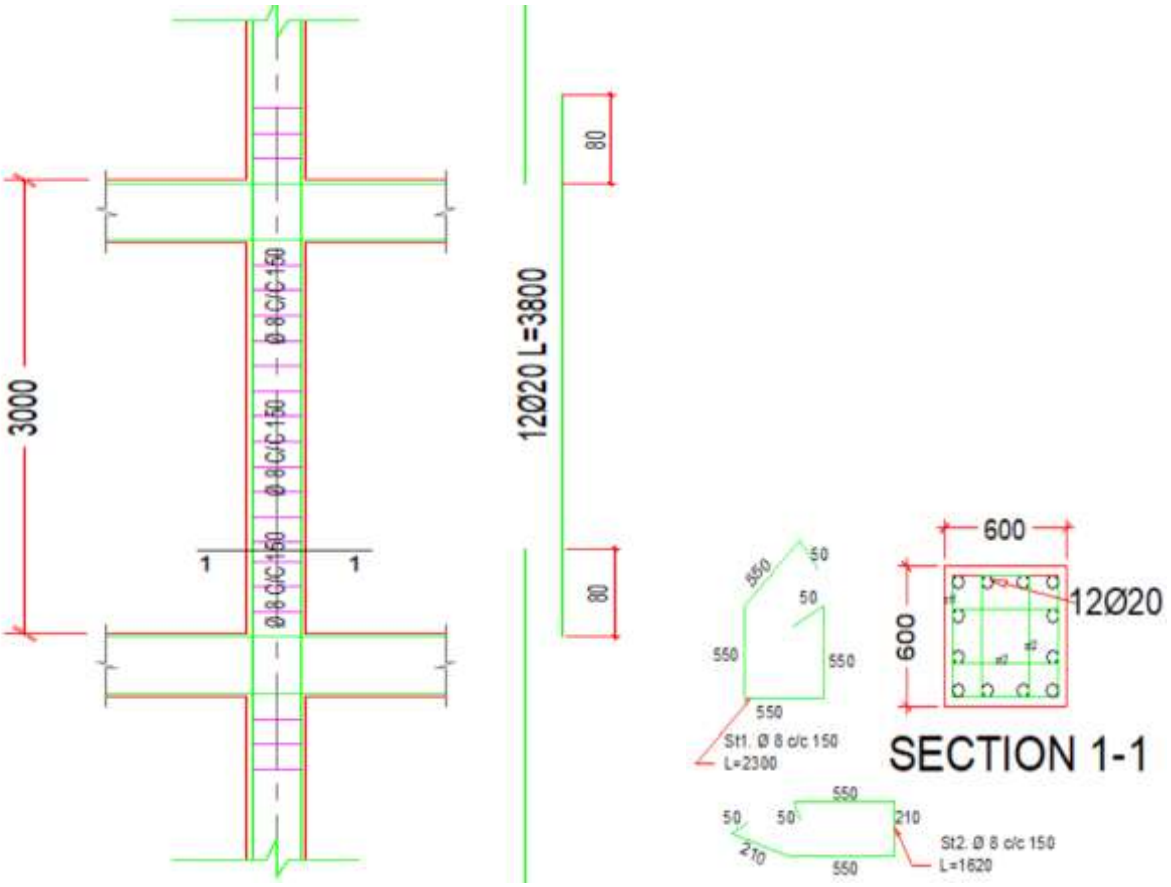

Figure Appendix 5: Sample detailing of a column in DCM favorable model

Table Appendix 10: Parameter evaluation as per the limit requirements for a column in DCM 10 favorable mode.

Parameter	Limit requirement	Provided from design out put	Remark
Longitudinal bars (L):			
Cross-section sides, hc, bc	25cm	60cm	Ok
ρ_{min}	1%	1.045%	Ok
ρ_{max}	4%	1.045%	Ok
dbL	8mm	20mm	Ok
bars per side	3	4	Ok
Spacing between restrained bars	≤ 200mm	178mm	Ok
distance of unrestrained to nearest restrained bar	≤ 150mm	-	Ok
Transverse bars (w):			
Outside critical region			
Dbw	≥ 6mm	8mm	Ok
Spacing sw	≤ 400mm	150mm	Ok
sw in splices	≤ 240mm	150mm	Ok
ii) In critical regions			
Dbw	≥ 6mm	8mm	Ok
Sw	≤ 160mm	150mm	Ok
ω_{wd} ≥	-	-	-
$\alpha\omega_{wd}$ ≥	-	-	-
In critical region at column base:			
ωwd≥	0.08	0.358	Ok
αωwd≥	0.042	0.303	Ok
Capacity design check at beam-column joints:	1.3* M_{Rb} < M_{RC}	From section designer output we have, M_{RC} = 768, M_{Rb} =231.4,	Ok

		1.3* M_{Rb} = 300.82 Thus, 1.3* M_{Rb} < M_{RC}	
Verification for Mx-My-N:	Truly Biaxial		
Axial load ratio $\nu_d = \frac{N_{Ed}}{Acfcd}$	< 0.65	3100/6000 = 0.527	Ok

2. Ductility Class High.

a) Beam detailing

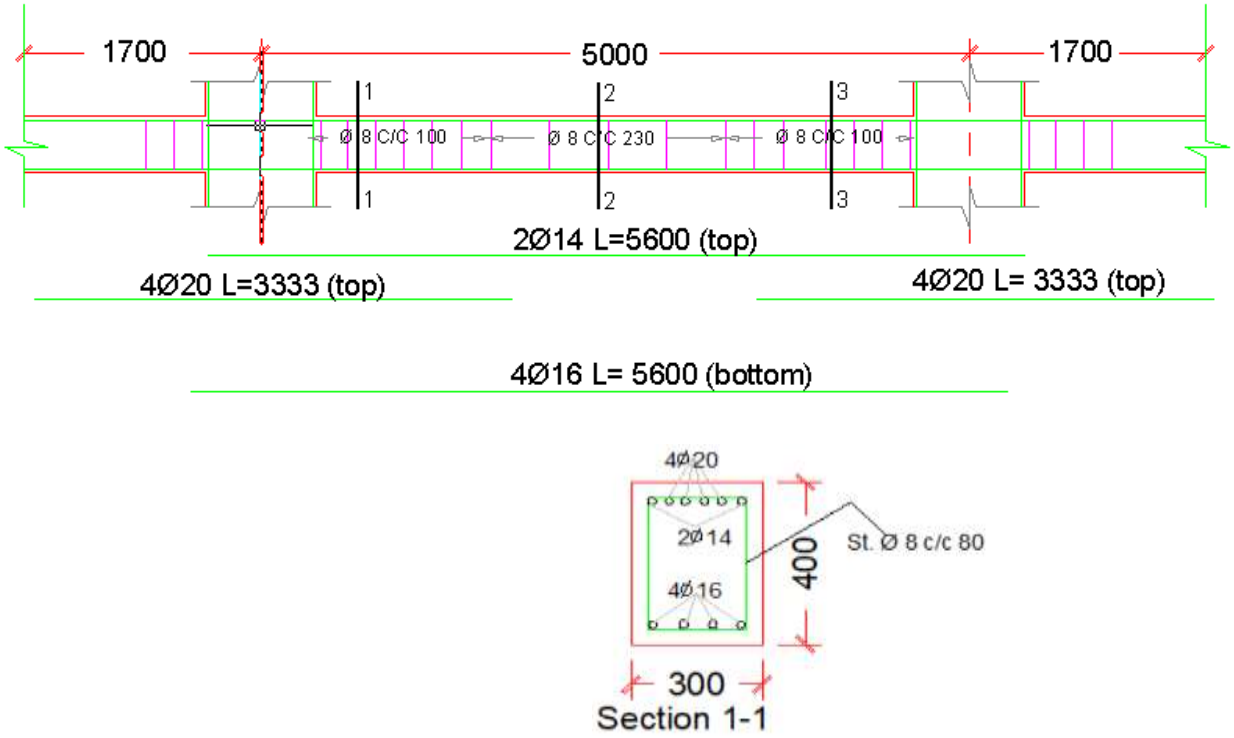

Figure Appendix 6: Sample detailing of a beam in DCH 10 favorable model

Table Appendix 11: Parameter evaluation as per the limit requirements for a beam in DCH 10 favorable model

Parameter	Limit requirement	Provided from design out put	Remark
Critical region length	1.5*hw = 900mm	900mm	Ok
ρ_{min}, tension side	0.003625	0.0055 > ρmin	Ok
ρ_{max}, critical regions	0.0178	0.0119	Ok
$A_{s,\,min}$, top & bottom	308mm^2	308mm^2	Ok
$A_{s,\,min}$, top-span	392.5 mm^2	628 mm^2	Ok
$A_{s,\,min}$, critical regions bottom	785 mm^2	1005 mm^2	Ok
$A_{s,\,min}$, supports bottom	251.25 mm^2	1005 mm^2	Ok
$\frac{dbL}{hc}$ - bar crossing interior joint	< 0.0675	0.05	Ok
$\frac{dbL}{hc}$ - bar anchored at exterior joint	< 0.0855	0.05	Ok
Transverse bars (w):			
iii) Outside critical region			
spacing sw≤	267.75mm	120mm	Ok
$\rho w \geq \frac{0.08fck}{2fyk}$, fck, fyk (Mpa)	0.001	0.0039	
ii) In critical regions			
dbw≥	6mm	8mm	Ok
spacing sw≤	150mm	80mm	Ok

b) Column detailing

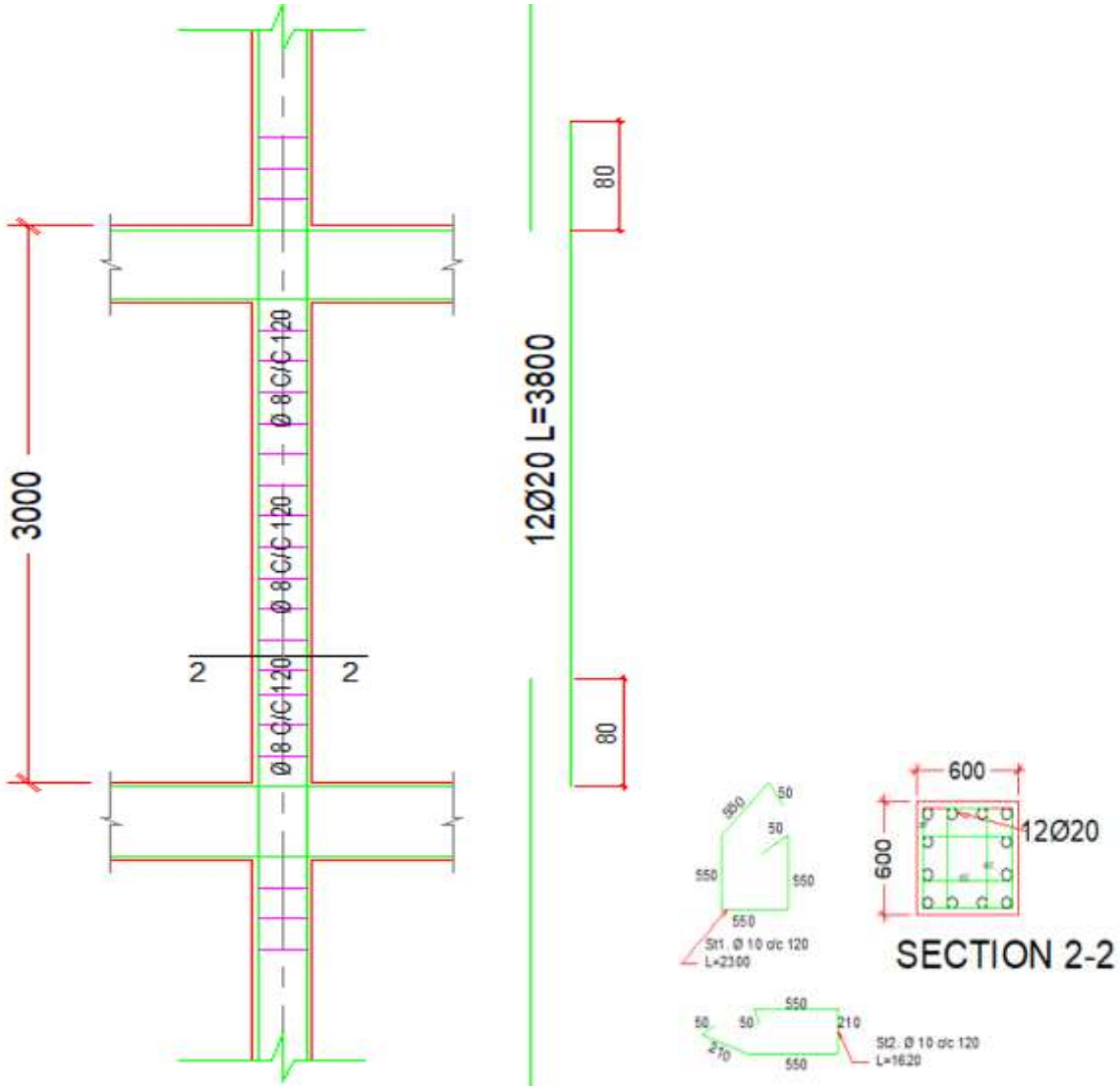

Figure Appendix 7: Sample detailing of a column in DCH favorable mode

Table Appendix 12: Parameter evaluation as per the limit requirements for a column in DCH 10 favorable model

Parameter	Limit requirement	Provided from design out put	Remark
Longitudinal bars (L):			
Cross-section sides, hc, bc	25cm	60cm	Ok
ρmin	1%	1.045%	Ok

ρmax	4%	1.045%	Ok
dbL	8mm	20mm	Ok
bars per side	3	4	Ok
Spacing between restrained bars	≤ 200mm	178mm	Ok
distance of unrestrained to nearest restrained bar			
Transverse bars (w):			
Outside critical region			
Dbw	≥ 6mm	8mm	Ok
Spacing sw	≤ 400mm	120mm	Ok
sw in splices	≤ 240mm	120mm	Ok
ii) In critical regions			
dbw (3)	≥ 6mm	8mm	Ok
sw (3), (4)	≤ 160mm	120mm	Ok
ω_{wd} ≥ (5)	0.08	0.56	Ok
$\alpha\omega_{wd}$ ≥ (4), (5), (6), (7)	0.053	0.428	Ok
In critical region at column base:			
ωwd≥	0.12	0.56	Ok
αωwd≥ (4), (5), (6), (8), (9)	0.053	0.428	Ok
Capacity design check at beam-column joints: (10)	1.3* M_{Rb} < M_{RC}	From section designer output we have, M_{RC} = 865.7, M_{Rb} = 257.27 1.3* M_{Rb} = 334.45 Thus, 1.3* M_{Rb} < M_{RC}	Ok
Verification for Mx-My-N:	Truly Biaxial		
Axial load ratio $\nu d = \frac{N_{Ed}}{Acfcd}$	< 0.55	2726.44/6000 = 0.454	Ok